CNWRA 96-009

A PARAMETRIC STUDY OF DRIFT STABILITY IN JOINTED ROCK MASS

PHASE I: DISCRETE ELEMENT THERMAL-MECHANICAL ANALYSIS OF UNBACKFILLED DRIFTS

Prepared for

Nuclear Regulatory Commission
Contract NRC-02-93-005

Prepared by

Center for Nuclear Waste Regulatory Analyses
San Antonio, Texas

September 1996

9611220045 961030
PDR WASTE
WM-11 PDR

CNWRA 96-009

A PARAMETRIC STUDY OF DRIFT STABILITY IN JOINTED ROCK MASS

PHASE I: DISCRETE ELEMENT THERMAL-MECHANICAL ANALYSIS OF UNBACKFILLED DRIFTS

Prepared for

Nuclear Regulatory Commission
Contract NRC-02-93-005

Prepared by

Mikko P. Ahola
Rui Chen
Hengameh Karimi
Sui-Min (Simon) Hsiung
Asadul H. Chowdhury

Center for Nuclear Waste Regulatory Analyses
San Antonio, Texas

September 1996

CONTENTS

Section Page

FIGURES v
TABLES vii
ACKNOWLEDGMENTS ix
EXECUTIVE SUMMARY xi

1 INTRODUCTION 1-1
1.1 BACKGROUND AND OBJECTIVES 1-1
1.2 SCOPE 1-4

2 PARAMETERS AND INPUT INFORMATION 2-1
2.1 SELECTION OF PARAMETERS 2-1
2.2 THERMAL LOAD 2-5

3 THERMAL-MECHANICAL ANALYSIS 3-1
3.1 COMPUTER CODE 3-1
3.2 NUMERICAL MODEL 3-1
3.2.1 Selection of Material Model 3-1
3.2.2 Initial/Boundary Conditions 3-1
3.2.3 Model Setup 3-3
3.2.4 Solution Scheme 3-3
3.3 DESIGN OF 2^k FRACTIONAL FACTORIAL EXPERIMENTS 3-6

4 RESULTS AND DISCUSSIONS 4-1
4.1 DISCUSSION OF UDEC SCOPING RUN RESULTS 4-1
4.1.1 Effect of Thermal Load and Joint Pattern on Displacement 4-1
4.1.2 Effect of Thermal Load and Joint Pattern on Stresses 4-10
4.1.3 Temperature Distribution 4-13
4.1.4 Summary of Scoping Analyses 4-13
4.2 GENERAL MODELING RESULTS FROM FINAL SET OF UDEC RUNS 4-20
4.2.1 Joint Shear Displacement 4-20
4.2.2 Convergence and Displacement 4-33
4.2.3 Stress Distribution 4-33
4.2.4 Failure Zones 4-37
4.2.5 Joint Opening and Closure 4-37
4.3 SIGNIFICANCE OF MAIN PARAMETERS AND TWO-PARAMETER INTERACTIONS 4-46
4.3.1 Thermal Load 4-47
4.3.2 Thermal Expansion Coefficient 4-48
4.3.3 Intact Rock Young's Modulus 4-49
4.3.4 Subvertical Joint Inclination 4-49
4.3.5 Subhorizontal Joint Inclination 4-50
4.3.6 Subvertical Joint Spacing 4-50
4.3.7 Joint Friction Angle 4-51

CONTENTS (cont'd)

Section Page

4.3.8 Intact Rock Cohesion 4-52
4.3.9 Intact Rock Friction Angle 4-52

5 CONCLUSIONS AND RECOMMENDATIONS 5-1
5.1 CONCLUSIONS 5-1
5.2 RECOMMENDATIONS 5-3

6 REFERENCES 6-1

APPENDIX A A-1

FIGURES

Figure		Page
2-1	Heat flux from typical waste package assuming 20-year-old fuel at time of emplacement (solid line) as well as UDEC input based on a best exponential fit using a single decay constant. Note: Curves represent necessary 2D tunnel wall heat flux required to establish areal mass loading of 100 MTU/acre	2-6
2-2	Wall temperatures calculated by UDEC for areal mass loadings of 100 MTU/acre and 20 MTU/acre assuming 20-year-old fuel	2-8
2-3	Portion of ABAQUS finite-element mesh for radiative heat transfer analysis	2-9
2-4	ABAQUS 2D radiative heat transfer analysis showing (a) temperature contours 50 yr after heating, and (b) comparison of tunnel roof temperature history with UDEC	2-10
3-1	UDEC model showing block geometry for one particular joint set pattern and thermal loading	3-4
3-2	Method of running a coupled thermal-mechanical simulation with UDEC (Board, 1989)	3-5
4-1	Vertical displacement after 100 yr of heating along a vertical section through model centerline above the tunnel for different joint patterns for 100 MTU/acre thermal load.	4-2
4-2	Vertical displacement after 100 yr of heating along a vertical section through model centerline above the tunnel for different joint patterns for 20 MTU/acre thermal load	4-3
4-3	Vertical displacement after 100 yr of heating along a vertical section through model centerline above the tunnel for joint pattern C	4-4
4-4	Vertical displacement at roof as a function of time for different joint patterns for the thermal load of 100 MTU/acre	4-5
4-5	Vertical displacement at floor as a function of time for different joint patterns for the thermal load of 100 MTU/acre	4-6
4-6	Vertical displacement at roof as a function of time for different joint patterns for the thermal load of 20 MTU/acre	4-8
4-7	Vertical displacement at floor as a function of time for different joint patterns for the thermal load of 20 MTU/acre	4-9
4-8	Horizontal stress after 100 yr of heating along a vertical section through the tunnel for the thermal loading of 100 MTU/acre	4-11
4-9	Horizontal stress after 100 yr of heating along a vertical section through the tunnel for the thermal loading of 20 MTU/acre	4-12
4-10	Horizontal stress after 100 yr of heating along a vertical section through the tunnel for joint pattern C	4-14
4-11	Vertical stress after 100 yr of heating along a horizontal section through the tunnel for the thermal loading of 100 MTU/acre	4-15
4-12	Vertical stress after 100 yr of heating along a horizontal section through the tunnel for the thermal loading of 20 MTU/acre (refer to figure 4-11 for curve definitions)	4-16
4-13	Vertical stress after 100 yr of heating along a horizontal section through the tunnel for joint pattern C	4-17

FIGURES (cont'd)

Figure		Page
4-14	Temperature histories on tunnel wall at roof for various joint patterns for the thermal loading of 100 MTU/acre	4-18
4-15	Temperature histories on tunnel wall at roof for various joint patterns under the thermal load of 20 MTU/acre	4-19
4-16	Joint shear displacement following drift excavation for Case 12. Joint shear displacement is in meters.	4-30
4-17	Joint shear displacement after 50 yr of heating for Case 12. Joint shear displacement is in meters.	4-31
4-18	Joint shear displacement after 100 yr of heating for Case 12. Joint shear displacement is in meters.	4-32
4-19	Principal stress distribution following drift excavation for Case 12. Stress unit is MPa.	4-34
4-20	Principal stress distribution after 50 yr of heating for Case 12. Stress unit is MPa	4-35
4-21	Principal stress distribution after 100 yr of heating for Case 12. Stress unit is MPa	4-36
4-22	Failure distribution following drift excavation for Case 26	4-38
4-23	Failure distribution after 50 yr of heating for Case 26	4-39
4-24	Failure distribution after 100 yr of heating for Case 26	4-40
4-25	Distribution of joint opening and closure following drift excavation for Case 12. Red lines represent joints with zero normal stress and the thickness of green lines is proportional to the magnitude of joint closure. Joint closure unit is meter..	4-41
4-26	Distribution of joint opening and closure after 50 yr of heating for Case 12. Joint closure unit is meter.	4-42
4-27	Distribution of joint opening and closure after 100 yr of heating for Case 12. Joint closure unit is meter.	4-43

TABLES

Table		Page
2-1	UDEC scoping run matrix for 20 and 100 MTU/acre thermal loadings with different fracture geometry	2-2
2-2	Intact rock parameter values for scoping analysis	2-3
2-3	Rock joint parameter values for scoping analysis	2-3
2-4	Range of variable parameters for final TM parametric study	2-4
2-5	Fixed parameters for final TM parametric study	2-4
2-6	Heat flux decay parameters for 20-year-old fuel	2-7
3-1	Drift and waste package spacings corresponding to range of thermal loadings	3-2
4-1	Comparison of roof, floor, and maximum joint shear displacement for scoping runs	4-7
4-2	Maximum compressive and maximum tensile stresses for scoping runs	4-10
4-3	Values of performance measures for factorial UDEC run cases, (a) at 50 yr and (b) at 100 yr	4-21
4-4	Maximum depth of opening zone from drift wall after 100 yr	4-44
4-5	General summary of factorial experiment	4-48

ACKNOWLEDGMENTS

This report was prepared to document work performed by the Center for Nuclear Waste Regulatory Analyses (CNWRA) for the Nuclear Regulatory Commission (NRC) under Contract No. NRC-02-93-005. The activities reported here were performed on behalf of the NRC Office of Nuclear Material Safety and Safeguards, Division of Waste Management. The report is an independent product of the CNWRA and does not necessarily reflect the views or regulatory position of the NRC.

The authors thank Drs. W. Patrick and B. Sagar for their reviews of this report. The authors are thankful to Y. Lozano for skillful typing of the report and to B. Long, who provided a full range of expert editorial services in the preparation of the final document.

QUALITY OF DATA

All CNWRA-generated original data contained in this report meet quality assurance (QA) requirements described in the CNWRA Quality Assurance Manual. Sources for other data should be consulted for determining the level of quality for those data.

SOFTWARE QUALITY ASSURANCE

The distinct element code UDEC (Version 2.01), which was used for the 74 analyses runs contained in this report, is controlled under the CNWRA software QA procedure (TOP-018, Development and Control of Scientific and Engineering Software). Several simple software packages developed at CNWRA were used for analyses of data contained in this report. These computational software packages fall under the categories covered by QAP-014, Documentation and Verification of Routine Calculations, and are not controlled by configuration management procedure TOP-018.

EXECUTIVE SUMMARY

Emplacement of heat generating radioactive waste in the partially saturated and fractured geologic medium of Yucca Mountain (YM) will induce thermal, mechanical, hydrological, and chemical processes some of which may have significant effects due to couplings. A Nuclear Regulatory Commission (NRC) staff technical position (Nataraja and Brandshaug, 1992) provided an acceptable methodology for systematically considering thermal loads and thermally induced mechanical, hydrological, and chemical processes for the design and performance assessment (PA) of a proposed geologic repository. This staff technical position is applicable to the U.S. Department of Energy (DOE) demonstration of compliance with the NRC regulations on thermal loads (Nuclear Regulatory Commission, 1996). When processes are coupled, behavior of the repository and surrounding rock mass cannot be reasonably evaluated by considering each process independently (Wang et al., 1983; Tsang, 1987; Manteufel et al., 1993). The importance of various processes will depend upon the thermal loading of the repository, the design of the engineered barriers including backfills, the properties of the geologic medium, the time and spatial scales at which these processes are of interest, and the measure selected to evaluate performance. The binary one-way coupling between thermal and mechanical processes is investigated in this report.

A key technical issue (KTI) in the high-level nuclear waste (HLW) program is evaluation of time-dependent thermal-mechanical (TM) coupled response of the jointed rock mass. Postclosure PA requires an understanding of the TM response of the jointed rock mass over the compliance period (thousands of years) as it impacts near-field environment and waste package degradation, performance of seals, and flow and radionuclide transport mechanisms. Design for the preclosure operation period (≈ 100 yr) requires an understanding of the TM response of the jointed rock mass as it impacts drift stability and waste retrievability. Two activities that involve study of mechanical effects in the near-field environment of the proposed HLW repository are: (i) stability of underground excavations, including emplacement drifts, for both opening design and providing input for design and PA of waste packages and (ii) change of hydrological properties of rock fractures due to TM perturbation of the rock mass that may affect vaporization of water, recondensation of the vapor, and condensate dripping through potential preferential pathways, for providing input to the waste package and the system PA.

The TM response of a jointed rock mass may be affected by a number of parameters and conditions. These include: (i) rock properties such as Young's modulus, strengths (tensile, compressive, and shear), Poisson's ratio, density, cohesion, specific heat, friction angle, coefficient of thermal expansion, thermal conductivity, and their variations with temperature, time, moisture content, and space; (ii) joint properties such as normal and shear joint stiffnesses, cohesion, friction angle, tensile strength, orientation and spacing of joints, and their variations with temperature, time, moisture content, and space; and (iii) *in situ* stresses, construction of openings, seismic events including repeated seismic events, thermal loads, and their variations with time. Parametric analysis involving these parameters and conditions provides an effective means to identify important influences on TM response of a jointed rock mass for both opening stability and fracture permeability change.

The overall objective of the TM parametric study is to identify thermal and site specific natural phenomena and rock mechanical and thermal parameters that may significantly influence the pre- and postclosure performance of the repository under heated and seismic conditions. A phased approach was adopted for this purpose. The objective of the Phase I TM parametric study is to conduct a parametric investigation of emplacement drifts without backfill, rock support, and seismic load for 100 yr of heating using the distinct element computer code UDEC. A 2^k fractional factorial experimental design approach

was applied in this parametric study. The 2^k fractional factorial design studies the effect on rock mass response of k parameters, each at two levels. Nine parameters (k=9) were studied: subvertical and subhorizontal joint inclination [measured upward from horizontal axis assuming two-dimensional strike of joints that are parallel to the drift axis], subvertical joint spacing, joint friction angle, thermal load, intact rock cohesion, intact rock friction angle, intact rock Young's modulus, and thermal expansion coefficient. The two levels are low and high values of these parameters. Although a full 2^9 factorial plan would require 512 runs, in this analysis only 64 runs (i.e., 1/8 fractional factorial plan) were made. The performance measures used in this study include: maximum principal and minimum principal stresses around the excavation, maximum joint shear displacement, maximum joint closure, maximum joint separation, roof-to-floor convergence, and extent of yield zone around the excavation.

The TM parametric study of emplacement drifts without backfill, rock support, and seismic load for 100 yr of heating shows that thermal load is an important parameter that affects most of the performance measures studied herein. The effects of important parameters on affected performance measures are given below in a tabular form.

Parameter Increased	Performance Affected					
	Maximum Principal Stress	Maximum Joint Shear Displacement	Maximum Joint Closure	Maximum Joint Separation	Maximum Roof-to-Floor Convergence	Extent of Yield Zone
Subvertical Joint Inclination	I	N (50 yr) I (100 yr)	N	D	D (50 yr) N (100 yr)	N
Subhorizontal Joint Inclination	N	N	N	I	N	N
Subvertical Joint Spacing	I	N (50 yr) D (100 yr)	N	N	N (50 yr) D (100 yr)	D
Joint Friction Angle	N	N	N	D	D	D
Thermal Load	I	I	I	I	D	I
Intact Rock Friction Angle	N	N	N	N	N	D
Intact Rock Young's Modulus	I	N (50 yr) I (100 yr)	N (50 yr) I (100 yr)	I	D (50 yr) N (100 yr)	I
Thermal Expansion Coefficient	I	N	I	I	D (50 yr) N (100 yr)	I

Note: I = increase; D = decrease; N = no effect

1 INTRODUCTION

1.1 BACKGROUND AND OBJECTIVES

Yucca Mountain (YM), in southern Nevada, has been designated by the United States Congress for characterization as a potential repository site for high-level nuclear waste (HLW) disposal. A general description of the YM site for the proposed HLW repository was presented in the U.S. Department of Energy (DOE) Site Characterization Plan (SCP) (U.S. Department of Energy, 1988). In addition, updated YM site characteristics data are provided by DOE through its semi annual SCP Reports. The YM area is characterized by north to northwest-trending mountain ranges composed of volcanic strata that dip eastward. The strata are broken into en-echelon fault blocks. The geomechanical conditions at the site are characterized by a highly fractured rock mass with prominent vertical and sub-vertical faults and joints that transgress the site environs. Arid climate prevails in the YM area, with less than 25 cm of rain per year, and no perennial streams exist in this region. The potential repository location is in the densely welded, devitrified part of the Topopah Spring (TSw2 unit) member of the Paintbrush tuff, which is about 350 m below the ground surface and 225 m above the water table (Klavetter and Peters, 1986). At YM, the zone above the water table contains capillary water held in pores with evidence of perched water zones. The emplacement of radioactive waste in this partially saturated geologic medium will induce thermal, mechanical, hydrological, and chemical processes some of which may have significant effects due to couplings. When processes are coupled, behavior of the repository and its surrounding rock mass cannot be reasonably evaluated by considering each process independently (Wang et al., 1983; Tsang, 1987; Manteufel et al., 1993). The importance of various processes will depend on the thermal loading of the repository, the design of the engineered barriers including backfill, the properties of the geologic medium, the time and spatial scales at which these processes are of interest, and the measure selected to evaluate performance.

The fractured rock mass will be perturbed in several ways. First, construction of the repository alters the state of stress, which in turn, causes mechanical deformation of the rock, including joint normal and shear deformations. Joint normal and shear deformations affect excavation stability. They also affect fluid flow and solute transport in the rock mass, which are particularly important to the performance of a HLW geologic repository and its environment. Second, nuclear waste provides a heat source that is active over an extended period of time. This thermal load induces rock expansion. Rock expansion may cause dilation, closure, and shear failure of fractures. Permeability of both matrix and fracture may change accordingly. The thermal load may also cause (i) degradation of the mechanical properties of the rock mass (Martin et al., 1993, 1994; Price et al., 1987); (ii) changes to the chemical sorption and retardation capabilities; (iii) vaporization, vapor flow, condensation, and condensate flow; and (iv) dissolution or healing of rock fractures (Lin and Daily, 1989; de Marsily, 1987). Third, dynamic ground motions due to earthquakes and nearby underground nuclear weapons testing, may induce additional stresses. The dynamic ground motions, including the cumulative effect of repeated seismic motions, will cause further dilation, closure, and shear of fractures, which may change fracture and matrix permeabilities (Kana et al., 1991 and 1995).

A recent Nuclear Regulatory Commission (NRC) staff technical position provided an acceptable methodology for systematically considering thermal loads and thermally induced mechanical, hydrological, and chemical processes (Nataraja and Brandshaug, 1992). The primary purpose of the NRC technical position is to outline an acceptable method of comprehensively, systematically, and logically understanding and evaluating coupled process response for design and performance assessment (PA) of

a proposed geologic repository. This staff technical position is applicable to the DOE demonstration of compliance with NRC regulations on thermal loads (Nuclear Regulatory Commission, 1996).

A key technical issue (KTI) identified by the NRC in the HLW program is evaluation of time-dependent thermal-mechanical (TM) coupled response of the jointed rock mass. Postclosure PA requires an understanding of the TM response of the jointed rock mass over the compliance period (thousands of years) as it impacts near-field environment and waste package degradation, performance of seals, and flow and radionuclide transport mechanisms. Designing for the preclosure or operations period ($\approx$ 100 yr) requires an understanding the TM response of the jointed rock mass as it impacts drift stability and retrievability.

In general, there are two factors that involve mechanical effects in the near-field environment of the proposed HLW repository: (i) stability of underground excavations, including emplacement drifts, for both opening design and providing input for design and PA of waste packages and (ii) change of hydrological properties of rock fractures due to TM perturbation of the repository rock mass that may affect vaporization of water, recondensation of the vapor, and condensate dripping through the potential preferential pathways, for providing input for both the waste package and the system PA.

Stability of underground openings, including emplacement drifts, will primarily depend on TM effects. The TM effects are those due to *in situ* and excavation-induced stresses, dynamic motions, including the cumulative effect of repeated seismic motions, and thermally induced stresses and deformations (Ghosh et al., 1994). Movement along joints in the disturbed jointed rock mass forms the primary mode of deformation of the near-field rock mass (Kana et al., 1991, 1995; Hsiung et al., 1992). Excessive slippage of a rock block along failed joints may affect performance of the waste canisters inside emplacement drifts. In addition to the TM effects, behavior of the joints is also influenced by the presence of water (Jaeger and Cook, 1979; Hoek and Brown, 1980), temperature, and time-dependent degradation of mechanical properties of rock matrix and joints (Kemeny and Cook, 1990; Price et al., 1987).

It is well recognized that rock strength and joint properties are a function of time (or stress) and temperature that is, rock mass deteriorates as time passes and/or temperature increases (Martin, 1972; Nimick and Connolly, 1991; Price et al., 1987; Carter, 1975, 1976). Time-dependent decrease in shear strength of joints may be due to: (i) fracture wall-rock alteration as a result of extended exposure to heat and moisture, (ii) slow deformation of asperities as a result of sustained stress concentration, and (iii) possible increase in fracture wall-rock ductility as a result of exposure to heat. The time-dependent decrease in strength of intact rock is generally associated with (i) gradual slip on grain contacts under sustained stress concentration, (ii) subcritical crack growth due to sustained concentration at microcrack tips, and (iii) possible increase in ductility (decrease in viscosity) of minerals due to exposure to heat.

Backfill could be placed in the emplacement drifts by the DOE (TRW Environmental Safety Systems, Inc., 1994a) for four major reasons: (i) to prevent deleterious rock movement in the strata between the surface and the repository horizon that may cause surface subsidence; (ii) to provide a predetermined environment around waste packages to enhance long-term performance of the waste package exterior; (iii) to protect or cushion the waste package from rock falls; and (iv) to retard transport of radionuclides to the accessible environment. Stability of emplacement drifts and the thermal environment in these drifts will be significantly affected by the absence or presence of backfill in the emplacement drifts. Consequently, TM effects on waste packages will also be significantly influenced by backfill. The effect of backfill on the stability of emplacement drifts and on the thermal environment of these drifts is not considered in this Phase I study. It will be considered in a subsequent phase of study.

If the temperature in the rock mass due to emplaced waste reaches the boiling point, pore water in the rock matrix is likely to vaporize and flow from the emplacement areas condensing in regions where temperatures are below boiling conditions—creating a dryout zone (Buscheck and Nitao, 1993). Condensate in the zones above the emplacement areas tends to drain toward the emplacement areas due to gravity or capillary effect. It has been argued (Buscheck and Nitao, 1994) that at YM fracture flow may be the most likely means for condensate to flow toward the waste packages since matrix permeability of the TSw2 unit is extremely small. In this condition, fracture flow tends to persist for a long distance before the condensate is re-vaporized or imbibed by rock matrix. Therefore, it would appear that the hydrological properties of fractures (Mohanty et al., 1994) (taking into consideration the buoyant pressure of vapor flow) along with the extent of dryout zone and amount of condensate available above the emplacement areas (note that the amount may be enhanced by infiltration of rainfall) are the predominant factors that will determine the rate and time of condensate flow towards the waste packages.

The behavior described above is complicated further by the possibility that the hydrological properties of fractures may not remain constant throughout the life of the waste packages and repository due to TM perturbation of the repository rock mass, including cumulative effect of repeated seismic motions as discussed earlier. Hydrologic changes have been observed in connection with several earthquakes (Ofoegbu et al., 1994; Rojstaczer and Wolf, 1992). At YM, the change of fracture permeability may occur because of the ground motion from earthquakes and underground nuclear explosions at the Nevada Test Site. Recent observations (Hill et al., 1993) that a large earthquake can induce smaller earthquakes at great distances from its epicenter makes this issue more significant than previously thought. TM perturbation of YM along with cumulative effects of repeated seismic loads may form preferential pathways connecting the emplacement area with condensation zones above the emplacement area, perched water zones, or neighboring steep hydraulic gradient zones that could increase significantly the chance for water to contact waste packages. The effect of earthquakes on stability of emplacement drifts and hydrological properties of fractures is not considered in this Phase I study; it will be considered in the next phase.

The time-dependent deterioration of rock joints is likely to change the capability of fractures to conduct flow. Furthermore, pore water or vapor in the rock matrix tends to expand as temperature increases, causing development of excess pore pressure. Since the rock matrix permeability at YM is low, excess pore pressure may not dissipate quickly. Laboratory data presented by Althaus et al. (1994) suggest that such pressure increase in the rock matrix may weaken the rock enough to increase the likelihood for microfracturing. The occurrence of microfracturing may cause considerable increase in the rock-mass permeability. However, it is not yet clear how such changes in rock-mass permeability may affect the performance of the proposed repository. The effect of time-dependent degradation of rock on fracture properties is not considered in this Phase I study; it will be considered in a subsequent phase of study.

The TM response of a jointed rock mass is affected by a number of parameters and conditions: (i) rock properties such as Young's modulus, strengths (tensile, compressive, and shear), Poisson's ratio, density, cohesion, specific heat, friction angle, coefficient of thermal expansion and thermal conductivity, and their variations with temperature, time, moisture content, and space; (ii) joint properties such as normal and shear stiffnesses, cohesion, angle of internal friction, tensile strength, orientation and spacing of joints, and their variations with temperature, time, moisture content, and space; and (iii) *in situ* stresses, construction of openings, seismic events including repetitive seismic events, thermal loads, and their variations with time. Parametric analysis involving these parameters and conditions provides an

effective means to identify important influences on coupled TM response of a jointed rock mass for both opening stability and fracture permeability change.

The overall objective of the TM parametric study is to identify thermal and site specific natural phenomena and rock mechanical and thermal parameters that may significantly influence the pre- and postclosure performance of the repository under heated and seismic conditions. A phased approach was adopted for this purpose. The objective of the Phase I TM parametric study is to conduct a parametric investigation of emplacement drifts without backfill, rock support, and seismic load for 100 yr of heating using the universal distinct element code (UDEC).

1.2 SCOPE

The scope of Phase I of the multiphase parametric study includes

- scoping analysis to assist selection of parameters for TM parametric study
- selection of parameters and input data based on available YM site specific and DOE design specific information. Sources for this information include the DOE YM Reference Information Base (RIB) (U.S. Department of Energy, 1994), YM region borehole drilling data (Brechtel and Kessler, 1995), and the DOE thermal study reports (TRW Environmental Safety Systems, Inc., 1994a,b, 1995, 1996)
- design of 2^k fractional factorial experiments
- TM analysis of emplacement drifts without backfill, rock support, and seismic load using the two-dimensional (2D) UDEC. The loads include *in situ* stresses, excavation induced stresses, and thermal load. Analysis is for 100 yr of thermal load (i.e., preclosure operation period)
- identification of important parameters that may significantly influence the preclosure ($\approx$ 100 yr) performance of the proposed repository under heated condition

2 PARAMETERS AND INPUT INFORMATION

2.1 SELECTION OF PARAMETERS

The YM rock and thermal properties used in this study are based on information available from a number of sources including the DOE YM RIB (U.S. Department of Energy, 1994), borehole drilling data from the YM region (Brechtel and Kessler, 1995), as well as from the DOE thermal study reports (TRW Environmental Safety System, Inc., 1994a,b, 1995, 1996). The thermal loads used in this study were 100 and 20 MTU/acre encompassing, respectively, the DOE hot and cold repository concepts.

It is recognized that current information and the level of understanding regarding the long-term thermal degradation of the rock mass within the near-field repository environment is limited at best. As a result, this study uses the ranges of mechanical and thermal parameters measured in the laboratory or field to account for the variation of parameters at the YM site as well as how they may change or degrade with temperature, time, stress, and moisture content. Currently, material inelastic behavior in the model takes place in the form of plastic yield when stress conditions are such that a predefined yield limit is met. The strength properties defining this yield limit surface, however, are independent of other parameters such as temperature, moisture content, etc. Further experimental and field studies are necessary to determine how such parameters may change in a repository environment and the importance of their inclusion in the models. Version 2.01 of UDEC used for this study does not have the ability to model temperature dependent mechanical and thermal properties.

Because of the large number of variables (e.g., joint geometries and orientations, mechanical and thermal properties) for conducting a TM drift stability parametric study with UDEC, it was decided that to limit the number and range of certain parameters to be studied in the factorial experiments, a set of scoping calculations first be conducted looking only at variations in the joint patterns (i.e., spacings, inclinations, and number of joint sets) while the mechanical properties of the rock matrix and joints as well as thermal properties remain fixed at their representative mean values. These scoping calculations analyzed the near-field response based on five distinct joint patterns under low and high areal mass loadings (20 and 100 MTU/acre, respectively). Each of the five joint patterns contained at least two joint sets; one subhorizontal and one subvertical. Several cases contained an additional subvertical or ubiquitous joint set. The subhorizontal joint set inclination varied between 0-10° with a constant spacing of 1.25 m. For cases with only one subvertical joint set, the inclination varied between 85-90° with a constant spacing of 0.625 m. For cases with an additional subvertical joint set (i.e., three joint sets total) the inclinations were 70° or 60° and spacing fixed at 1.25 m. This joint geometry data was extracted from Christianson and Brady (1989) as well as borehole mappings of the North Ramp (Brechtel and Kessler, 1995). In general, the published results show the primary jointing being near vertical with spacings a few tenths of a meter, with some horizontal jointing due to bedding foliations within the tuff with spacings on the order of meters. As the inclinations approach vertical, published data shows joint frequency increases. However, there is a practical limit to modeling such high joint frequencies, especially when considering three joint sets. Table 2-1 shows the matrix of UDEC runs for the first set of scoping analyses. The remaining fixed mechanical and thermal parameters for the scoping calculations are given in tables 2-2 and 2-3.

Table 2-1. UDEC scoping run matrix for 20 and 100 MTU/acre thermal loadings with different fracture geometry

Areal Mass Loading (MTU/acre)	Data File Name	Spacing		Thermal Load[1]		Joint Sets (Inclination and Spacing)			Young's Modulus E (GPa)	Joint Friction Angle
		Drift (m)	Waste Package (m)	Initial Heat Generation Rate (W/m^2)	Decay Exponent (s^{-1})	Set No. 1	Set No. 2	Set No. 3		
100	TM100A.dat	22.5	18.0	28.4701	-3.220×10^{-10}	90° 0.625 m	0° 1.25 m	—	32.3	38°
	TM100B.dat					85° 0.625 m	10° 1.25 m	—		
	TM100C.dat							70° 1.25 m		
	TM100D.dat							60° 1.25 m		
	TM100F.dat					85° ubiquitous		70° 1.25 m		
20	TM20A.dat	40.0	50.6	10.1633	-3.220×10^{-10}	90° 0.625 m	0° 1.25 m	—		
	TM20B.dat					85° 0.625m	10° 1.25 m	—		
	TM20C.dat							70° 1.25 m		
	TM20D.dat							60° 1.25 m		
	TM20F.dat					85° ubiquitous		70° 1.25 m		

[1]Equation for thermal decay is expressed as $q=q_0 \exp(-\alpha t)$, where q_0 is initial strength (W/m^2) and α is the decay exponent (1/s).

Table 2-2. Intact rock parameter values for scoping analysis

Parameters	Values	Units
Young's Modulus	32.3	GPa
Poisson's Ratio	0.21	-
Density	2297.0	kg/m^3
Uniaxial Compressive Strength	166.0	MPa
Cohesion	2.1	MPa
Tensile Strength	1.05	MPa
Angle of Internal Friction	49.0	degrees
Thermal Conductivity	2.1	W/m-K
Coefficient of Thermal Expansion	8.8×10^{-6}	K^{-1}
Specific Heat	932.0	J/kg-K

Table 2-3. Rock joint parameter values for scoping analysis

Parameters	Values	Units
Normal Stiffness	1.0×10^5	MPa/m
Shear Stiffness	1.0×10^5	MPa/m
Cohesion	0.08	MPa
Tensile Strength	0.04	MPa
Friction Angle	38.0	degrees

Based on the results of the scoping analysis, it was determined that the joint patterns did not appear to have a large impact on either magnitude or distribution of stresses [shown in results discussed in chapter 4 (section 4.1.2)]. However, it was generally observed that simulating three joint sets resulted in more fluctuation in the stress and in a slightly higher maximum stress magnitude. Similar agreement occurred in the displacement field for the various joint patterns as discussed in chapter 4 (section 4.1.1). Based on these results and also that simulation of three joint sets was much more computationally intensive, it was decided that for the final set of 64 UDEC TM runs [i.e., 1/8 fractional factorial plan (section 3.3)] only two joint sets would be simulated—one subvertical and one subhorizontal. Using only two joint sets would also allow incorporation of a higher joint frequency, which would be more representative of the subvertical joints. It was decided that for the final set of UDEC TM runs, the subvertical joint set spacing and the two joint set inclinations would be variable. The subhorizontal joint set spacings are much larger (on the order of meters in the field) and were thus chosen to remain constant at 1.25 m for all runs. The additional variable parameters (besides the joint pattern and thermal loading

for the final UDEC runs) included joint friction angle, intact rock cohesion, intact rock friction angle, intact rock Young's modulus, and thermal expansion coefficient. This choice of parameters was based partly on the observation that DOE published field data showed some parameters (e.g., joint cohesion and joint tensile strengths) had values measured close to zero. Selection of variable parameters was also based on past studies and literature reviews (e.g., Manteufel et al., 1993) concerning their importance in overall TM response. To limit the number of runs, the likely high and low extreme values were chosen based on the DOE RIB and other reports mentioned earlier. The variable parameters and their ranges for the final set of TM runs are presented in table 2-4. The remaining fixed parameters were similar to those used for the scoping calculations and are given in table 2-5.

Table 2-4. Range of variable parameters for final TM parametric study

Parameters	Upper Limit	Lower Limit	Units
Subvertical Joint Inclination	85.0	70.0	degrees
Subhorizontal Joint Inclination	20.0	10.0	degrees
Subvertical Joint Spacing	0.5	0.2	m
Joint Friction Angle	38.0	28.0	degrees
Thermal Loading	100	20	MTU/acre
Intact Rock Cohesion	43.0	18.0	MPa
Intact Rock Friction Angle	50.0	20.0	degrees
Intact Rock Young's Modulus	32.0	16.0	GPa
Thermal Expansion Coefficient	12.0×10^{-6}	6.0×10^{-6}	K^{-1}

Table 2-5. Fixed parameters for final TM parametric study

Parameters	Values	Units
Number of Joint Sets	2	-
Horizontal Joint Spacing	1.25	m
Poisson's Ratio	0.21	-
Density	2297.0	kg/m^3
Uniaxial Compressive Strength	166.0	MPa
Uniaxial Tensile Strength	5.0	MPa

Table 2-5. Fixed parameters for final TM parametric study (cont'd)

Parameters	Values	Units
Thermal Conductivity	2.1	W/m-K
Specific Heat	932.0	J/kg-K
Joint Normal Stiffness	1.0×10^5	MPa/m
Joint Shear Stiffness	1.0×10^5	MPa/m
Joint Cohesion	0.08	MPa
Joint Tensile Strength	0.04	MPa

2.2 THERMAL LOAD

For the 2D UDEC analysis, it was decided to analyze two bounding thermal loading strategies to limit the number of computational runs and vary other mechanical and thermal material properties as discussed in section 2.1. These two input thermal loadings included a high (100 MTU/acre) and a low (20 MTU/acre) level. The DOE current baseline thermal loading is approximately 84 MTU/acre. Heat generation due to decay of spent fuel within the waste package in the DOE in-drift configuration is modeled in UDEC as a thermal flux applied directly to the wall of the circular emplacement drift. In reality, heat transfer from the waste package to surrounding rock in an unbackfilled drift would consist of a combination of radiative heat transfer to the wall of the emplacement drift as well as conductive heat transfer to the tunnel floor through the waste package support system. Depending on whether the unbackfilled drifts are ventilated, heat transfer could also take place in the form of forced convection. Because Version 2.01 of UDEC is incapable of modeling cavity radiation (i.e., currently it is set up to handle only boundary radiation to an infinite domain), it was decided to neglect modeling of the waste package itself and apply the volumetric heat generation directly as a heat flux to the drift wall. In essence, the analysis neglects heat removal from ventilation. For this study, the age of the fuel within the MPC was assumed to be 20 yr old at the time of waste emplacement. The surface heat flux (in W/m^2) applied to the tunnel wall in the 2D UDEC models is calculated by dividing the total waste package heat output (W) by the circumferential perimeter of the drift and the waste package spacing. For UDEC analyses, emplacement drift diameter was taken to be 5 m.

Version 2.01 of UDEC currently allows a thermal flux boundary condition to be input as either a constant or simple exponentially decaying flux with a single decay coefficient of the form

$$q = q_o \exp(-\alpha t) \tag{2-1}$$

where q_o is the initial surface heat flux (W/m^2) applied to the drift wall at time of emplacement and α is the decay constant (1/s). In actuality, a number of exponentially decaying terms are usually required to model the heat generation rate. For instance, a recent DOE thermomechanical analysis (TRW Environmental Safety Systems, Inc., 1995) used a decaying source term with four decay coefficients. As a result, for the UDEC analysis, a best exponential fit using a single decay constant was made (as shown in figure 2-1) from a more general and realistic decay function (U.S. Department of Energy, 1987). Table 2-6 shows the values for q_o and α for different areal mass loadings obtained from the curve fitting

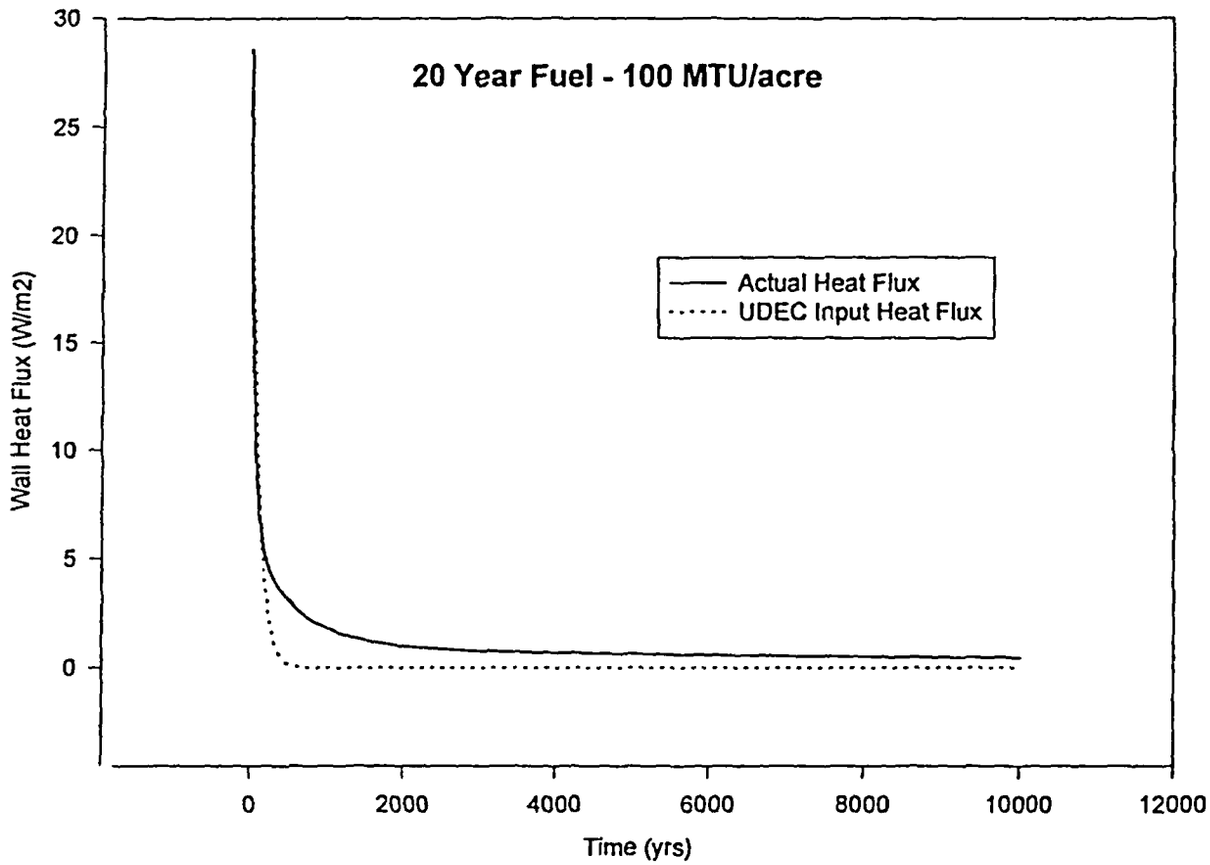

Figure 2-1. Heat flux from typical waste package assuming 20-year-old fuel at time of emplacement (solid line) as well as UDEC input based on a best exponential fit using a single decay constant. Note: Curves represent necessary 2D tunnel wall heat flux required to establish mass loading of 100 MTU/acre.

exercise, however as indicated previously, only areal mass loadings of 20 and 100 MTU/acre were considered in the analyses conducted.

Table 2-6. Heat flux decay parameters for 20-year-old fuel

Areal Mass Loading (MTU/Acre)	q_0 (W/m^2)	α (1/s)
100	28.570	3.2197×10^{-10}
80	25.459	3.2197×10^{-10}
40	15.260	3.2197×10^{-10}
20	10.163	3.2197×10^{-10}

Histories of tunnel wall temperatures calculated by UDEC based on use of the decaying heat flux given by Eq. (2-1) along with the decay coefficients for 100 and 20 MTU/acre thermal loadings are presented in figure 2-2. This figure shows peak wall temperatures of about 192 °C for the 100 MTU/acre thermal loading and 63 °C for the 20 MTU/acre thermal loading. The peak temperatures occur approximately 60-70 yr after emplacement.

As a check to determine how much error is incurred by neglecting the radiative heat transfer effects, an ABAQUS (Hibbitt, Karlsson, and Sorenson, Inc., 1995) model was set up to analyze radiative heat transfer within the emplacement drift. Based on a simplified in-drift waste emplacement geometry, a finite element mesh was created for the ABAQUS (Version 5.5) simulation, a portion of which is shown in figure 2-3. Using this geometry, a view factor matrix was created by ABAQUS to simulate the cavity radiation between the waste package and wall of the emplacement drift. The waste package was modeled as a lumped heat source. Conductive heat transfer was also allowed across the contact between the waste package and concrete invert segment. Figure 2-4a shows the temperature profile after 50 yr of heating (emissivities of 0.85 and 0.80 chosen for the rock and canister surface, respectively). The figure indicates that fairly uniform heating occurs around the drift, which supports the uniform wall flux approach chosen for the UDEC analyses. As shown in figure 2-4b, the peak wall temperature, calculated by ABAQUS is approximately 20 °C lower (i.e., approximately 172 °C). Thus, applying the thermal loading as a uniformly decaying heat flux around the tunnel perimeter as well as the exponential fit approach required for the UDEC analysis as discussed earlier results in overestimation of the calculated wall temperature by just over 10 percent.

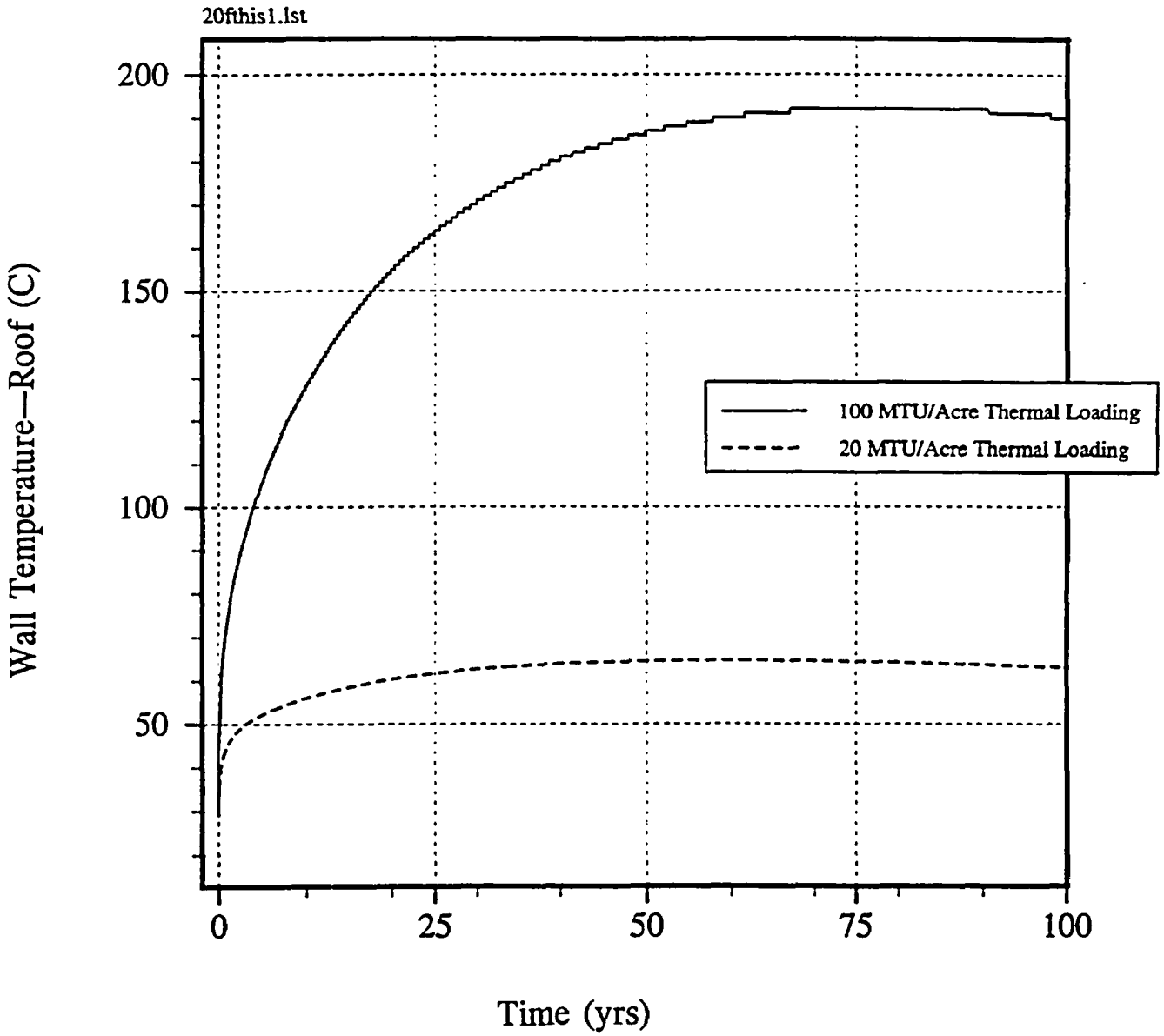

Figure 2-2. Wall temperatures calculated by UDEC for areal mass loadings of 100 MTU/acre and 20 MTU/acre assuming 20-year-old fuel

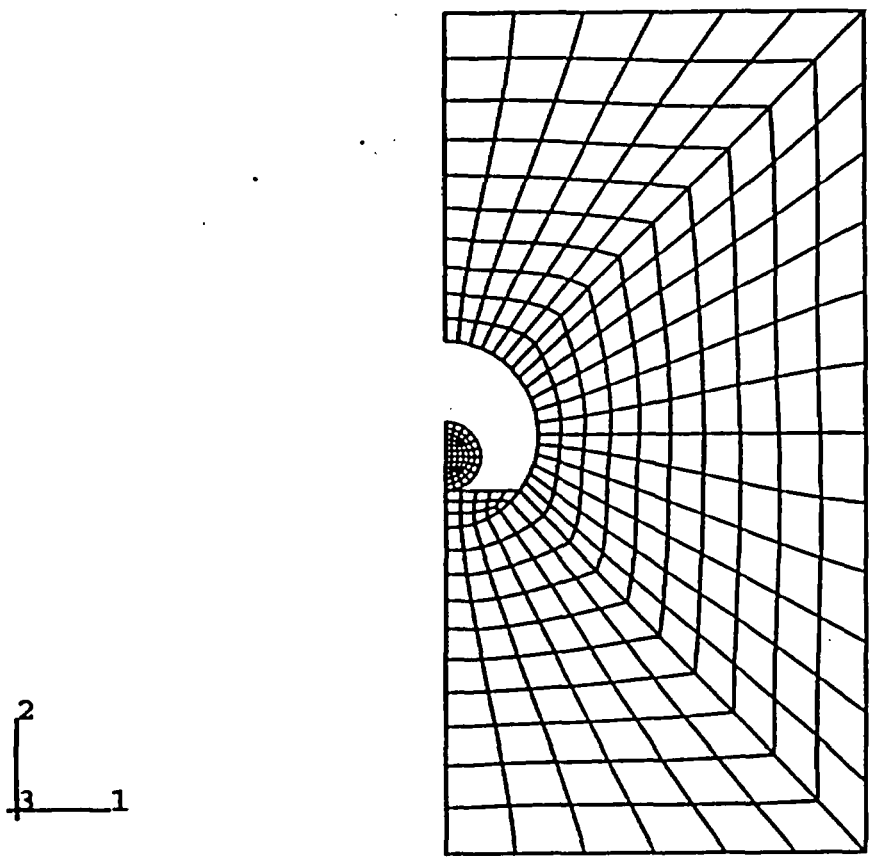

Figure 2-3. Portion of ABAQUS finite-element mesh for radiative heat transfer analysis

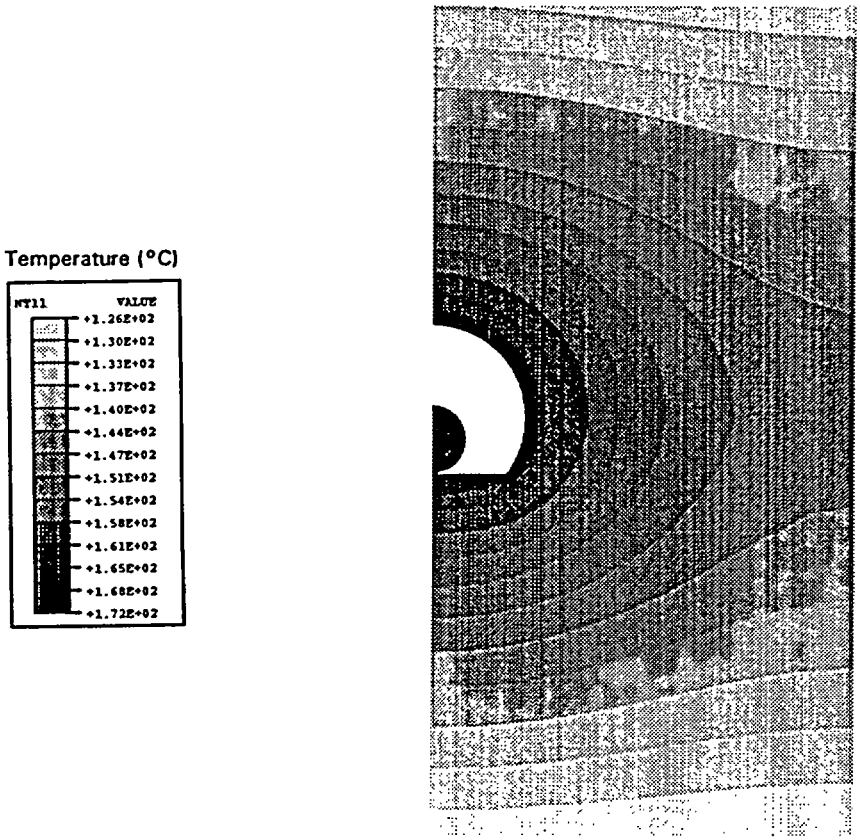

(a)

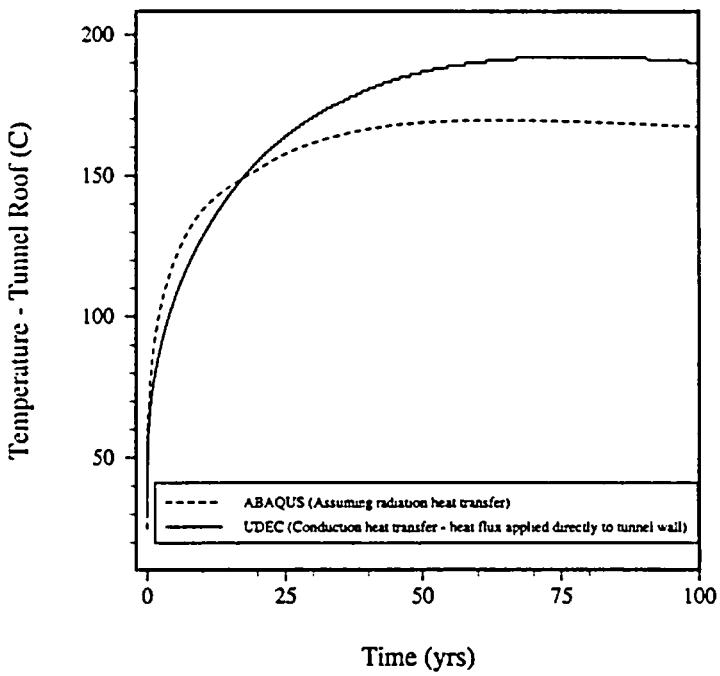

(b)

Figure 2-4. ABAQUS 2D radiative heat transfer analysis showing (a) temperature contours 50 yr after heating, and (b) comparison of tunnel roof temperature history with UDEC

3 THERMAL-MECHANICAL ANALYSIS

3.1 COMPUTER CODE

Version 2.01 of the 2D distinct element computer code UDEC was used to conduct a coupled TM analysis of one unbackfilled emplacement drift out of a series of parallel emplacement drifts within the repository block. UDEC has capabilities for effectively modeling the joint network. Specifically, the code can simulate relatively large shear displacements along block interfaces with proper redistribution of resulting stresses (Itasca Consulting Group, Inc., 1993).

3.2 NUMERICAL MODEL

3.2.1 Selection of Material Model

The Mohr-Coulomb plasticity formulation was selected for intact rock behavior in the TM analysis. This plasticity formulation consists of a yield function and plastic flow rule. The Mohr-Coulomb plasticity model represents a material that only yields in shear and is a conventional model for plasticity in rock mechanics. The shear yield surface corresponds to the Mohr-Coulomb criterion in which only the major and minor principal stresses are active in the formulation. The shear yield function f_s is defined as (Itasca Consulting Group, Inc., 1993)

$$f_s = \sigma_1 - \sigma_3 N_\phi + 2c\sqrt{N_\phi} \tag{3-1}$$

where $N_\phi = (1+\sin\phi)/(1-\sin\phi)$, ϕ is the friction angle, and c is the cohesion. Shear yield is detected if $f_s<0$. In this case plastic flow is allowed to occur to restore the condition $f_s=0$. In the Mohr-Coulomb plasticity formulation, a nonassociated flow rule is used, the formulation of which is discussed in depth in Itasca Consulting Group, Inc. (1993). Input properties for this plasticity formulation include the elastic bulk modulus, elastic shear modulus, mass density, cohesion, dilation angle, internal angle of friction, and tension limit.

Behavior of the joints was governed by a Mohr-Coulomb slip criterion based on user defined values for the joint cohesion, dilation angle, friction angle, and tensile strength. For this analysis, both the normal and shear joint stiffnesses were assumed to be constant.

3.2.2 Initial/Boundary Conditions

For the 2D UDEC models, vertical boundaries represented lines of symmetry based on the assumption of multiple parallel emplacement drifts within the repository. These vertical boundaries were located mid-way between the drifts depending on the areal thermal loading chosen, and assigned zero normal (e.g., x-direction) velocity as well as zero heat flux to account for mechanical and thermal symmetry. It was necessary to model the entire drift to avoid erroneously introducing symmetric joints on left and right halves of the drift. The lateral extent of the model is governed by the drift to drift spacing which itself depends on the areal thermal loading chosen. Typical drift and waste package spacings for various thermal loading strategies are listed in table 3-1, where areal thermal loading is given in units of MTU/acre.

Table 3-1. Drift and waste package spacings corresponding to range of thermal loadings

Areal Mass Loading (MTU/acre)	Drift Spacing (m)	Waste Package Spacing (m)
100.0	22.5	18.0
80.0	25.0	20.0
40.0	30.0	33.7
20.0	40.0	50.6

The drift and waste package spacings in table 3-1 lie within the ranges considered by DOE (TRW Environmental Safety Systems, Inc., 1994), however, DOE noted that the areal mass loadings of 20 and 40 MTU/Acre are less favorable since they lead to waste package spacings greater than the drift to drift spacings. The vertical extent of the UDEC models was determined so that the ambient temperatures applied along the upper and lower boundaries did not artificially impact the results for the total selected simulation time of 100 yr. The method suggested by St. John (1985) was used to determine the distance of influence of a single waste container on rock temperatures as a function of time to determine the vertical extent of the UDEC model. The equation for temperature change at a distance, R, from a decaying point source of initial strength, Q_o, is given by Christianson (1979) as

$$\Delta T = \frac{Q_0}{\pi^{3/2}} \exp(-At) \frac{\sqrt{\pi}}{4\kappa} \exp(-R^2/4\kappa t) \; Re[w\,(\sqrt{At} + \frac{iR}{\sqrt{4\kappa t}})] \tag{3-2}$$

where

i	=	imaginary number
A	=	thermal constant
κ	=	thermal diffusivity
t	=	time(s)
$w(z)$	=	complex error function
Re	=	real part of argument

It is seen that the temperature change decays from the point source approximately proportional to

$$\exp\,(-R^2/4\kappa t) \tag{3-3}$$

St. John (1985) suggested that $R^2/4\kappa t = 4$ is sufficient to ensure a small temperature change. This expression requires that

$$R \geq 4\sqrt{\kappa t} \tag{3-4}$$

where t is time in yr.

Applying the above equation to the present UDEC model for a simulation time period of 100 yr and a thermal diffusivity of 31.3 m^2/yr, the vertical extent of thermal influence, R, is determined to be approximately 225 m. Thus, in all the UDEC runs, both the upper and lower boundaries are located 225 m from the drift centerline.

The initial temperature at the repository horizon was selected at 29 °C (Christianson and Brady, 1989), with a gradient of 0.02 °C/m. The *in situ* vertical stress at the repository horizon was taken to be 7.0 MPa (Christianson and Brady, 1989) with a gradient of 0.0225 MPa/m. The *in situ* horizontal stress, σ_h, was assumed to be related to the vertical stress, σ_v, by the following equation

$$\sigma_h = \frac{\nu}{(1 - \nu)} \sigma_v \tag{3-5}$$

where ν is the Poisson's ratio and the horizontal gradient was determined to be 0.0059 MPa/m.

3.2.3 Model Setup

To maintain a reasonable number of blocks and finite difference zones, only a region approximately one tunnel diameter into the rock mass was modeled as having the specified joint spacings assigned for each case. Beyond this region, primarily because of the fairly small subvertical joint spacings (i.e., 0.2 and 0.5 m), it was necessary to scale up the size of the blocks as depicted in figure 3-1. The very far-field region, needed to allow propagation of heat over the 100 yr heating period, consisted of even larger discrete element blocks. Zoning of the individual blocks was also scaled accordingly. Rock support around the emplacement drift was neglected for this study and the study only considered the unbackfilled scenario (i.e., preclosure period up to 100 yr of operation). As a conservative analysis, the emplacement drifts were assumed to be nonventilated.

3.2.4 Solution Scheme

The analysis scheme consisted of first obtaining model equilibrium under the *in situ* applied stresses. Once accomplished, the tunnel blocks were excavated and a new equilibrium stage was reached. At this stage, the mechanical time was reset to zero for the TM analyses. In conducting a TM analysis, UDEC uses a sequential coupling approach as depicted in figure 3-2. This approach consists of running the thermal analysis for a period of time during which nodal or gridpoint temperatures are updated. The thermal time is then held fixed while mechanical cycling is conducted to update zone stresses, nodal displacements, block rotations, etc. to reach a new mechanical equilibrium with this thermal state. In such analyses, thermal time is the actual simulation time while the mechanical time is more of a pseudo-time for the intermediate calculations. For the TM analyses conducted here, the thermal time increments between mechanical cycling started out at one week, gradually progressing to a month and eventually to 1 yr for the first 5 yr of the analyses mainly because of the large gradient in the decay function as shown in section 2.2. During later stages of the 100 yr TM analyses, thermal increments were increased to 25 yr as a result of much smaller temperature gradients throughout the model. An implicit thermal solution scheme based on the Crank-Nicholson method (Itasca Consulting Group, Inc., 1993) was chosen allowing the user to specify a thermal time-step. Although this method is flexible, it is not completely arbitrary since a stability criteria for the implicit method must be satisfied. For the set of analyses conducted in this study, the maximum allowable thermal time-step within each thermal increment varied greatly among the various runs. For the cases run with low thermal loadings, thermal time-steps on the order of days

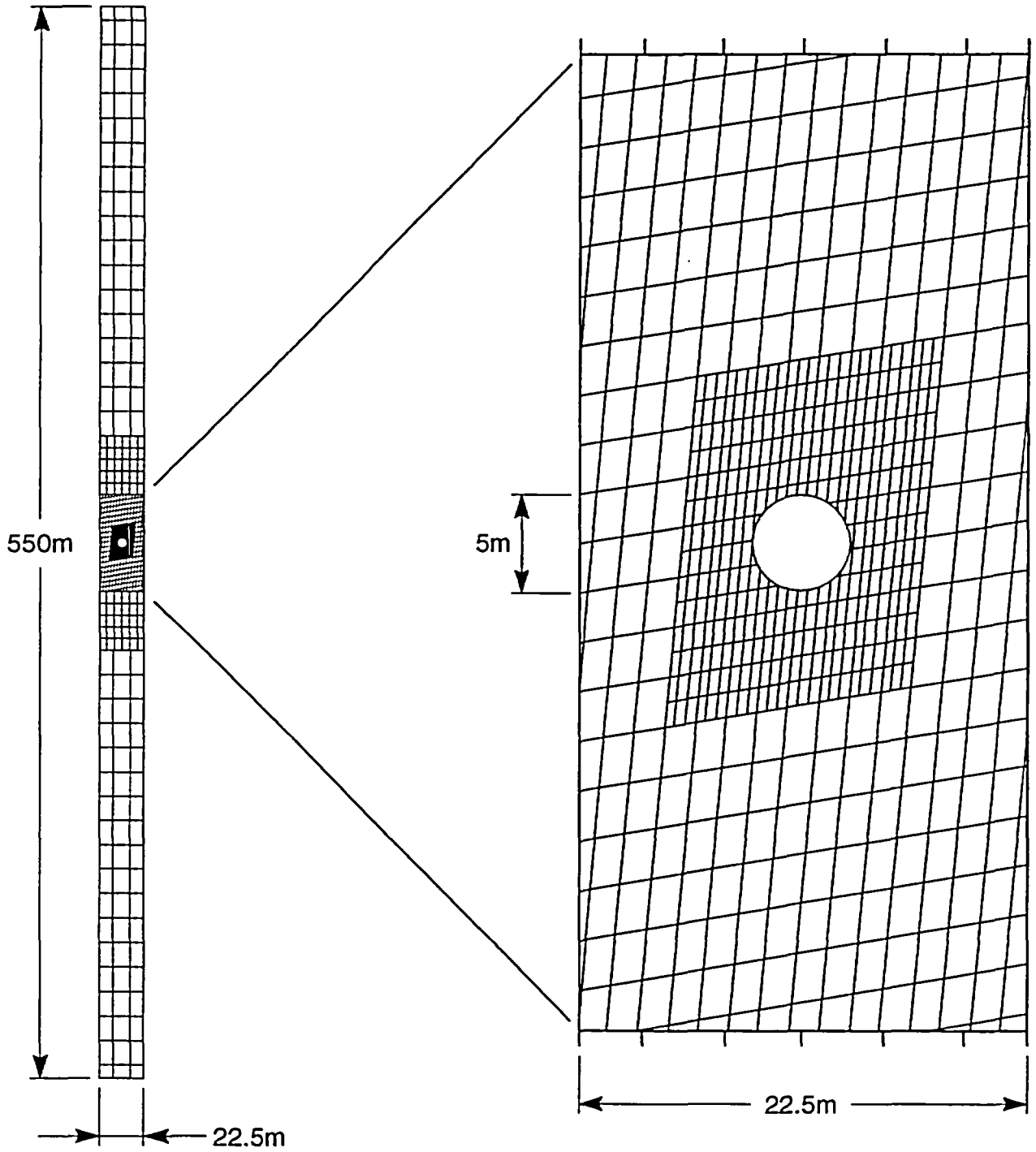

Figure 3-1. UDEC model showing block geometry for one particular joint set pattern and thermal loading

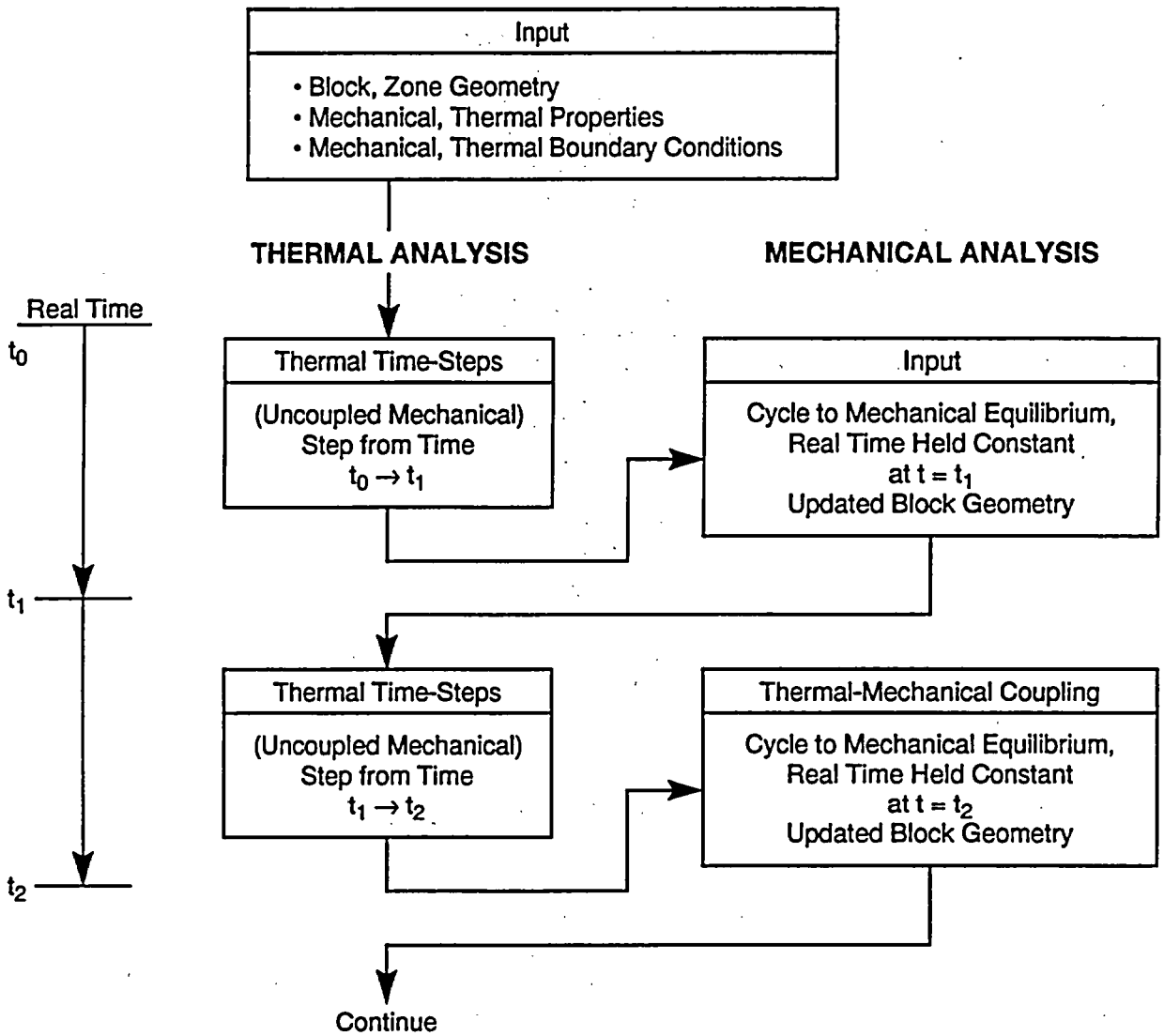

Figure 3-2. Method of running a coupled thermal-mechanical simulation with UDEC (Board, 1989)

and possibly greater were allowed. However, for the high thermal loading cases, thermal time-steps had to be reduced as low as 0.5 hrs for the entire 100-yr TM simulation. As a result, run times varied from an overnight job to several days depending on the thermal loading scheme and type of computer (i.e., Sun Sparcstations or 486 IBM compatibles).

The reason for the small thermal time-steps for the cases run with high thermal loadings was likely due to increase in plastic yielding around the drift, especially those specified with high thermal expansion coefficients and low intact block strength properties. Also, it is recommended for UDEC plasticity calculations (Itasca Consulting Group, Inc., 1993) that the finite difference zones within a block be generated so that the zones all share a common central gridpoint for more accurate plasticity results. Meeting this criterion was not possible in this study for those blocks immediately surrounding the tunnel due to their irregular shapes. Consequently, some accuracy in the results for the plastic stress state were sacrificed and it is not clear whether the inability to meet this zoning criterion for some blocks affected the thermal time-step. Finally, it should be noted that in the near-field region of the emplacement drift, blocks were separating and in some cases falling into the tunnel which could have again affected the thermal time-step, since the thermal analysis scheme assumes the material to be a continuum. This problem was somewhat mitigated by specifying a larger thermal tolerance parameter in UDEC, which essentially still lumps two contacts or gridpoints together as a single gridpoint for the thermal calculation even though mechanically they have separated. During the simulation, those blocks that were beginning to fall into the tunnel could have easily been deleted from the analysis, however, the thermal flux (applied over a thin annular region encompassing the nodes along the perimeter of the tunnel) would have been altered since the total required flux assumes that it is applied over all the circular tunnel segments. During the analysis, mechanical cycling was done to reach equilibrium within the rock mass except for those few unstable tunnel blocks. As a result, those unstable blocks around the tunnel did not have a chance to move much even though they had a finite velocity and carried no mechanical stress. Thus, the thermal flux could still be applied to those blocks to generate the required areal thermal loading. There were some fluctuations in the wall temperatures of 10-20 degrees indicating that some of the unstable blocks may have displaced outside the annular heat flux region resulting in a discontinuity in the flux applied around the circumference of the tunnel. The small variances in these temperatures were believed not to have a great effect on the overall TM response of the rock mass, since this fluctuation in temperature near the tunnel wall represents only approximately 5 percent of the peak wall temperature of 190 °C.

3.3 DESIGN OF 2^k FRACTIONAL FACTORIAL EXPERIMENTS

As discussed earlier, the purpose of this analysis was to perform a parametric study on and identify important parameters that may affect the stability of the emplacement drifts under heated conditions. To achieve this goal, a large number of parameters would need to be examined and their impacts assessed. As a result, the number of numerical runs could be exceedingly large and complex if all possible effects of these parameters and, to the extent reasonable, their potential interactions were to be evaluated adequately. These large numbers of runs were not practical given the constraints of resources and time. Therefore, it was necessary to use a systematic approach so that meaningful work could be completed within the constraints. Toward this end, the concept of a 2^k fractional factorial experimental design was adopted in this study.

In this study, 10 parameters were identified to have potential effects on the behavior of underground excavations at the proposed repository site. These parameters were number of joint sets, subvertical and subhorizontal joint inclinations, subvertical joint spacing, joint friction angle, thermal

load, intact rock cohesion, intact rock friction angle, intact rock Young's modulus, and thermal expansion coefficient. Horizontal joint spacing was not included because, based on the current understanding, horizontal spacing is large (i.e., a few meters). Consequently, it was our judgment that its impact might be relatively small compared to subvertical joint spacing which is a fraction of a meter. Another consideration was that too many parameters might make this study unmanageable. Number of joint sets was not included in the development of a numerical modeling plan because it may substantially change the block size of UDEC models such that comparison between results from a UDEC run with a large number of joint sets and those with a small number of joint sets becomes difficult, if not impossible. Consequently, only nine parameters were included in the design.

With nine parameters chosen for the study ($k = 9$), a full 2^k factorial plan requires 512 UDEC runs. While it was desirable to adopt this modeling plan so that each interaction between parameters allows only a degree of freedom, it may not be necessary since certain interactions may not be of interest or may be negligible. Furthermore, the available resources and time did not support this level of effort. Therefore, it was decided to use a fractional factorial experiment approach in which one-eight of the total factorial plan was actually carried out. A detailed discussion regarding the 1/8 fraction of the 2^k factorial experimental design is provided in appendix A.

4 RESULTS AND DISCUSSIONS

As described in chapter 3, 74 UDEC runs were performed during FY96 TM analyses, including 10 scoping runs and 64 final runs. The scoping runs were aimed at identifying the effects of joint patterns on near-field thermal-mechanical responses. The final runs were based on a fractional factorial experiment design methodology to systematically probe the effects of joint patterns and thermal and mechanical parameters. UDEC modeling results are presented and discussed in this section. Section 4.1 discusses results from 10 scoping runs. Section 4.2 presents results of 64 final runs in a general way. Section 4.3 presents and discusses the results from analyses of fractional factorial experiments. Some output parameters from numerical modeling have been considered as performance measures for the factorial analyses based on observation of general results and engineering judgment. The observations are used both in discussing the general results in section 4.2 and in assessing the effects of input parameters on drift stability in section 4.3.

4.1 DISCUSSION OF UDEC SCOPING RUN RESULTS

As discussed in section 2.1, the 10 UDEC scoping runs were designed to isolate that the effects of input parameters related to joint patterns and thermal loads. Decisions regarding fractional factorial runs were made and the important parameters were selected based on the results of scoping runs. This section discusses some of the results from the scoping runs. For the scoping analysis, a total of five different joint patterns were analyzed, each under thermal loadings of 20 and 100 MTU/acre. Table 2-1 lists different joint patterns noted by the letters A, B, C, D, and F in the file names for a particular run.

4.1.1 Effect of Thermal Load and Joint Pattern on Displacement

Figure 4-1 compares vertical displacement after 100 yr of heating along a vertical section through the model centerline above the tunnel for five different joint patterns considered in the scoping run cases (see table 2-1) for the thermal load of 100 MTU/acre. Distribution of vertical displacement for different joint patterns is similar (i.e., upward expansion increases with extended vertical distance from the tunnel). However, the magnitude of vertical expansion is slightly different for different joint patterns. Vertical expansion at a given depth is the largest for joint pattern F (ubiquitous joint model with a subvertical and a subhorizontal joint set, see table 2-1) and is the smallest for joint pattern B (a subvertical and a subhorizontal joint set with inclinations similar to those in joint pattern F, see table 2-1). For the thermal load of 20 MTU/acre, vertical displacement at a given depth is the highest for joint pattern A and the lowest for joint pattern C (figure 4-2). Figures 4-1 and 4-2 show that the effect of joint pattern on the magnitude of vertical displacement is rather arbitrary and not consistent for the high and low thermal load strategies considered in this analysis (i.e., 100 MTU/acre and 20 MTU/acre).

Figures 4-3 compares vertical expansion for different thermal loads for a specific joint pattern C. This figure indicates that higher thermal load results in greater vertical expansion. In general, the maximum vertical expansion of the high thermal load (100 MTU/acre) is about five times greater than that of the low thermal load (20 MTU/acre).

Figures 4-4 and 4-5 compare vertical displacements at the roof and floor, respectively, as a function of time for different joint patterns for the thermal load of 100 MTU/acre. Although different joint pattern produces different roof and floor displacements, the effect of joint pattern on roof displacement is not consistent with its effect on floor displacement. The ubiquitous model (joint pattern F)

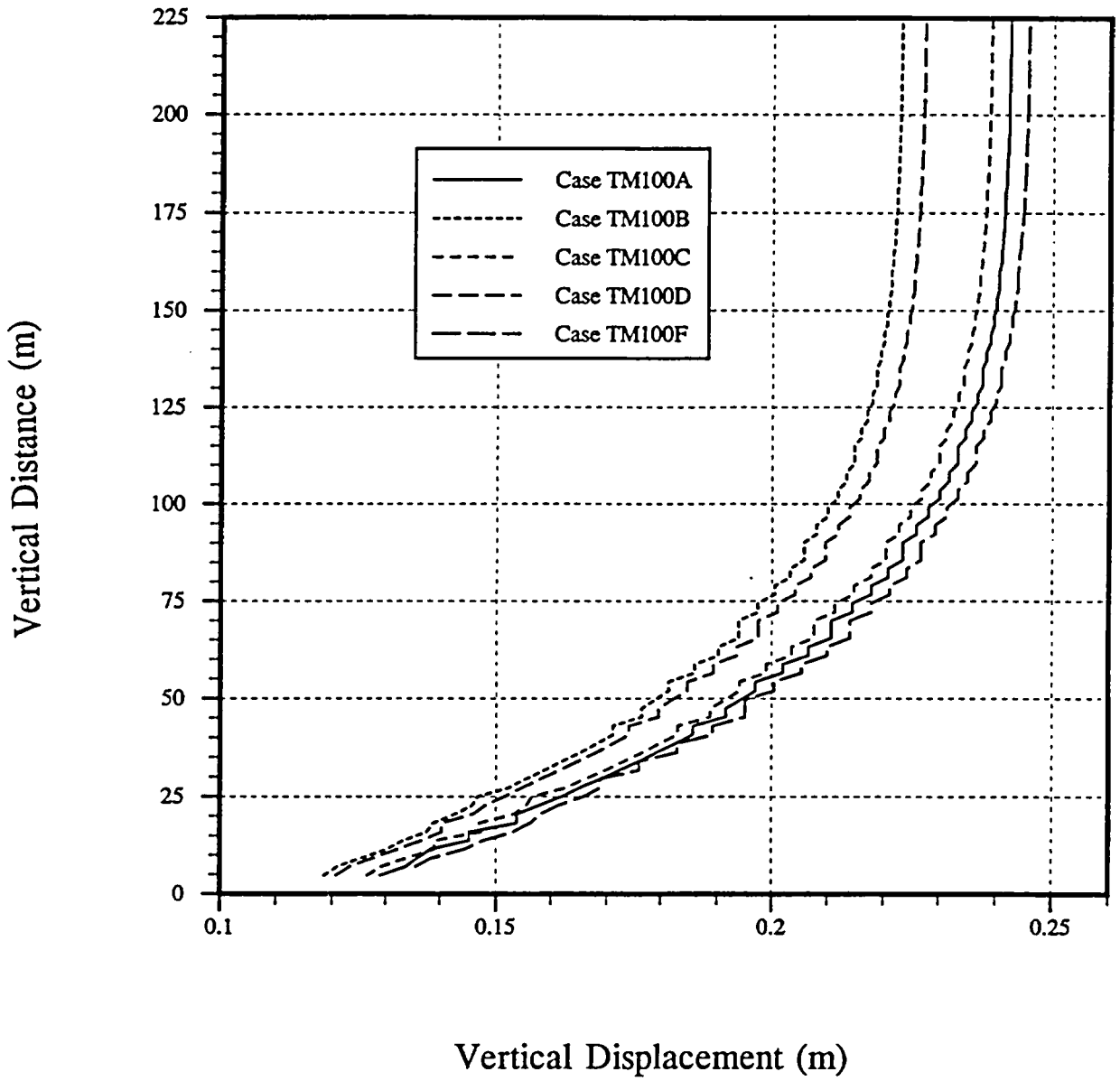

Figure 4-1. Vertical displacement after 100 yr of heating along a vertical section through model centerline above the tunnel for different joint patterns for 100 MTU/acre thermal load

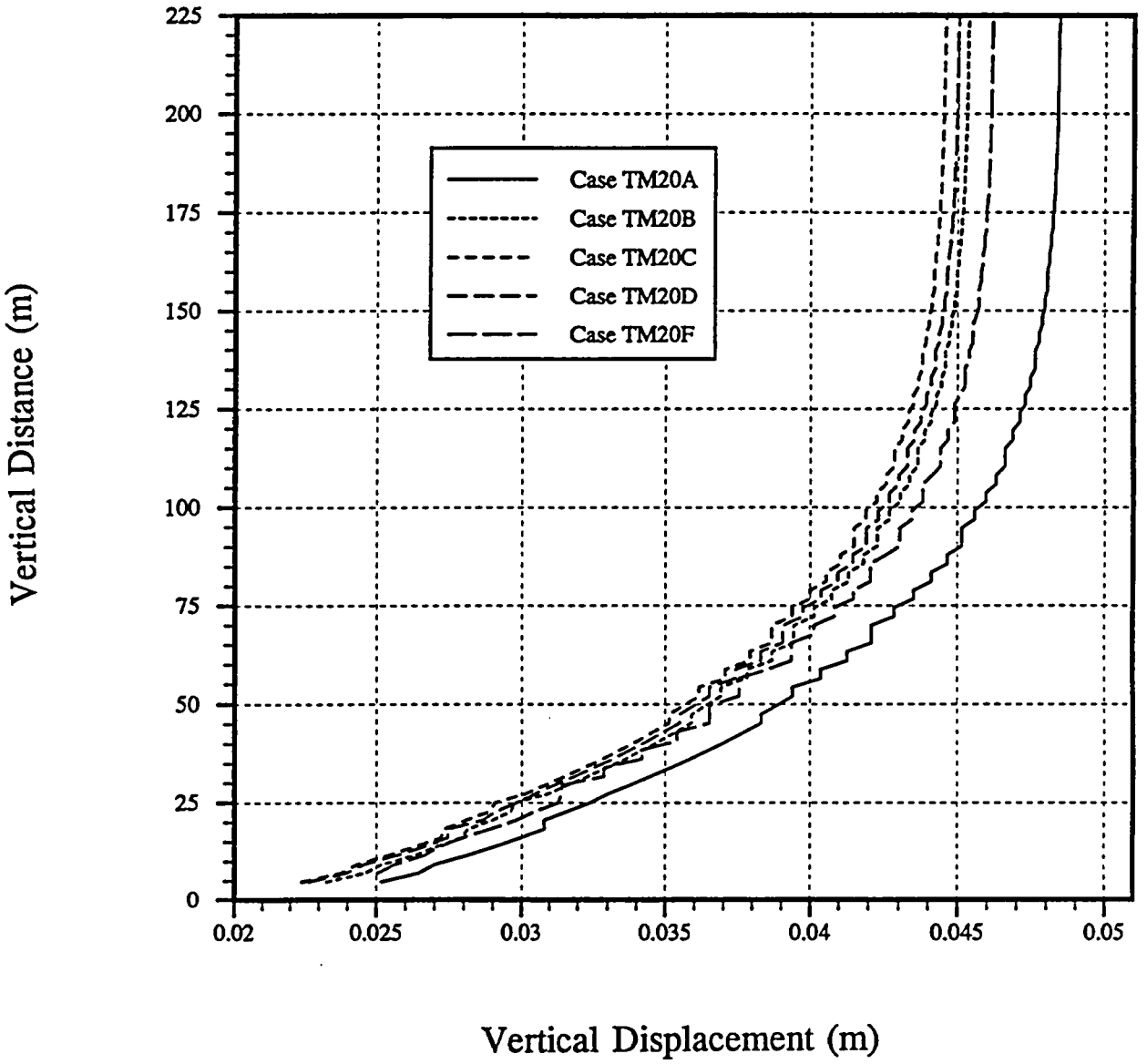

Figure 4-2. Vertical displacement after 100 yr of heating along a vertical section through model centerline above the tunnel for different joint patterns for 20 MTU/acre thermal load

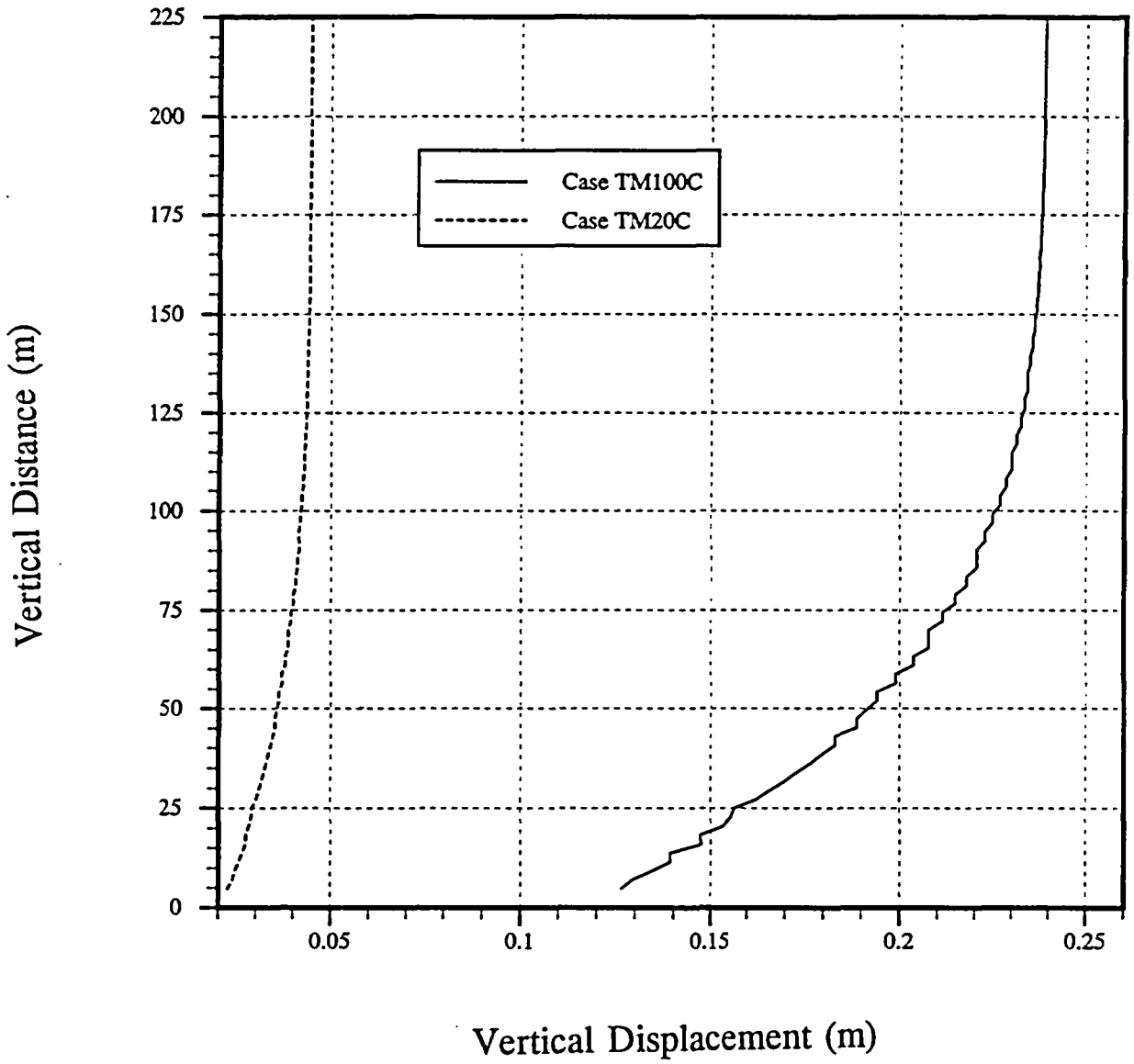

Figure 4-3. Vertical displacement after 100 yr of heating along a vertical section through model centerline above the tunnel for joint pattern C

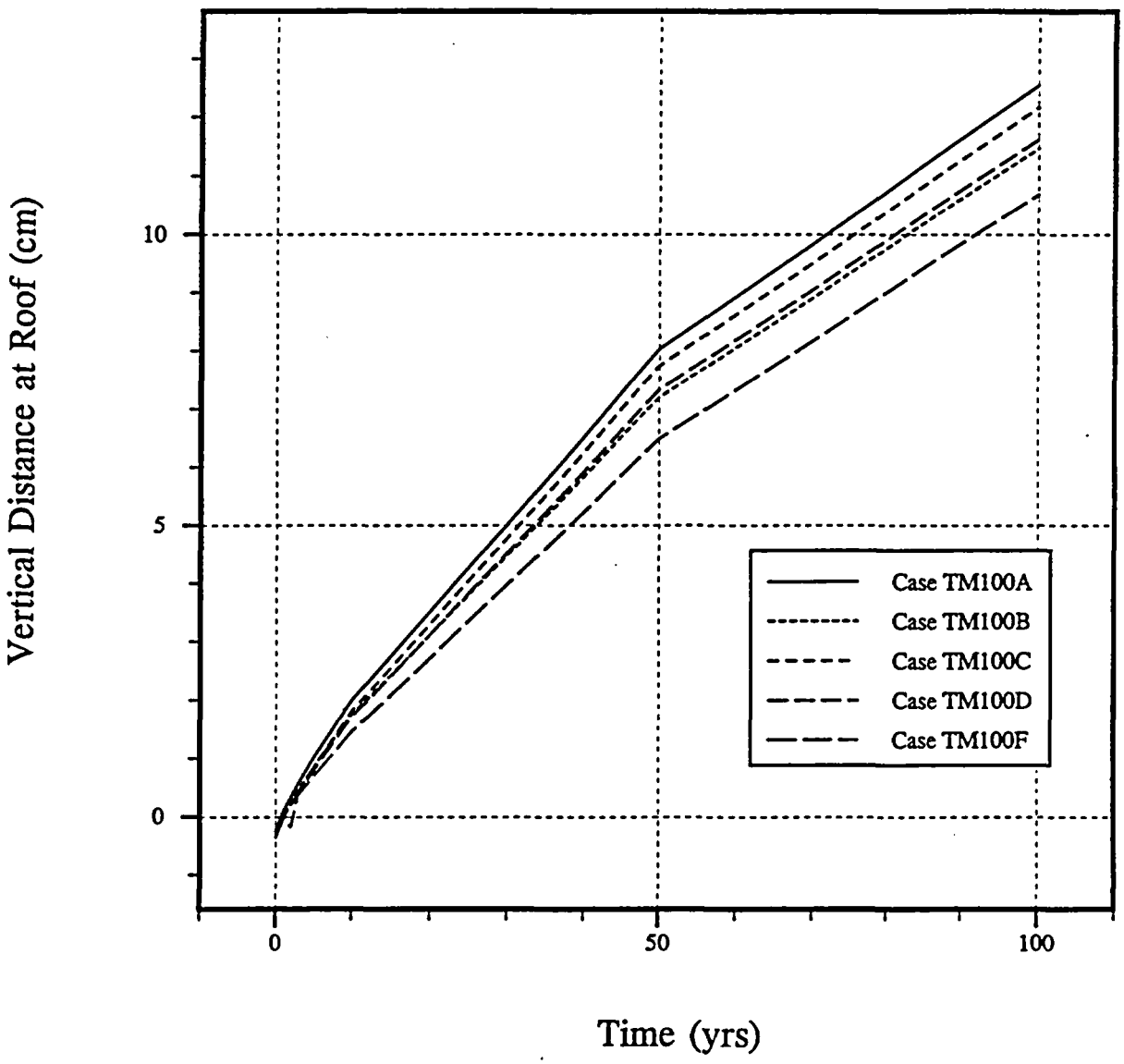

Figure 4-4. Vertical displacement at roof as a function of time for different joint patterns for the thermal load of 100 MTU/acre

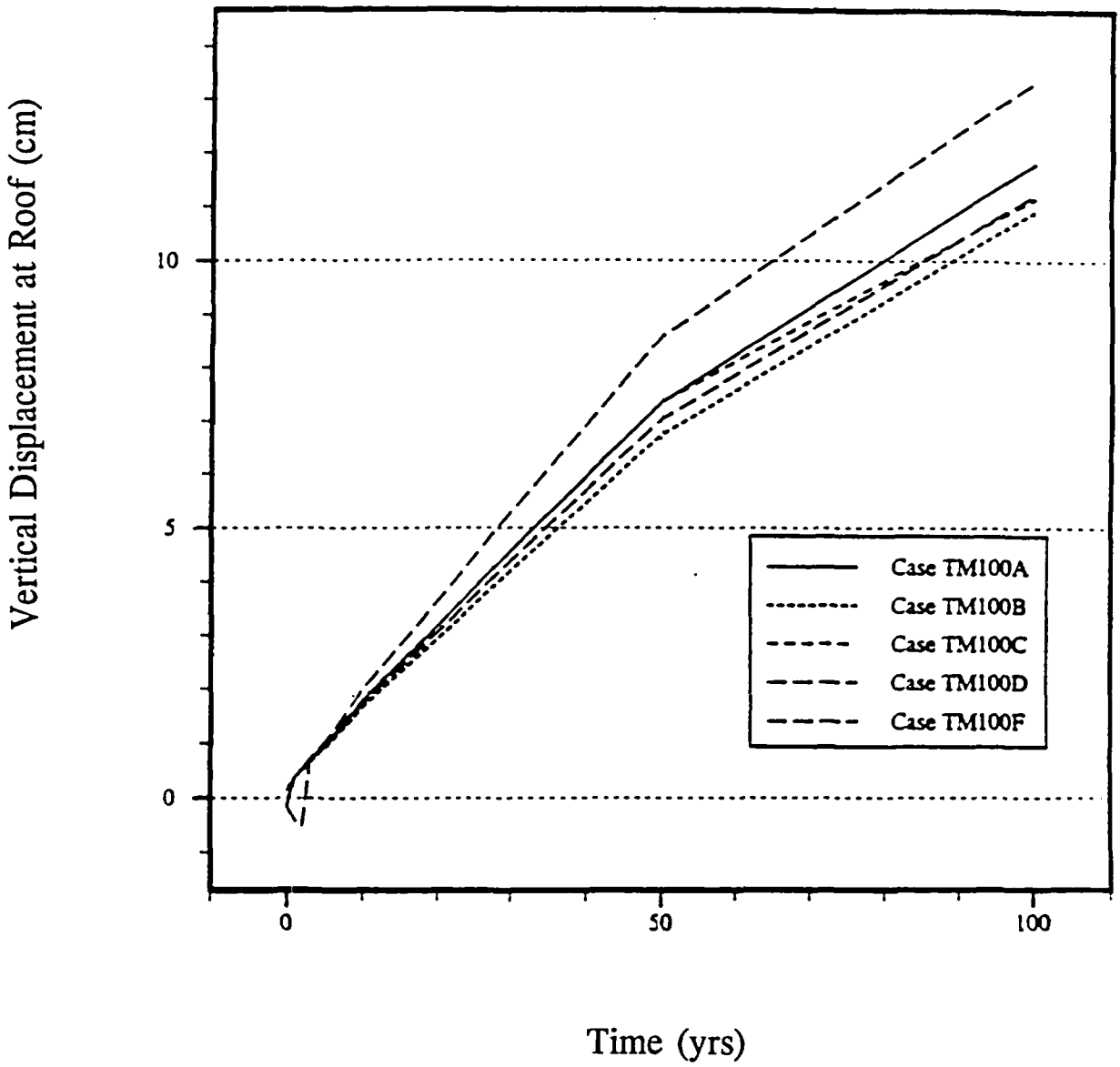

Figure 4-5. Vertical displacement at floor as a function of time for different joint patterns for the thermal load of 100 MTU/acre

has the largest floor displacement and the smallest roof displacement, resulting in drift convergence (see table 4-1). For all other joint patterns, the difference between roof and floor expansion is rather nominal, although in general, the roof expands slightly more than the floor, resulting in drift divergence. Figures 4-6 and 4-7 compare vertical displacement at the roof and floor, respectively, as a function of time for different joint patterns for the thermal load of 20 MTU/acre. Joint patterns show larger effect on roof displacement than on floor displacement. An interesting observation for this low thermal loading strategy, rather different from the high thermal loading strategy, is that floor displacement is always larger than roof displacement (see table 4-1), resulting in drift convergence. Also, joint pattern F behaves in a way similar to other cases. These observations show that the effect of thermal loading and joint pattern on drift convergence is rather complicated. In general, thermal loading reduces drift convergence or causes the roof and floor of the drift to diverge, depending on rock mass deformability and the level of thermally induced rock expansion. For example, a sufficiently high thermal loading causes the drift in explicit joint models (joint patterns A through D) to diverge after 100 yr of heating, while a drift in the ubiquitous joint model continues to converge. This observation is consistent with the fact that an ubiquitous joint model produces greater rock mass deformability. Also, in all joint models under the low thermal loading, the drift continues to converge, i.e., decrease in diameter after 100 yr of heating, signifying that the thermally induced rock expansion is not great enough to compensate mechanically induced convergence.

Table 4-1. Comparison of roof, floor, and maximum joint shear displacement for scoping runs

Case	Roof Displacement (cm)		Floor Displacement (cm)		Maximum Joint Shear Displacement (cm)	
	Excavation	100 yr	Excavation	100 yr	Excavation	100 yr
TM100A	−0.23	12.55	0.16	11.82	0.80	1.06
B	−0.26	11.48	0.17	10.93	0.20	1.40
C	−0.34	12.17	0.16	11.17	0.37	1.47
D	−0.35	11.63	0.16	11.24	0.38	16.00
F	−0.29	10.69	0.14	13.36	0.30	1.70
TM20A	−0.21	2.41	0.17	2.52	0.19	16.87
B	−0.23	2.21	0.18	2.40	0.26	7.93
C	−0.29	2.12	0.20	2.40	0.54	7.59
D	−0.30	2.13	0.19	2.44	0.38	1.92
F	−0.25	2.23	0.17	2.44	0.34	3.0

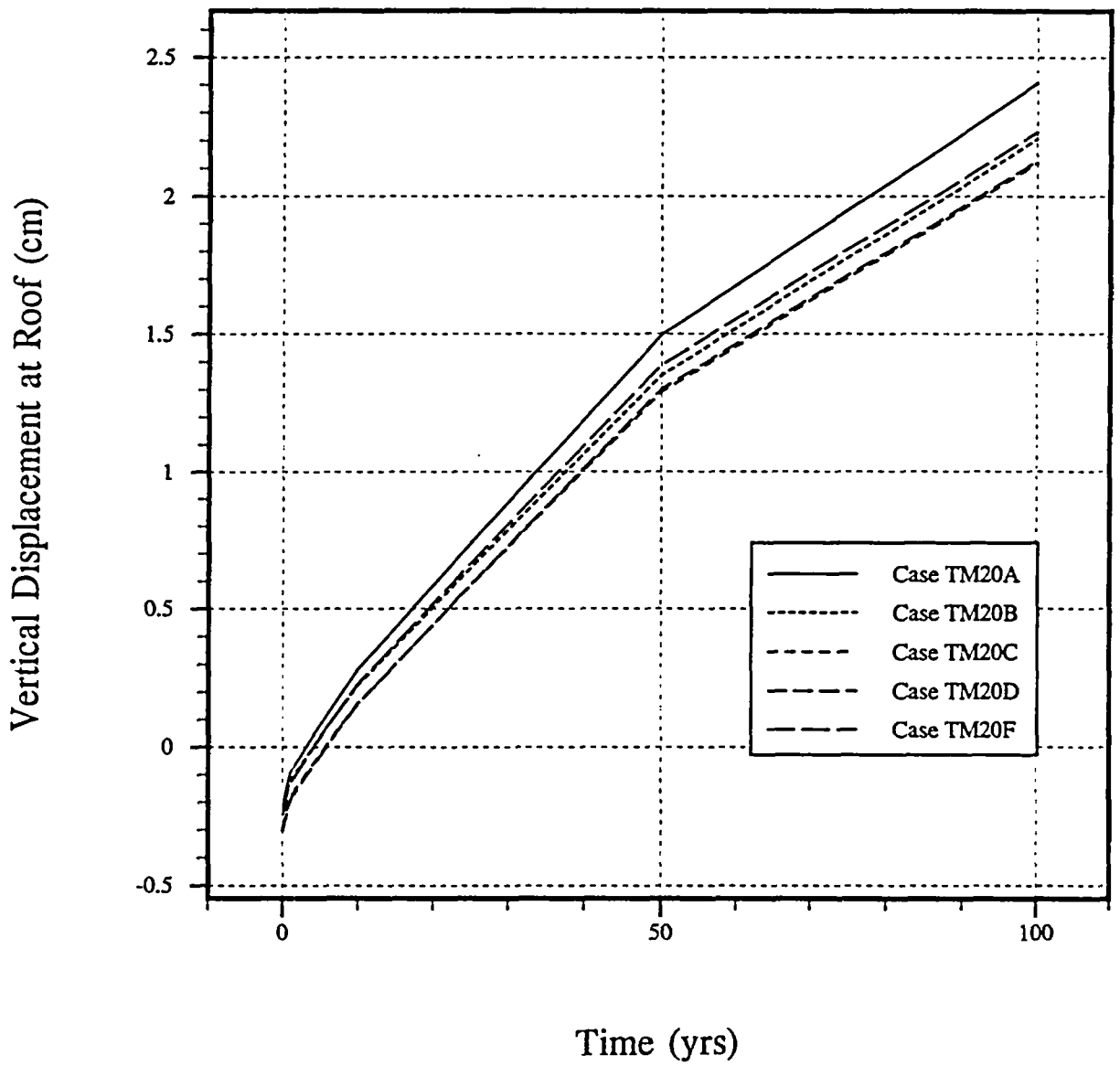

Figure 4-6. Vertical displacement at roof as a function of time for different joint patterns for the thermal load of 20 MTU/acre

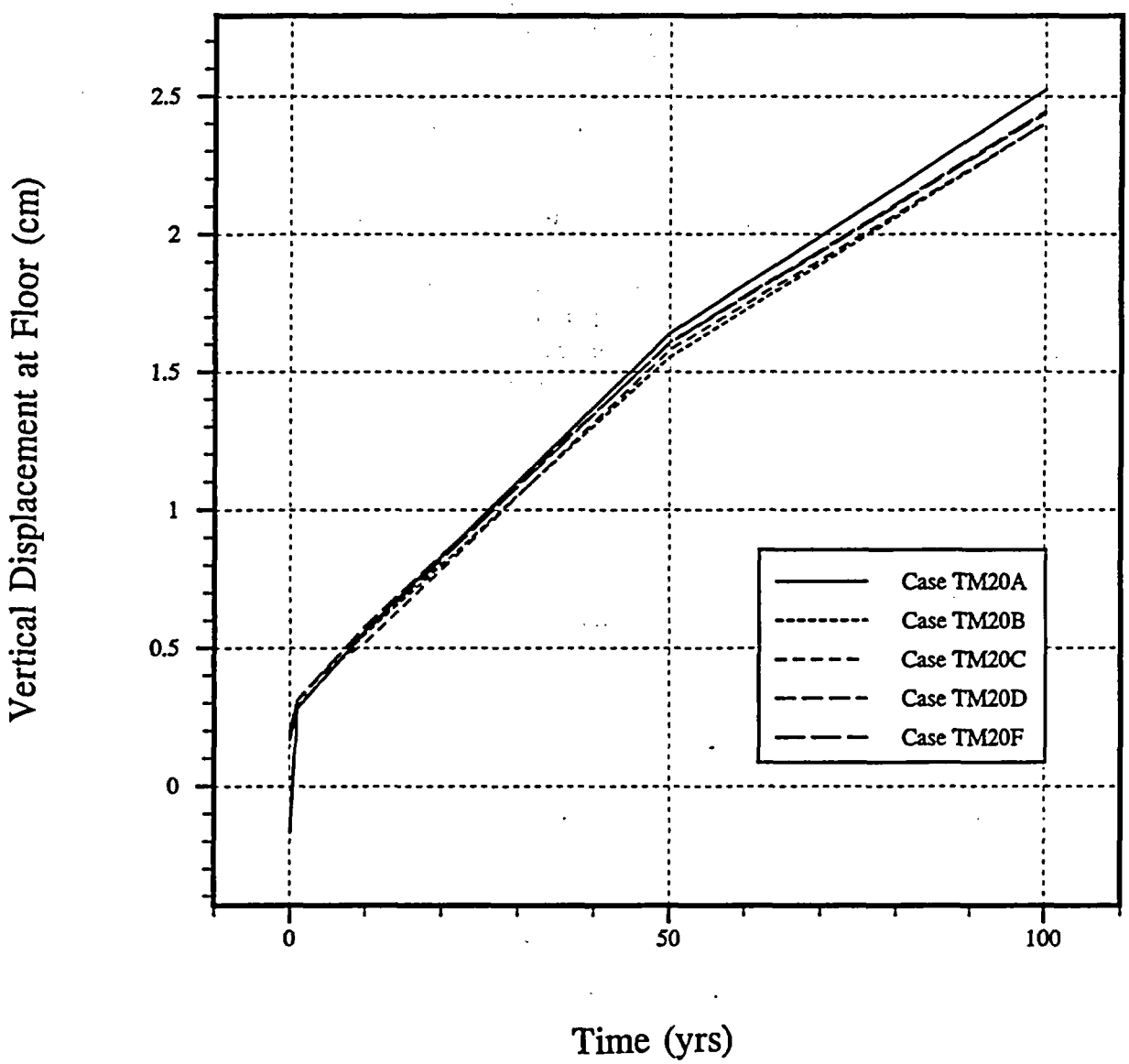

Figure 4-7. Vertical displacement at floor as a function of time for different joint patterns for the thermal load of 20 MTU/acre

Table 4-1 compares roof displacement, floor displacement, and maximum joint shear displacement after excavation and 100 yr of heating for different joint patterns and thermal loads. This table shows that joint pattern D has the highest maximum joint shear displacement for 100 MTU/acre thermal loading and joint pattern A has the highest maximum joint shear displacement for 20 MTU/acre thermal loading. These maximum joint shear displacements are mainly due to falling of blocks at drift ribs in these models. Joint shear displacement after 100 yr of heating is, in general, an order of magnitude higher than joint shear displacement immediately after excavation. Neither the magnitude of thermal loads nor joint patterns appear to have altered the maximum joint shear displacement in a consistent way.

4.1.2 Effect of Thermal Load and Joint Pattern on Stresses

Figure 4-8 compares horizontal stress after 100 yr of heating along a vertical section through the tunnel for different joint patterns for the 100 MTU/acre thermal loading. Differences in joint patterns do not seem to significantly affect either the magnitude or distribution of horizontal stresses, except in the immediate roof and floor where stress fluctuates considerably due to the existence of joints. Similar effects can also be observed in the case of 20 MTU/acre thermal loading (figure 4-9). It appears that the more complex the joint pattern, the more fluctuation in the stress and the higher the maximum tensile stress magnitude (see table 4-2).

Table 4-2. Maximum compressive and maximum tensile stresses for scoping runs

Case	Maximum Compressive Stress (MPa)		Maximum Tensile Stress (MPa)	
	Excavation	100 yr	Excavation	100 yr
TM100A	15.0	86.0	0.7	1.5
B	11.5	75.0	0.7	4.0
C	20.0	63.0	1.6	6.4
D	20.0	61.0	1.5	5.0
F	13.0	56.2	0.0	0.0
TM20A	14.9	21.7	0.8	0.8
B	10.9	19.4	0.8	1.0
C	21.3	19.2	1.1	3.0
D	18.7	16.6	1.4	3.4
F	13.7	22.3	0.0	0.0

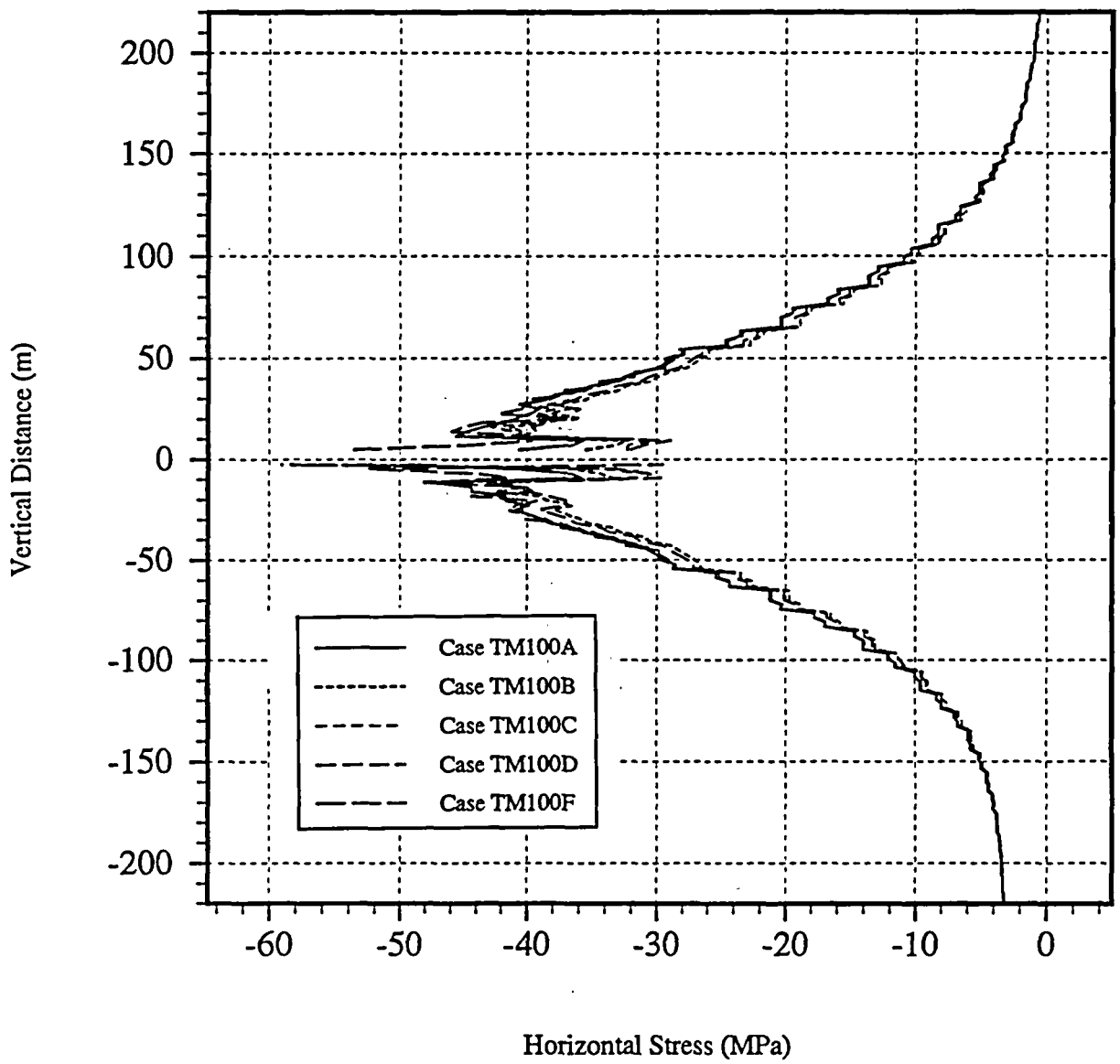

Figure 4-8. Horizontal stress after 100 yr of heating along a vertical section through the tunnel for the thermal loading of 100 MTU/acre

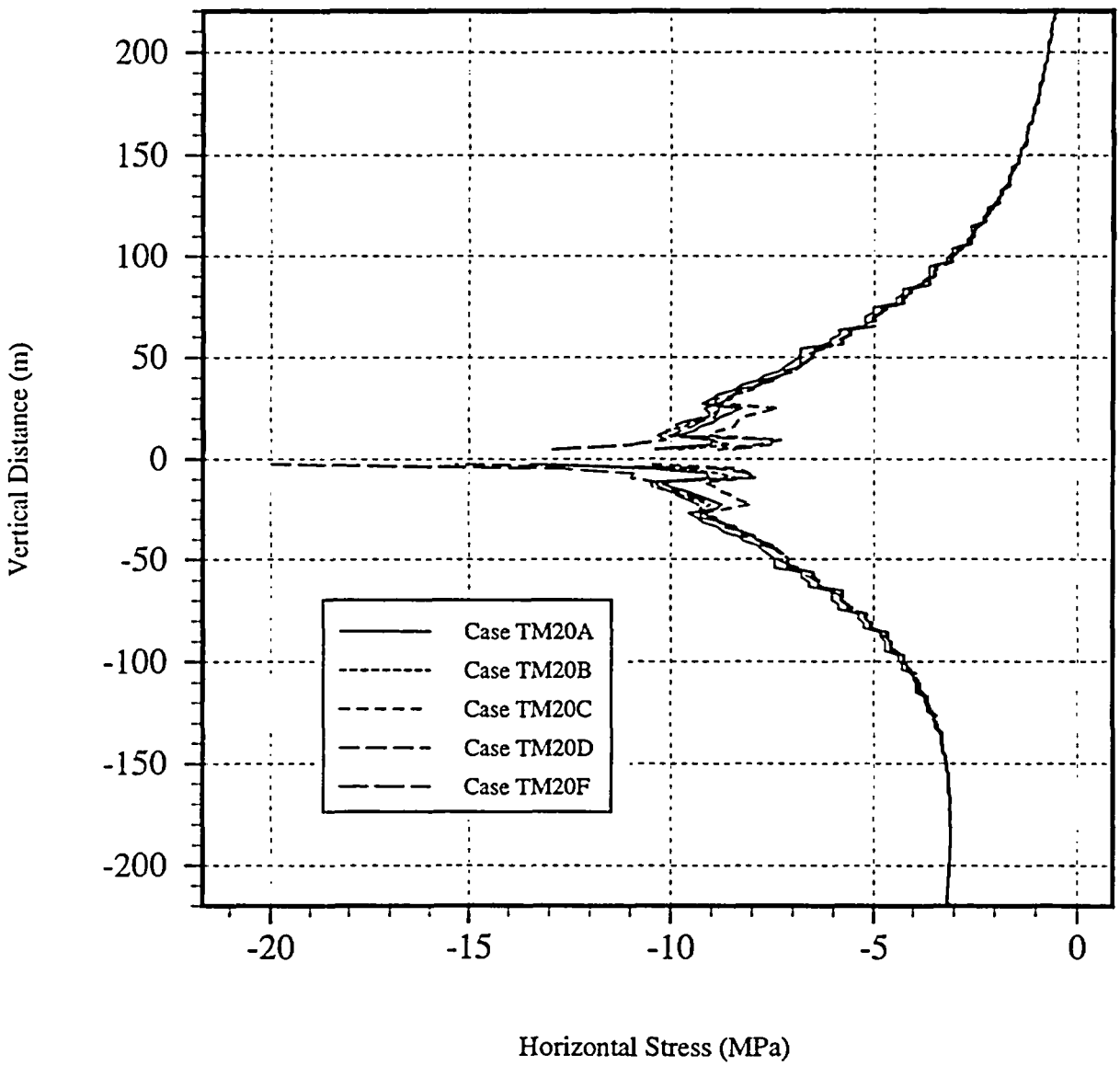

Figure 4-9. Horizontal stress after 100 yr of heating along a vertical section through the tunnel for the thermal loading of 20 MTU/acre

Figure 4-10 compares horizontal stress along a vertical section through the tunnel resulting from 100 yr of heating at the 100 MTU/acre and 20 MTU/acre loading cases for joint pattern C. In general, increasing thermal load from 20 MTU/acre to 100 MTU/acre increases horizontal compressive stress four to six times in the roof and floor areas. Similar observations apply to other joint patterns.

Figure 4-11 compares vertical stress after 100 yr of heating along a horizontal section through the tunnel for different joint patterns for 100 MTU/acre thermal loading. Because of the short distance and high fluctuation in the magnitude of the vertical stresses, it is difficult to observe the effect of joint pattern on the magnitude and distribution of stresses. Figure 4-12 presents information for 20 MTU/acre thermal loading. This figure shows that joint pattern does not significantly alter the trend of vertical stress distribution along this horizontal section. However, it appears that the simpler joint patterns (e.g., joint patterns A and B) result in smoother stress curves. Different joint pattern does result in different stress magnitude close to the drift wall.

Figure 4-13 compares vertical stress after 100 yr of heating along a horizontal section through the tunnel resulting from the 100 MTU/acre and 20 MTU/acre loading cases for joint pattern C. The maximum vertical compressive stress along this horizontal section is higher for the higher thermal load. This observation applies to other joint patterns as well.

Table 4-2 summarizes the maximum tensile and compressive stresses for each UDEC run (taking into account any yielding that may have occurred). Tensile stresses occur immediately after excavation in all cases except the ubiquitous joint model. Maximum tensile stress is the highest for cases with three joint sets (i.e., joint patterns C and D).

4.1.3 Temperature Distribution

Figures 4-14 and 4-15 depict temperature histories on the tunnel wall at the roof for all of the joint patterns under thermal loads of 100 MTU/acre and 20 MTU/acre, respectively. In 100 MTU/acre loading case, temperature at the tunnel wall increases to a maximum of 180 to 190 °C and reaches the maximum at about 80 yr after heating. In the 20 MTU/acre loading case, temperature at the tunnel wall increases to a maximum of 62 to 63 °C and reaches the maximum at about 60 yr after heating.

4.1.4 Summary of Scoping Analyses

TM scoping analyses of waste emplacement drift considered five joint patterns and two thermal loading strategies—100 MTU/acre and 20 MTU/acre. The following observations can be summarized from these UDEC analyses:

- The maximum upward expansion due to thermal load is about 24 cm for 100 MTU/acre thermal loading and about 4.6 cm for 20 MTU/acre thermal loading.

- In general, upward movement of roof due to thermal loading is slightly higher than that of floor for the 100 MTU/acre thermal loading case, causing the drift to diverge. However, for the 100 MTU/acre thermal loading and ubiquitous joint model, the upward movement of roof is smaller than that of floor, resulting in drift convergence. For all joint models at the 20 MTU/acre thermal loading case, the upward movement of floor is always greater than that of the roof, signifying drift convergence.

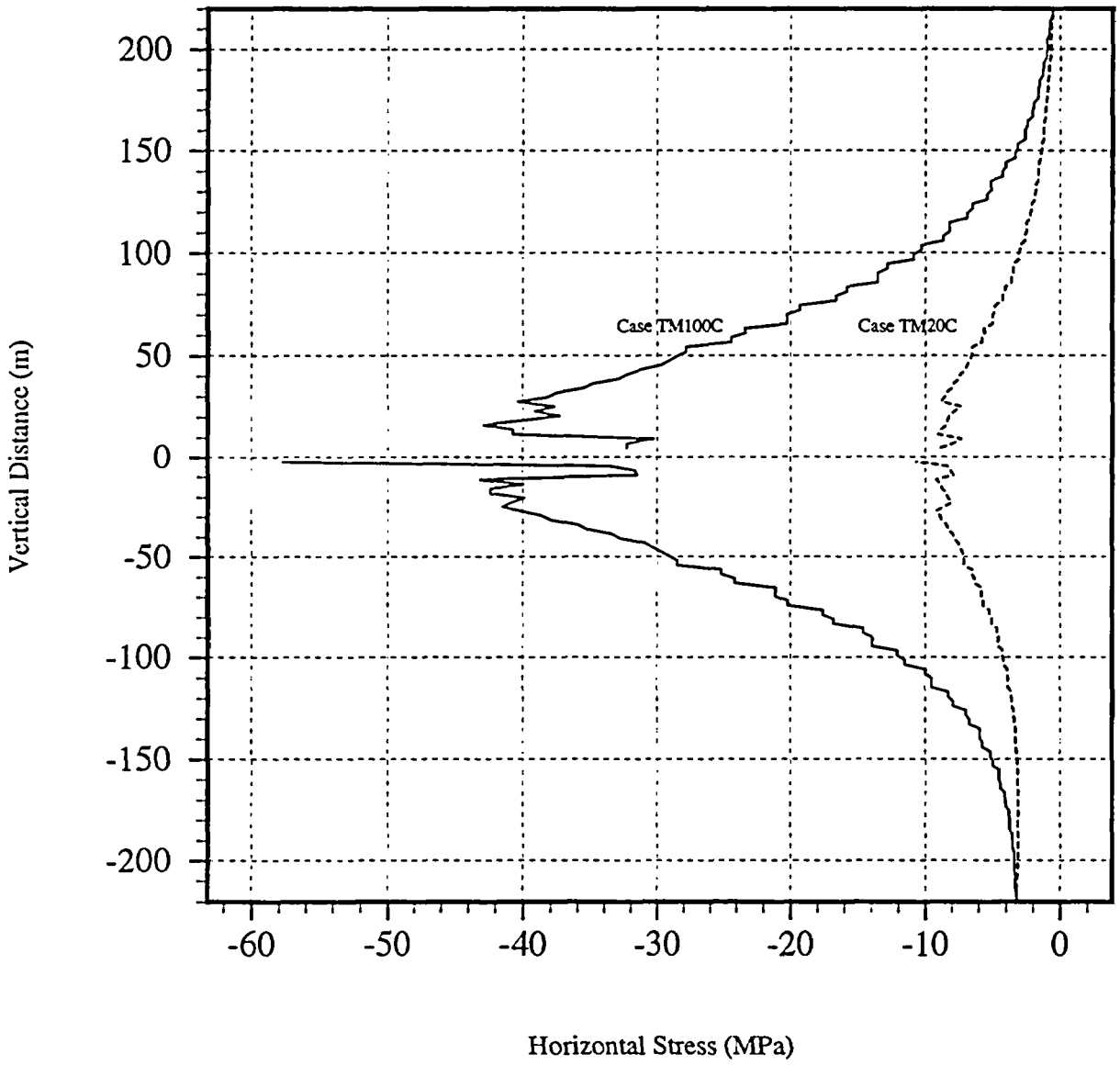

Figure 4-10. Horizontal stress after 100 yr of heating along a vertical section through the tunnel for joint pattern C

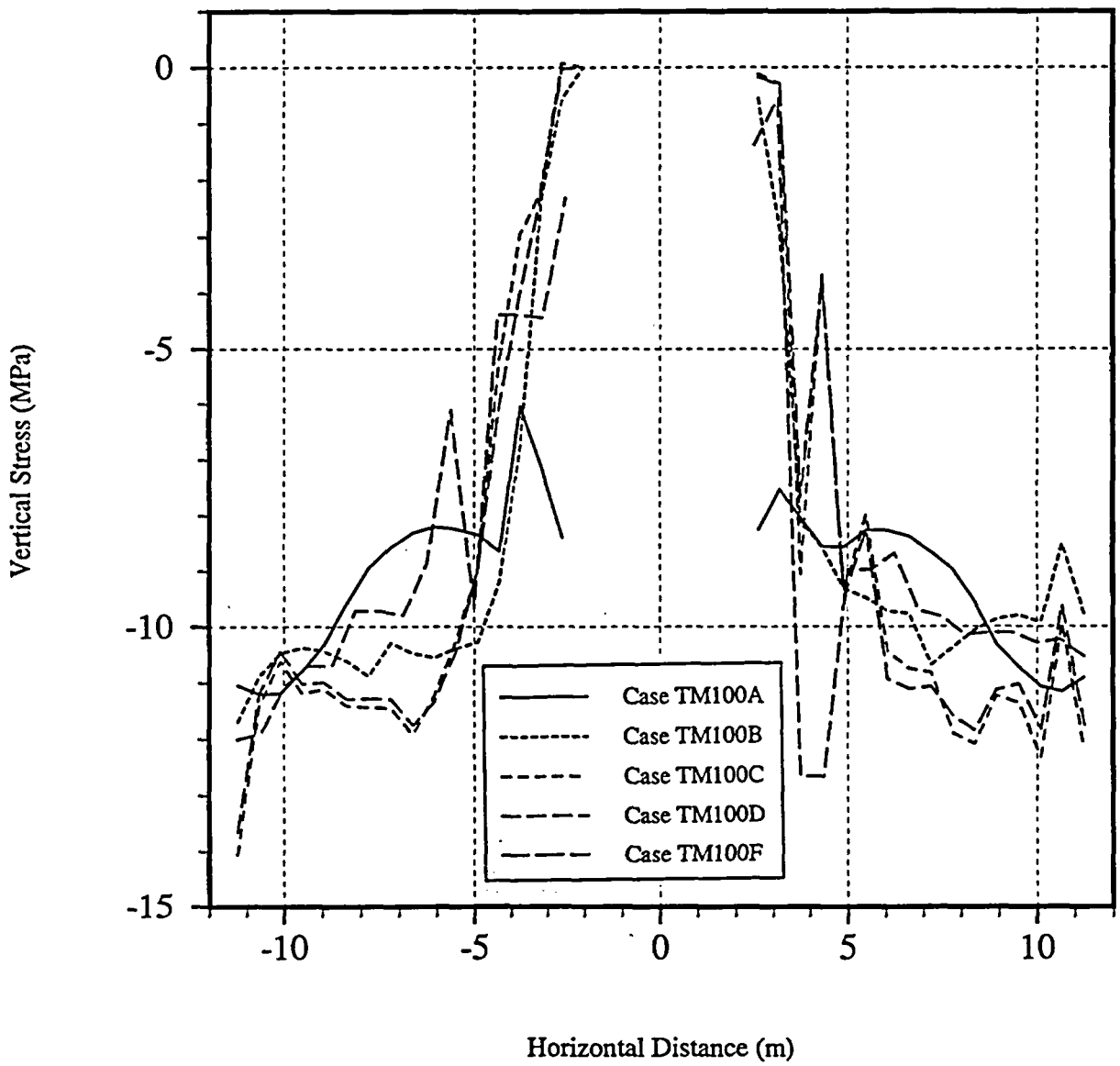

Figure 4-11. Vertical stress after 100 yr of heating along a horizontal section through the tunnel for the thermal loading of 100 MTU/acre

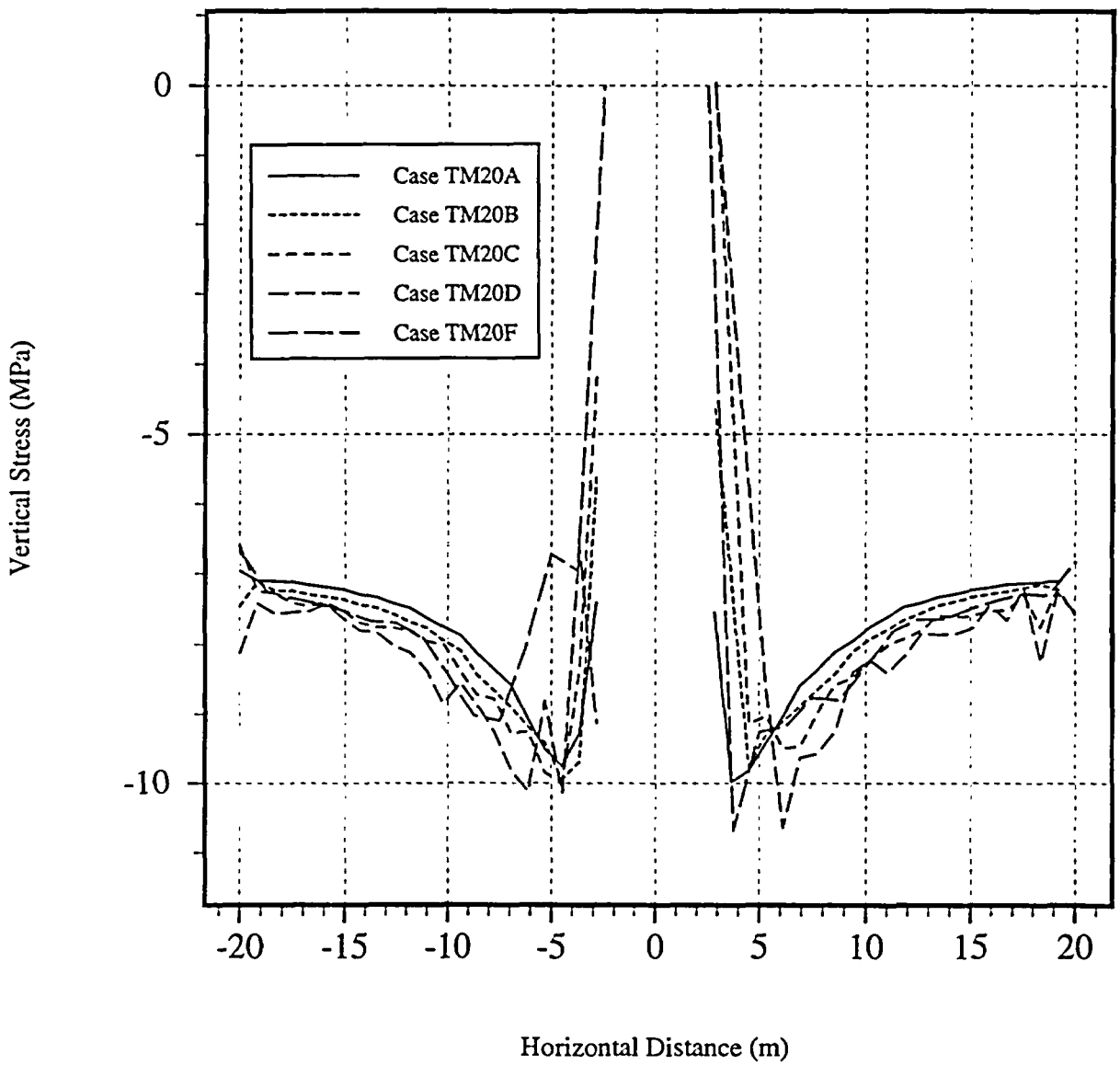

Figure 4-12. Vertical stress after 100 yr of heating along a horizontal section through the tunnel for the thermal loading of 20 MTU/acre (refer to figure 4-11 for curve definitions)

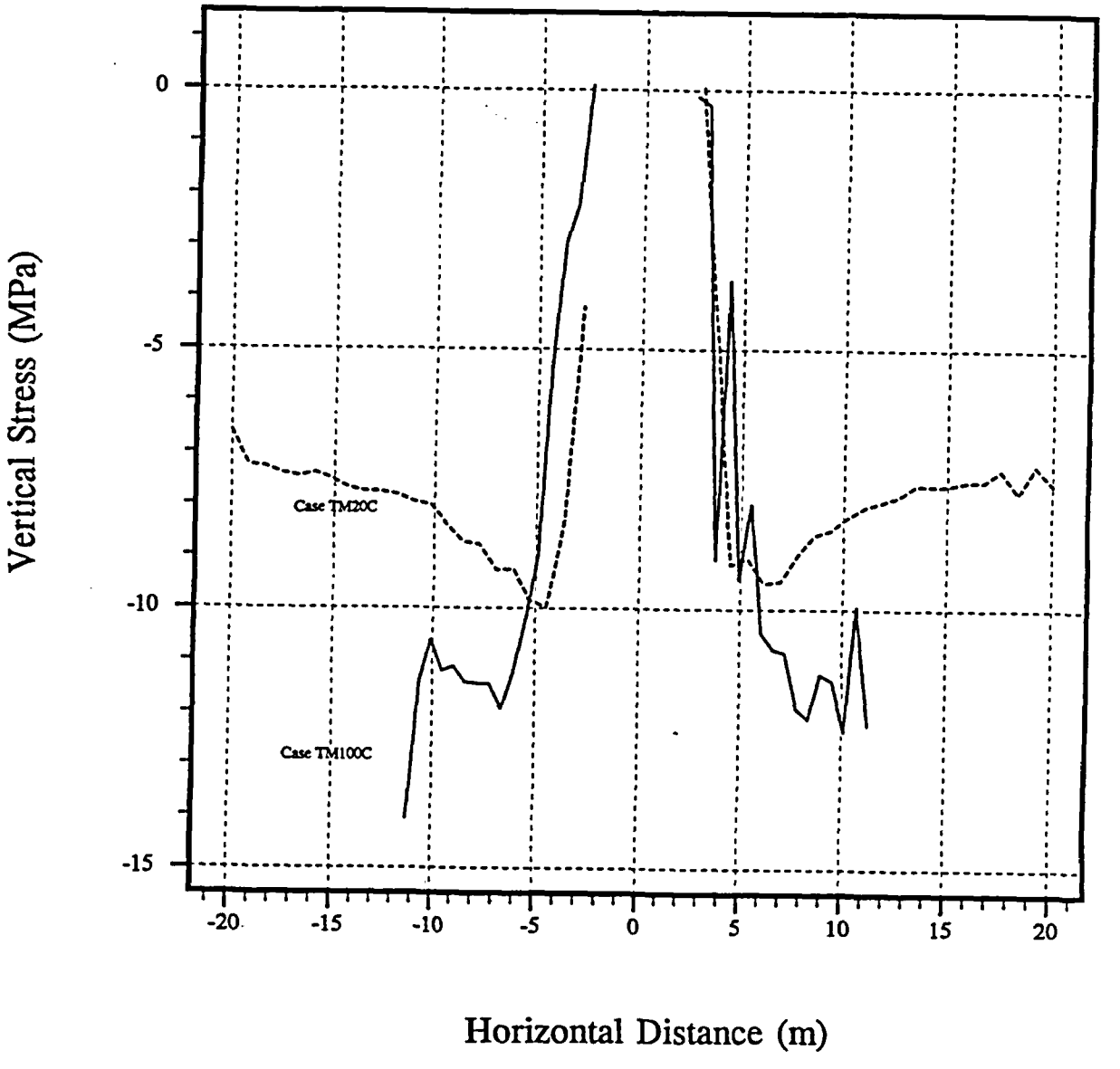

Figure 4-13. Vertical stress after 100 yr of heating along a horizontal section through the tunnel for joint pattern C

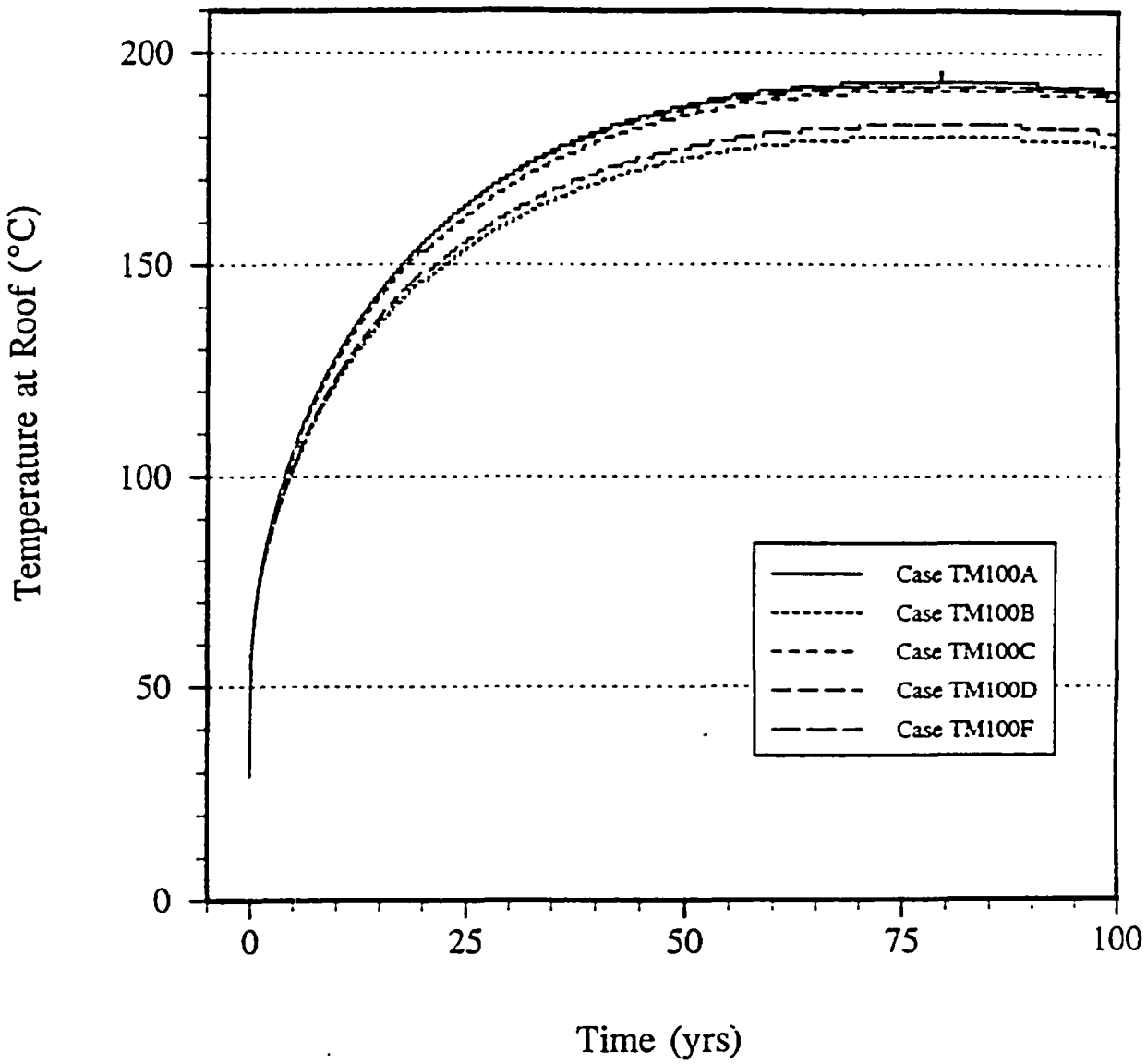

Figure 4-14. Temperature histories on tunnel wall at roof for various joint patterns for the thermal loading of 100 MTU/acre

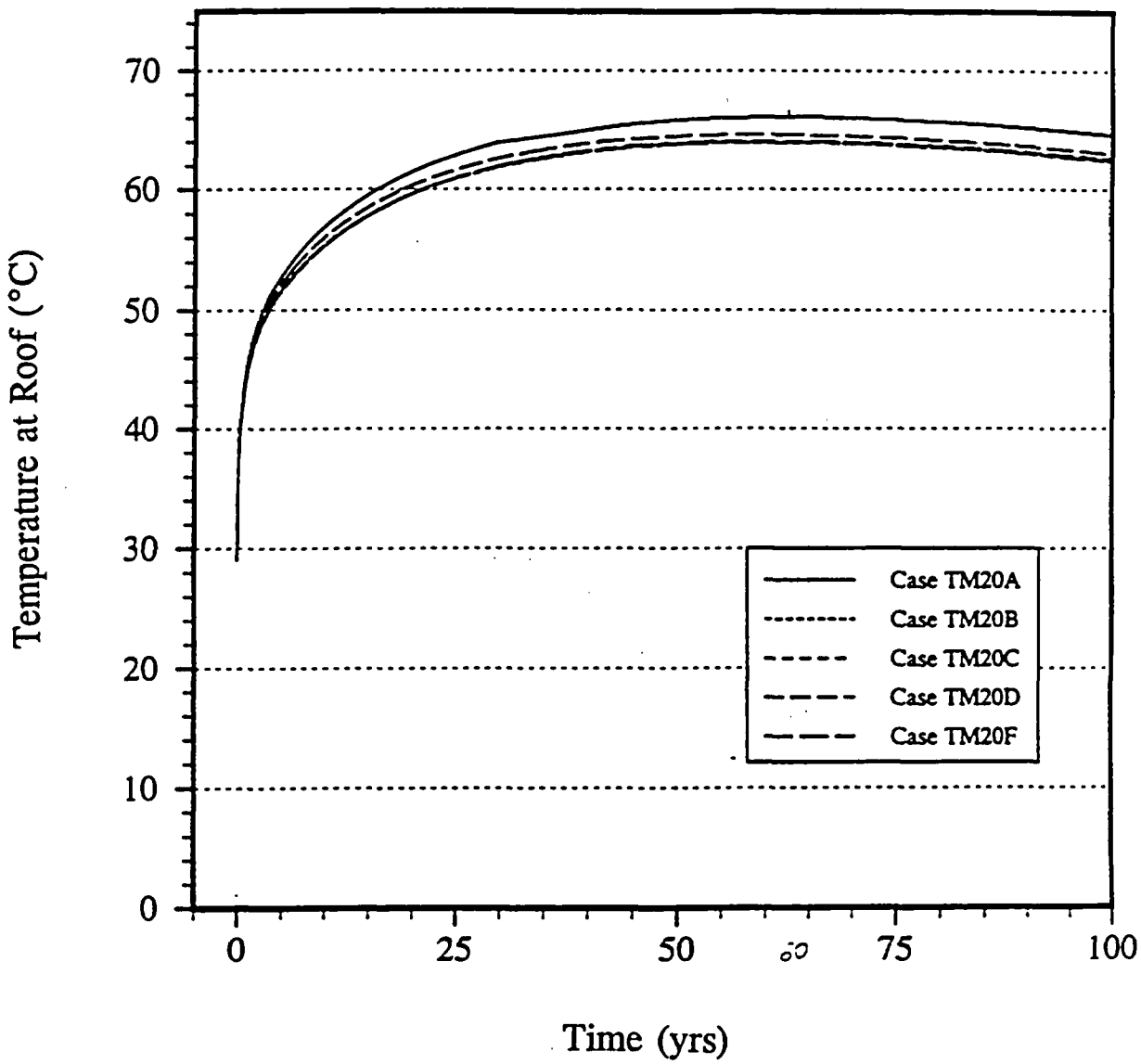

Figure 4-15. Temperature histories on tunnel wall at roof for various joint patterns under the thermal load of 20 MTU/acre

- Although, it appears that thermal expansion increases the maximum joint shear displacement, neither the magnitude of thermal load nor joint pattern appear to affect the magnitude of maximum joint shear displacement in a systematic way.

- Joint pattern does not seem to affect the magnitude and distribution of stresses at a distance away from the tunnel, while it does affect both the magnitude and distribution of stresses in the immediate tunnel areas (about five diameters into the wall).

- Tensile stresses occur in most cases (except the ubiquitous joint models) that may cause localized failure, depending on local compressive stresses. In most cases, there are blocks falling from the rib areas of the tunnel.

- The maximum temperature is 180 to 190 °C for 100 high thermal loading case and 62 to 63 °C for thermal loading cases. For high thermal loading, the temperature reaches the maximum at about 80 yr after heating. For low thermal loading, it reaches the maximum at about 60 yr after heating.

Based on some of these observations, in future analyses, it does not appear necessary to consider joint patterns consisting of more than three joint sets. It would seem sufficient to consider a vertical-subvertical joint set with reasonable ranges of spacing and orientation and a horizontal-subhorizontal joint set with reasonable ranges of orientation and spacing.

4.2 GENERAL MODELING RESULTS FROM FINAL SET OF UDEC RUNS

This section describes general results from the final set of 64 UDEC runs that are important in discussing overall drift stability and effectiveness of waste isolation. The effects of input parameters on these general results are also briefly discussed in a qualitative manner, provided such effects are pronounced. As discussed at the beginning of section 4, some output parameters from numerical modeling have been considered as performance measures for the factorial analysis based on observation of the general results and engineering judgment. Table 4-3 presents these performance measures and their values from all the 64 factorial run cases after 50 and 100 yr of heating, respectively.

4.2.1 Joint Shear Displacement

Shear displacements usually occur along joints near the drift following excavation. Thermal loading in most cases increases joint shear displacement. Figures 4-16 through 4-18 show joint shear displacement following excavation after 50 and 100 yr of heating, respectively, for Case 12. As noted in these figures, the maximum joint shear displacements increase from around 0.6 cm following drift excavation to about 1 cm at 100 yr for this particular case of high thermal loading. Thermal loading results primarily in increased shear displacements along the horizontal-subhorizontal joints. Although the extensiveness and magnitude of joint shear vary from case to case, joint shear displacement occurs in most cases. The maximum joint shear displacement at 100 yr ranges from 0.4 cm (Case 15) to 4.8 cm (Case 26) for high thermal loading and from 0.2 cm (Case 45) to 4 cm (Case 44) for low thermal loading, while the maximum joint shear displacement after 50 yr ranges from 0.4 cm (Case 8) to 4.3 cm (Case 16) for high thermal loading and from 0.1 (Case 51) to 7.2 (Case 60) for low thermal loading. Table 4-3 lists the maximum joint shear displacement for each of the 64 fractional factorial runs.

Table 4-3. Values of performance measures for factorial UDEC run cases, (a) at 50 yr and (b) at 100 yr

Table 4-3a. UDEC results after 50 yr of emplacement drift heating

UDEC RUNS	Parameter Values*	σ_{min} (MPa)	σ_{max} (MPa)	Jc_{max} ($\times 10^{-2}$cm)	Jo_{max} ($\times 10^{-2}$cm)	Jd_{max} (cm)	Area of Yield Zone (m^2)	Roof/Floor Convergence (cm)
Case1.dat	de	2.7	−20.1	1.940	12.000	0.640	0	0.175
Case2.dat	abde	2.9	−23.6	2.150	0.300	0.500	0	−0.032
Case3.dat	acef	3.0	−10.0	4.590	9.300	0.530	0.007	0.305
Case4.dat	bcef	2.8	−34.5	2.870	19.100	0.790	0	0.528
Case5.dat	aeg	2.6	−27.4	3.800	20.500	0.750	0	0.623
Case6.dat	beg	3.2	−30.7	2.340	90.300	1.900	0.010	0.650
Case7.dat	cdefg	2.9	−36.0	2.960	3.100	0.440	0	−0.166
Case8.dat	abcdefg	2.6	−37.1	3.540	1.900	0.410	0	−0.117
Case9.dat	acdeh	3.7	−54.0	5.660	11.800	0.480	0.041	−0.175
Case10.dat	bcdeh	3.9	−54.1	4.360	95.900	0.480	0.585	−0.448
Case11.dat	efh	3.8	−33.3	4.920	106.100	3.400	1.889	1.178
Case12.dat	abefh	4.3	−35.9	4.590	105.400	1.180	0.240	0.406
Case13.dat	cegh	4.8	−56.6	4.640	3.100	0.440	0.096	−0.377
Case14.dat	abcegh	3.9	−49.1	4.510	24.800	0.420	0.190	−0.382
Case15.dat	adefgh	3.8	−33.7	4.020	18.500	0.420	0.216	−0.117
Case16.dat	bdefgh	4.9	−35.5	3.140	75.300	4.310	0.248	−0.337
Case17.dat	cei	4.4	−63.8	5.340	57.600	1.610	0.690	0.160
Case18.dat	abcei	3.3	−44.6	5.580	43.900	1.290	0.341	−0.270

* For consistency with appendix A, a lower case letter indicates a high value used for that particular parameter (see table 4-3c for parameter identification) while the absence of a letter indicates a low extreme value. In the case all parameters are low, the notation (1) is used (see table 3-1).

Table 4-3a. UDEC results after 50 yr of emplacement drift heating (cont'd)

UDEC RUNS	Parameter Values*	σ_{min} (MPa)	σ_{max} (MPa)	jc_{max} ($\times 10^{-2}$cm)	jo_{max} ($\times 10^{-2}$cm)	jd_{max} (cm)	Area of Yield Zone (m^2)	Roof/Floor Convergence (cm)
Case19.dat	adefi	4.0	−48.8	5.970	25.400	0.750	0.080	−0.429
Case20.dat	bdefi	3.0	−27.7	2.400	3.800	0.540	0.013	−0.072
Case21.dat	acdegi	4.4	−62.5	6.417	20.400	1.287	0.134	−0.529
Case22.dat	bcdegi	4.8	−51.2	4.455	100.200	3.017	0.255	0.080
Case23.dat	efgi	4.7	−57.8	7.070	82.200	2.881	2.273	0.954
Case24.dat	abefgi	4.6	−123.9	8.272	41.000	1.605	0.393	−0.290
Case25.dat	aehi	4.1	−77.1	7.652	114.400	1.722	112.700	−0.626
Case26.dat	behi	4.6	−64.1	7.351	109.000	3.842	197.700	1.240
Case27.dat	cdefhi	4.7	−123.1	10.500	14.200	1.934	1.640	−1.570
Case28.dat	abcdefhi	4.3	−124.2	8.070	96.100	1.830	8.250	−1.205
Case29.dat	deghi	4.8	−98.6	9.342	50.400	1.980	5.350	−1.730
Case30.dat	abdeghi	3.9	−103.3	7.573	114.000	1.646	4.890	−1.414
Case31.dat	acefghi	4.3	−98.2	9.641	29.100	1.773	4.140	−1.062
Case32.dat	bcefghi	4.6	−64.6	8.514	139.800	2.888	7.850	0.790
Case33.dat	(1)	1.5	−15.2	2.660	8.177	2.487	0	0.945
Case34.dat	ab	1.5	−14.7	2.480	3.774	0.551	0	0.843
Case35.dat	acdf	1.7	−33.9	1.074	2.453	0.319	0	0.457
Case36.dat	bcdf	1.6	−12.1	0.738	2.501	0.437	0	0.384
Case37.dat	adg	0.9	−15.0	1.531	2.459	0.415	0	0.521

* For consistency with appendix A, a lower case letter indicates a high value used for that particular parameter (see table 4-3c for parameter identification) while the absence of a letter indicates a low extreme value. In the case all parameters are low, the notation (1) is used (see table 3-1).

Table 4-3a. UDEC results after 50 yr of emplacement drift heating (cont'd)

UDEC RUNS	Parameter Values*	σ_{min} (MPa)	σ_{max} (MPa)	$\int c_{max}$ ($\times 10^{-2}$cm)	$\int o_{max}$ ($\times 10^{-2}$cm)	$\int d_{max}$ (cm)	Area of Yield Zone (m^2)	Roof/Floor Convergence (cm)
Case38.dat	bdg	2.1	−10.6	0.681	3.428	0.505	0	0.480
Case39.dat	cfg	1.1	−14.6	1.718	12.230	0.565	0	0.748
Case40.dat	abcfg	1.5	−26.4	1.531	8.868	0.483	0	0.813
Case41.dat	ach	2.0	−29.4	1.657	3.770	0.275	0	0.297
Case42.dat	bch	3.4	−14.1	1.479	37.250	0.655	0.069	0.416
Case43.dat	dfh	2.1	−12.6	0.939	2.610	1.870	0	0.153
Case44.dat	abdfh	2.9	−14.8	1.407	2.649	2.328	0	0.235
Case45.dat	cdgh	2.5	−17.1	1.200	64.950	0.975	0	0.106
Case46.dat	abcdgh	1.5	−23.2	1.606	2.393	0.230	0	0.131
Case47.dat	afgh	2.0	−14.3	1.236	3.547	0.291	0	0.308
Case48.dat	bfgh	2.5	−13.3	1.179	24.980	0.594	0.050	0.512
Case49.dat	cdi	1.4	−14.4	0.791	1.008	0.393	0	0.387
Case50.dat	abcdi	1.8	−27.9	2.037	4.939	0.418	0	0.217
Case51.dat	afi	3.5	−18.0	2.511	42.200	0.127	2.055	0.814
Case52.dat	bfi	3.0	−16.7	1.532	49.200	1.102	0.052	1.148
Case53.dat	acgi	1.4	−16.9	2.046	7.721	0.586	0	0.658
Case54.dat	bcgi	3.0	−15.0	2.109	116.4	2.545	0.051	1.023
Case55.dat	dfgi	2.0	−16.3	1.520	1.300	0.500	0	0.318
Case56.dat	abdfgi	2.3	−27.3	1.809	3.588	0.427	0	0.462

* For consistency with appendix A, a lower case letter indicates a high value used for that particular parameter (see table 4-3c for parameter identification) while the absence of a letter indicates a low extreme value. In the case all parameters are low, the notation (1) is used (see table 3-1).

Table 4-3a. UDEC results after 50 yr of emplacement drift heating (cont'd)

UDEC RUNS	Parameter Values*	σ_{min} (MPa)	σ_{max} (MPa)	jc_{max} ($\times 10^{-2}$cm)	jo_{max} ($\times 10^{-2}$cm)	jd_{max} (cm)	Area of Yield Zone (m^2)	Roof/Floor Convergence (cm)
Case57.dat	adhi	1.5	−22.2	2.843	1.902	0.273	0	0.108
Case58.dat	bdhi	3.5	−23.0	1.996	46.200	0.333	0.102	0.188
Case59.dat	cfhi	2.3	−30.5	3.508	11.800	0.550	0	0.351
Case60.dat	abcfhi	43.1	−67.3	15.980	0.766	7.274	25.097	0.799
Case61.dat	ghi	2.4	−25.8	2.900	11.100	0.670	0	0.483
Case62.dat	abghi	2.4	−48.6	4.360	6.640	0.350	0	0.354
Case63.dat	acdfghi	1.5	−24.9	2.471	3.814	0.266	0	0.096
Case64.dat	bcdfghi	3.6	−38.5	2.265	6.882	0.270	0	0.106

Table 4-3b. UDEC results after 100-yr of emplacement drift heating

UDEC RUNS	Parameter Values*	σ_{min} (MPa)	σ_{max} (MPa)	jc_{max} ($\times 10^{-2}$cm)	jo_{max} ($\times 10^{-2}$cm)	jd_{max} (cm)	Area of Yield Zone (m^2)	Roof/Floor Convergence (cm)
Case1.dat	de	3.4	−20.4	1.830	21.000	3.390	0	0.095
Case2.dat	abde	3.4	−24.9	2.270	4.000	0.500	0	−0.025
Case3.dat	acef	3.3	−109.6	0.050	9.000	0.440	0.007	0.317
Case4.dat	bcef	2.7	−35.7	3.000	22.000	0.800	0	0.516
Case5.dat	aeg	2.9	−28.6	2.790	21.000	0.780	0	0.574
Case6.dat	beg	3.3	−32.1	2.430	26.000	3.350	0.007	0.632

* For consistency with appendix A, a lower case letter indicates a high value used for that particular parameter (see table 4-3c for parameter identification) while the absence of a letter indicates a low extreme value. In the case all parameters are low, the notation (1) is used (see table 3-1).

Table 4-3b. UDEC results after 100 yr of emplacement drift heating (cont'd)

UDEC RUNS	Parameter Values*	σ_{min} (MPa)	σ_{max} (MPa)	jc_{max} ($\times 10^{-2}$cm)	jo_{max} ($\times 10^{-2}$cm)	jd_{max} (cm)	Area of Yield Zone (m^2)	Roof/Floor Convergence (cm)
Case7.dat	cdefg	3.2	−38.0	3.130	4.000	0.450	0	−0.217
Case8.dat	abcdefg	2.9	−39.2	3.720	2.000	0.440	0	−0.177
Case9.dat	acdeh	4.2	−56.8	5.670	12.0000	0.530	0.041	−0.290
Case10.dat	bcdeh	4.1	−56.1	4.550	22.000	2.890	0.585	−0.533
Case11.dat	efh	3.7	−35.0	6.990	105.000	3.860	1.900	1.216
Case12.dat	abefh	4.6	−36.2	4.270	93.000	0.990	0.240	0.396
Case13.dat	cegh	4.1	−58.3	4.890	3.000	0.520	0.366	−0.424
Case14.dat	abcegh	4.1	−51.1	4.680	28.000	0.500	0.190	−0.439
Case15.dat	adefgh	4.3	−34.7	4.000	20.000	0.420	0.216	−0.166
Case16.dat	bdefgh	4.7	−37.2	3.280	85.000	4.340	0.248	−0.403
Case17.dat	ce	4.3	−66.2	5.360	57.000	1.700	1.000	0.060
Case18.dat	abcei	4.5	−52.3	6.080	93.000	2.200	1.600	−0.410
Case19.dat	adefi	3.8	−50.4	5.460	44.000	0.690	0.145	−0.520
Case20.dat	bdefi	3.4	−28.6	2.480	6.000	0.540	0.013	−0.135
Case21.dat	acdegi	4.3	−65.0	6.570	17.700	1.405	0.296	−0.620
Case22.dat	bcdegi	3.8	−51.3	492.000	122.800	2.487	0.493	−0.110
Case23.dat	efgi	4.8	−59.9	6.690	132.500	3.119	2.273	0.964
Case24.dat	abefgi	4.7	−122.3	8.164	43.600	1.691	0.362	−0.370
Case25.dat	aehi	4.4	−76.8	7.620	135.700	2.078	178.000	−0.690

* For consistency with appendix A, a lower case letter indicates a high value used for that particular parameter (see table 4-3c for parameter identification) while the absence of a letter indicates a low extreme value. In the case all parameters are low, the notation (1) is used (see table 3-1).

Table 4-3b. UDEC results after 100 yr of emplacement drift heating (cont'd)

UDEC RUNS	Parameter Values*	σ_{min} (MPa)	σ_{max} (MPa)	jc_{max} ($\times 10^{-2}$cm)	jo_{max} ($\times 10^{-2}$cm)	jd_{max} (cm)	Area of Yield Zone (m^2)	Roof/Floor Convergence (cm)
Case26.dat	behi	4.8	−68.1	7.350	136.500	4.820	255.300	2.310
Case27.dat	cdefhi	3.9	−115.0	10.300	22.000	2.149	3.160	−1.800
Case28.dat	abcdefhi	4.5	−66.8	9.584	92.600	2.285	12.750	−0.930
Case29.dat	deghi	4.3	−99.9	9.501	79.500	2.722	13.480	−1.970
Case30.dat	abdeghi	4.9	−70.8	9.263	62.200	2.742	11.330	1.490
Case31.dat	acefghi	4.7	−100.3	9.723	52.600	2.009	4.190	−1.280
Case32.dat	bcefghi	4.4	−66.6	8.790	128.000	3.614	9.330	0.760
Case33.dat	(1)	1.6	−15.2	2.179	8.797	2.498	0	0.929
Case34.dat	ab	1.7	−15.1	2.018	3.982	0.546	0	0.860
Case35.dat	acdf	1.7	−32.9	1.086	2.655	0.318	0	0.433
Case36.dat	bcdf	1.7	−11.5	0.758	2.515	0.432	0	0.366
Case37.dat	adgh	0.9	−14.0	1.455	2.616	0.415	0	0.502
Case38.dat	bdg	2.2	−10.8	0.663	3.674	0.490	0	0.461
Case39.dat	cfg	1.0	−14.8	1.730	11.960	0.587	0	0.731
Case40.dat	abcfg	1.5	−25.6	1.577	8.470	0.481	0	0.800
Case41.dat	ach	2.1	−27.3	1.728	3.860	0.267	0	0.280
Case42.dat	bch	3.5	−14.7	1.518	39.680	0.657	0.069	0.417
Case43.dat	dfh	2.2	−13.3	0.995	2.390	2.628	0	0.136
Case44.dat	abdfh	2.7	−15.6	1.490	2.841	3.407	0	0.224

* For consistency with appendix A, a lower case letter indicates a high value used for that particular parameter (see table 4-3c for parameter identification) while the absence of a letter indicates a low extreme value. In the case all parameters are low, the notation (1) is used (see table 3-1).

Table 4-3c. Information for tables 4-3a and 4-3b

Table 4-3a—Study Results after 50 yr of emplacement drift heating Table 4-3b—Study Results after 100 yr of emplacement drift heating		
Nomenclatures		
σ_{min}	=	maximum tensile principal stress (positive)
σ_{max}	=	maximum compressive principal stress (negative)
jc_{max}	=	maximum joint closure
jo_{max}	=	maximum joint opening
jd_{max}	=	maximum joint shear displacement
A lower case in tables 4-3a and 4-3b (column 2) indicates a high value for that particular variable input parameter. Absence of a letter indicates a low value. In the case all parameters are low, the notation (1) is used.		
A	=	Subvertical joint inclination (85–70) [degrees]
B	=	Subhorizontal joint inclination (20–10) [degrees]
C	=	Subvertical joint spacing (0.5–0.2) [m]
D	=	Joint friction angle (38–28) [degrees]
E	=	Thermal loading (100–20) [MTU/acre]
F	=	Intact rock cohesion (43–18) [MPa]
G	=	Intact rock friction angle (50-20) [degrees]
H	=	Intact rock Young's modulus (32–16) [GPa]
I	=	Thermal expansion coefficient ($12\times10^{-6} - 6\times10^{-6}$) [$K^{-1}$]
Fixed Input Parameters		
Number of joint sets	= 2	
Horizontal joint spacing	= 1.25 m	
Poisson's ratio	= 0.21	
Density	= 2297.0 kg/m^3	
Uniaxial compressive strength	= 166.0 MPa	
Uniaxial tensile strength	= 5 MPa	
Thermal conductivity	= 2.1 W/m-K	
Specific heat	= 932.0 J/Kg-K	
Joint normal stiffness	= 1.0×10^5 MPa/m	
Joint shear stiffness	= 1.0×10^5 MPa/m	
Joint cohesion	= 0.08 MPa	
Joint tensile strength	= 0.04 MPa	
Joint angle of friction	= 38°	

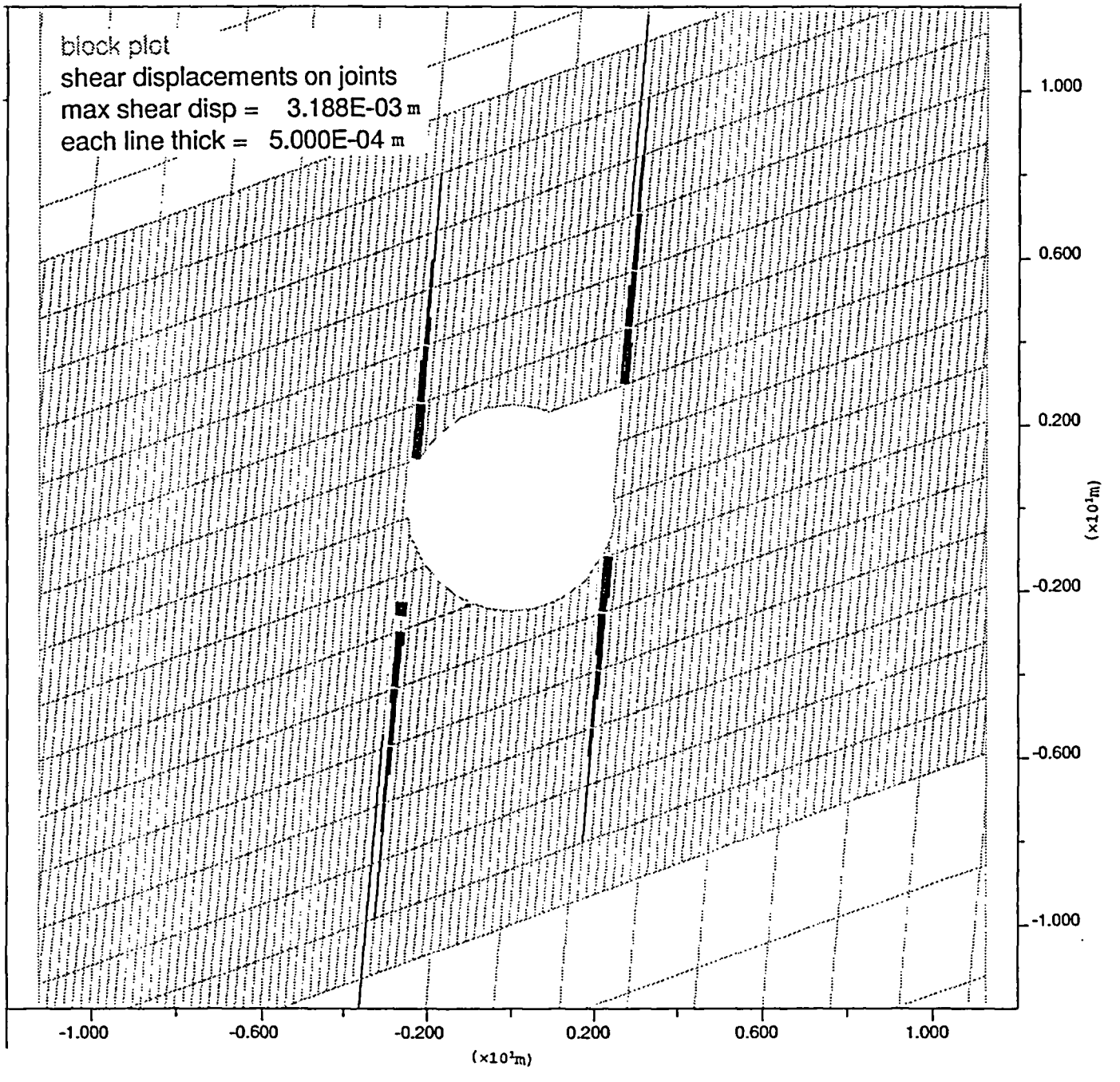

Figure 4-16. Joint shear displacement following drift excavation for Case 12. Joint shear displacement is in meters.

Table 4-3b. UDEC results after 100 yr of emplacement drift heating (cont'd)

UDEC RUNS	Parameter Values*	σ_{min} (MPa)	σ_{max} (MPa)	jc_{max} ($\times 10^{-2}$cm)	jo_{max} ($\times 10^{-2}$cm)	jd_{max} (cm)	Area of Yield Zone (m^2)	Roof/Floor Convergence (cm)
Case45.dat	cdgh	2.8	−17.5	1.271	1.140	0.220	0	0.088
Case46.dat	abcdgh	1.7	−24.1	1.732	2.671	0.227	0	0.015
Case47.dat	afgh	2.2	−14.6	1.258	3.959	0.280	0	0.297
Case48.dat	bfgh	2.4	−13.5	1.201	33.270	0.596	0.050	0.511
Case49.dat	cdi	1.5	−13.9	0.808	1.030	0.393	0	0.368
Case50.dat	abcdi	2.0	−29.2	2.162	6.000	0.413	0	0.186
Case51.dat	afi	3.9	−18.4	1.712	48.980	1.311	2.1200	0.584
Case52.dat	bfi	3.4	−17.0	1.547	52.830	1.113	0.052	0.959
Case53.dat	acgi	1.7	−17.6	2.053	7.435	0.575	0	0.621
Case54.dat	bcgi	3.2	−15.2	2.201	121.400	2.648	0.051	1.039
Case55.dat	dfgi	2.5	−16.6	1.530	2.000	0.490	0	0.278
Case56.dat	abdfgi	2.9	−28.6	1.863	4.760	0.426	0	0.441
Case57.dat	adhi	1.8	−22.8	2.631	4.719	0.271	0	0.071
Case58.dat	bdhi	3.3	−23.1	1.991	53.000	0.394	0.165	0.179
Case59.dat	cfhi	2.4	−31.7	3.467	11.500	0.568	0	0.321
Case60.dat	abcfhi	4.2	−65.4	15.750	76.690	0.115	26.042	0.799
Case61.dat	ghi	2.4	−24.2	0.2600	15.000	0.780	0	0.467
Case62.dat	abghi	2.8	−50.2	4.070	7.540	0.339	0	0.342
Case63.dat	acdfghi	2.0	−26.4	2.980	3.889	0.252	0	0.078

* For consistency with appendix A, a lower case letter indicates a high value used for that particular parameter (see table 4-3c for parameter identification) while the absence of a letter indicates a low extreme value. In the case all parameters are low, the notation (1) is used (see table 3-1).

Table 4-3b. UDEC results after 100 yr of emplacement drift heating (cont'd)

UDEC RUNS	Parameter Values*	σ_{min} (MPa)	σ_{max} (MPa)	jc_{max} ($\times 10^{-2}$cm)	jo_{max} ($\times 10^{-2}$cm)	jd_{max} (cm)	Area of Yield Zone (m^2)	Roof/Floor Convergence (cm)
Case64.dat	bcdfghi	3.2	−41.2	2.437	7.424	0.302	0.051	0.092

* For consistency with appendix A, a lower case letter indicates a high value used for that particular parameter (see table 4-3c for parameter identification) while the absence of a letter indicates a low extreme value. In the case all parameters are low, the notation (1) is used (see table 3-1).

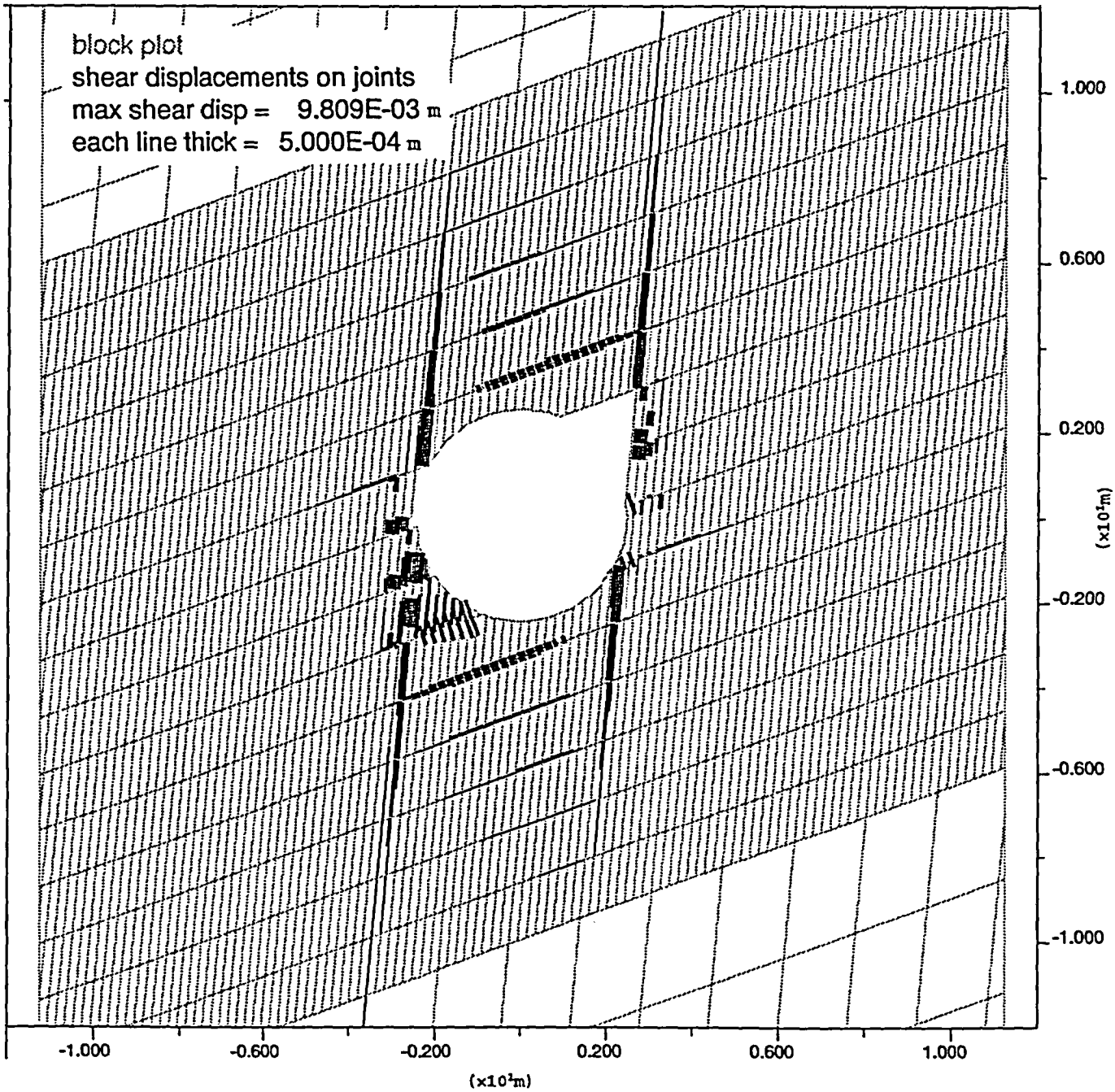

Figure 4-17. Joint shear displacement after 50 yr of heating for Case 12. Joint shear displacement is in meters.

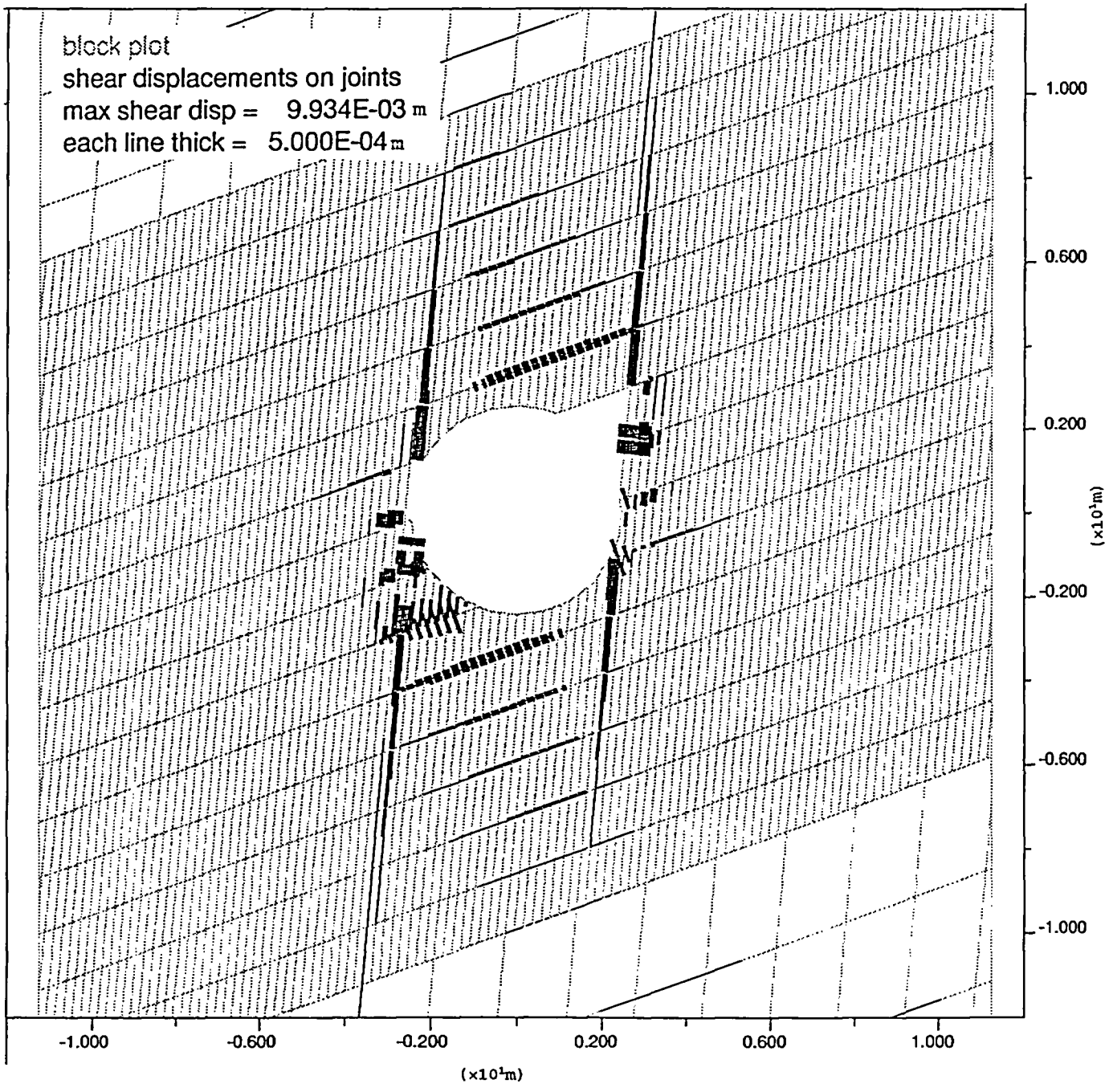

Figure 4-18. Joint shear displacement after 100 yr of heating for Case 12. Joint shear displacement is in meters.

The fact that both the magnitude and extent of joint shear displacement is largely increased by thermal loading might have significant meaning for the effectiveness of waste isolation. Although it is not explicitly modeled in this UDEC analyses, joint shear displacement could increase joint dilation and, thus, increase joint permeability (Barton et al., 1985). If joint permeability is increased by the thermal load to an extent shown in figure 4-18, it could increase the possibility of groundwater flow into the emplacement drift. However, it is not clear from this purely TM analysis what the combined effect of increased closure along some joints, increased dilation due to shear on other joints, and joint opening because of stress relaxation will be on the groundwater flow field and emplacement drift inflow.

4.2.2 Convergence and Displacement

Table 4-3 gives roof-to-floor convergence for each of the UDEC runs. In general, thermal loading causes upward heave. In some cases, floor upward movement is greater than the roof upward movement, resulting in positive convergence. In other instances, floor upward movement is less than the roof upward movement, resulting in negative convergence (i.e., the drift actually enlarges in the vertical direction). The convergence for high thermal loading cases ranges from −2.0 cm (Case 29) to 2.3 cm (Case 26) at 100 yr and from -1.7 cm (Case 29) to 1.2 cm (Case 26) at 50 yr. Convergence for low thermal loading cases ranges from 0.015 cm (Case 46) to 1.039 cm (Case 54) at 100 yr and from 0.096 cm (Case 63) to 1.148 cm (Case 52) at 50 yr. Most of the low thermal loading cases have positive convergence. Negative convergence occurs in about half of the high thermal loading instances.

4.2.3 Stress Distribution

As examples, figures 4-19 through 4-21 show principal stress distribution immediately after drift excavation, at 50 yr, and 100 yr, respectively, for Case 12. For most of the UDEC runs, maximum compressive stress immediately after excavation occurs in the drift side-walls, the maximum compressive principal stress usually increases after heating, and location of the maximum compressive principal stress usually shifts to the immediate roof and floor areas. Tensile stresses are predicted following drift excavation as well as after heating for most of the cases. However, heat load changes the location of the maximum tensile stress from roof and floor areas following drift excavation to side-walls of the drift. It is usual that the circumferential stress increases in the roof with heating, while it decreases in the ribs of the drift due to thermal expansion. As is shown in figures 4-19 through 4-22, the right and left drift ribs in this 100 MTU/acre loading case become almost completely destressed. This results in opening of joints and unstable rock along the ribs of the drift. The maximum tensile principal stress for the high thermal loading cases ranges from 2.7 MPa (Case 4) to 4.9 MPa (Case 30) at 100 yr and from 2.6 (Cases 5 and 8) to 4.9 MPa (Case 16) at 50 yr. The maximum compressive principal stress for the high thermal loading cases ranges from 20.4 MPa (Case 1) to 122.5 MPa (Case 24) at 100 yr and from 10 MPa (Case 3) to 124.2 MPa (Case 28) at 50 yr. The maximum tensile principal stress for the low thermal loading cases ranges from 0.9 MPa (Case 31) to 4.2 MPa (Case 60) at 100 yr and from 0.9 (Case 37) to 4.3 MPa (Case 60) at 50 yr. The maximum compressive principal stress for the low thermal loading cases ranges from 10.81 MPa (Case 38) to 65.4 MPa (Case 60) at 100 yr and from 10.61 MPa (Case 38) to 67.29 MPa (Case 60) at 50 yr. These tensile stresses take into account yielding that may have occurred in the model since a tensile strength cutoff of 5.0 MPa was assigned. Likewise, the maximum compressive stresses take into account yielding in blocks.

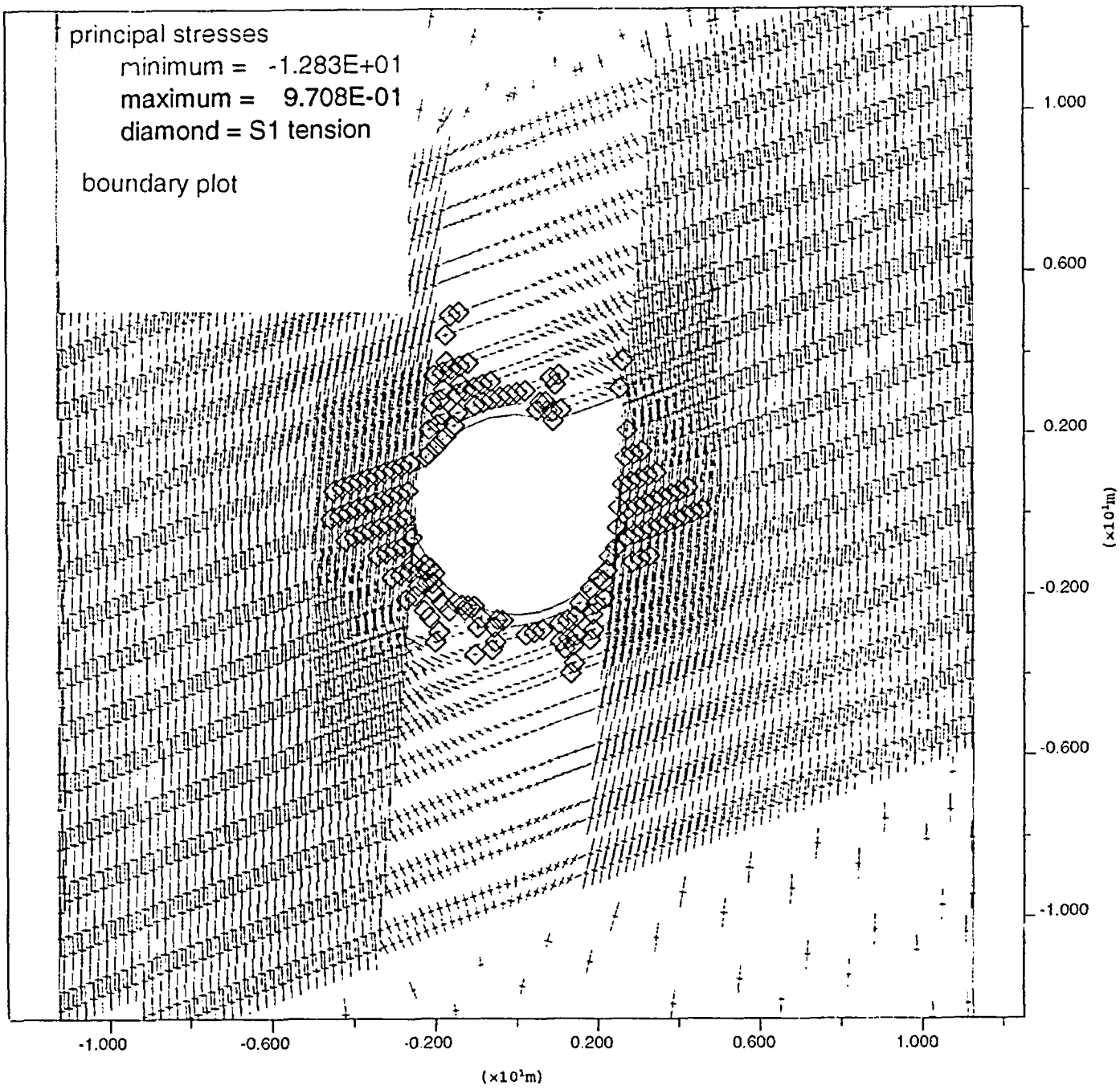

Figure 4-19. Principal stress distribution following drift excavation for Case 12. Stress unit is MPa.

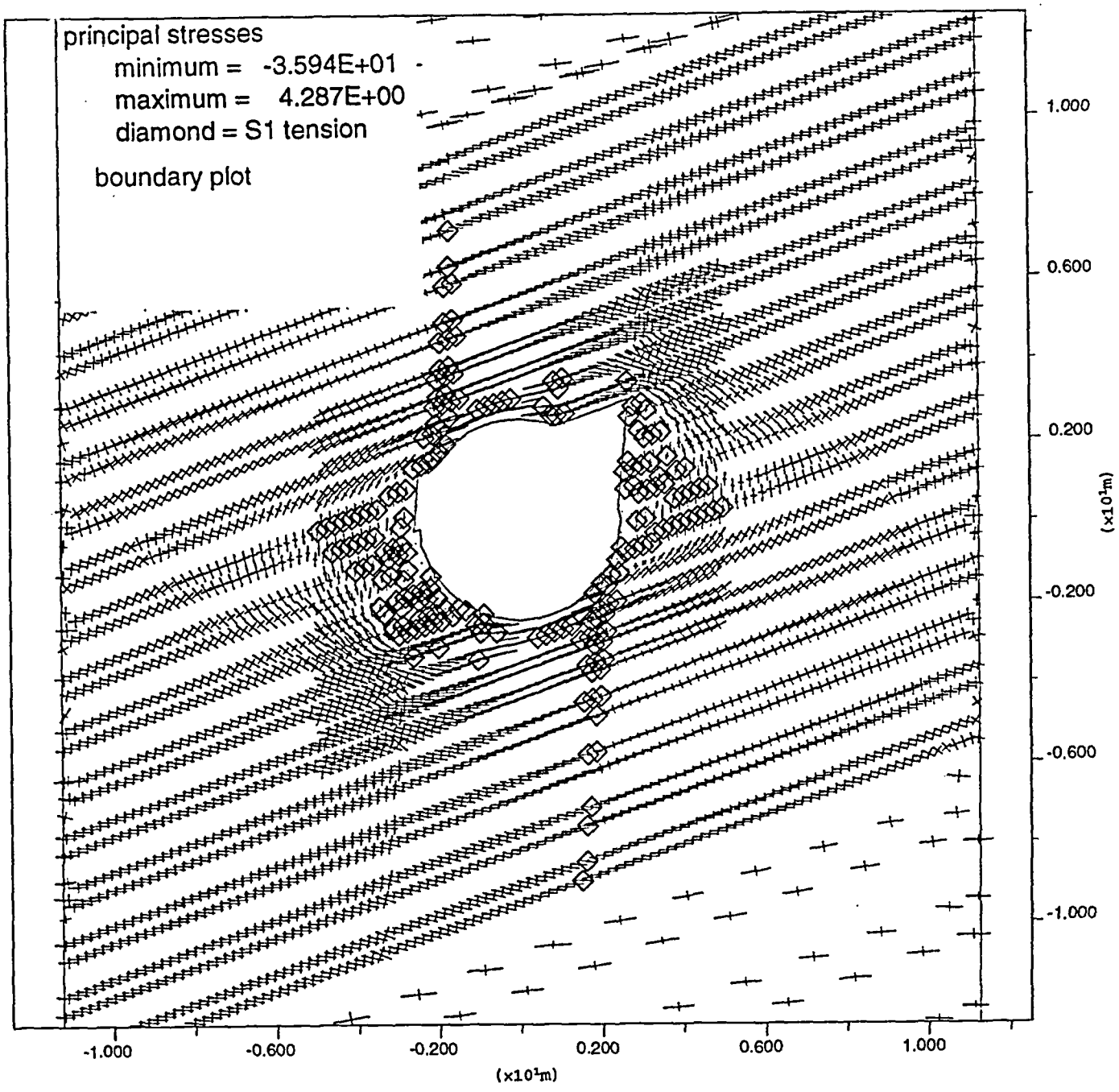

Figure 4-20. Principal stress distribution after 50 yr of heating for Case 12. Stress unit is MPa.

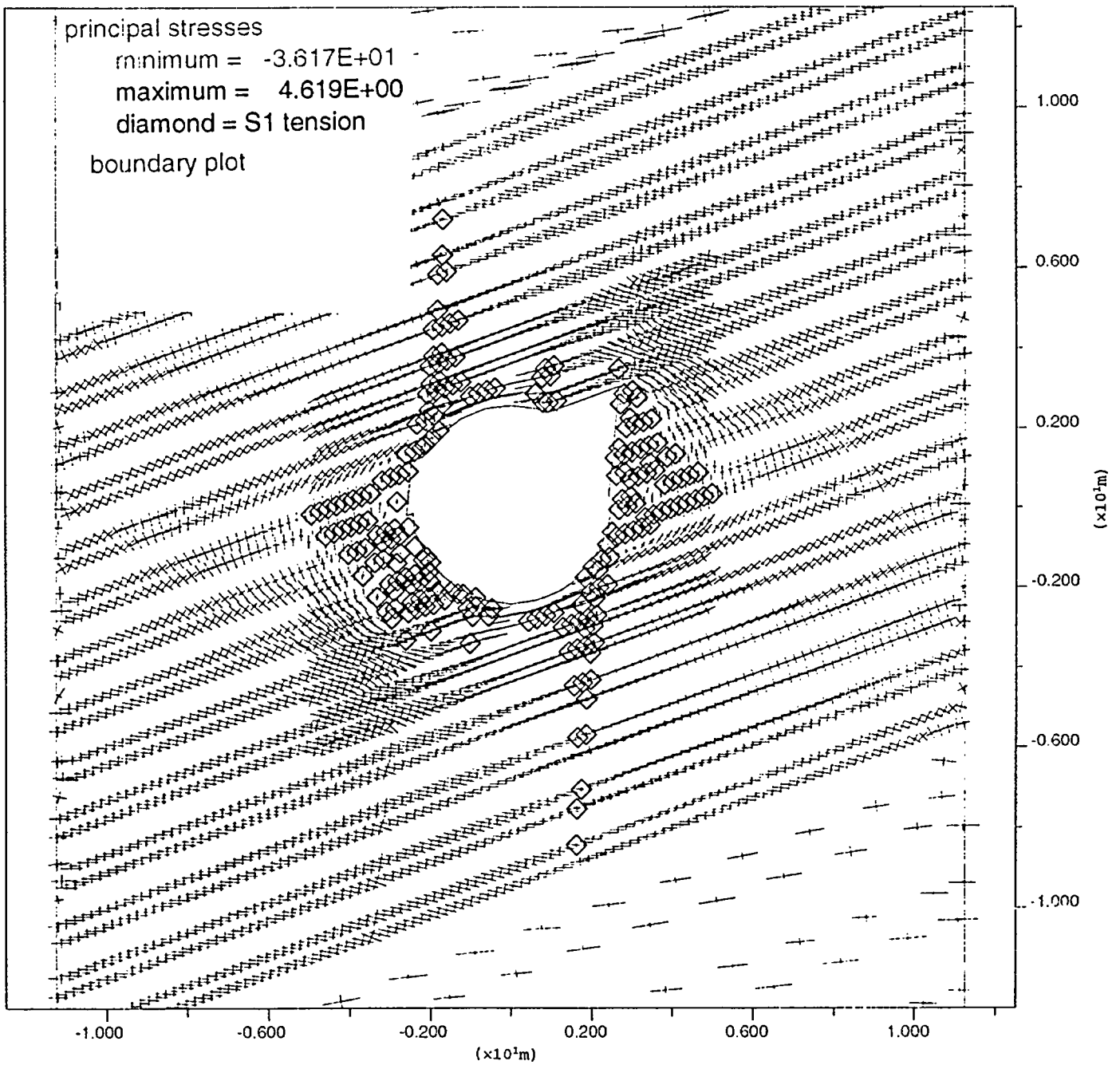

Figure 4-21. Principal stress distribution after 100 yr of heating for Case 12. Stress unit is MPa.

4.2.4 Failure Zones

Table 4-3 gives the approximate size of the area that experiences yielding for each of the UDEC runs. Yielding occurs in most of the high thermal loading cases. In most of these cases, the yielding zone is localized to the areas around the drift, extending less than 10 m^2. In the worst cases, the yielding zone can extend more than 250 m^2 (e.g., Cases 26 and 25). Both of these cases have high vertical-subvertical joint spacing, high thermal loading, high thermal expansion coefficient, low joint friction angle, and low intact rock cohesion and friction angle.

Case 26 has the most extensive yielding zone covering about 250 m^2 area around the drift. Figures 4-22 through 4-24 show failure distributions for Case 26 following drift excavation, 50 yr after heating, and 100 yr after heating, respectively. Yielding occurs only at one point following drift excavation (see figure 4-22). Extensive yielding occurs after heating (see figures 4-23 and 4-24). Therefore in this particular case, yielding is mainly a result of thermal loading. At 100 yr after heating, the failure zone almost covers the entire pillar.

Although the UDEC runs in this study do not couple the effect of water flow and the effect of yielding on rock permeability, most studies show that yielding of intact rock causes dilation which, in turn, would increase rock permeability (Wawersik and Brace, 1971; Wawersik and Fairhurst, 1970; Bieniawski, 1969; Ofoegbu and Curran, 1992). It is possible, though, that in some materials yielding might actually lead to further consolidation of the intact media and a permeability reduction. Such effects of yielding on the flow characteristics within a welded tuff should be addressed in separate studies, especially if such yielding is found to introduce microfractures in the tuff. Normally, from a mechanical stand point, the design of the emplacement drifts would incorporate thermal loadings, etc. so as to limit the extent of rock yielding.

4.2.5 Joint Opening and Closure

In most of the UDEC runs conducted in this study, subvertical joints near the side-walls of the drift tend to open because of stress relaxation after excavation of the drift. In addition, for many of the cases, portions of the subhorizontal joints immediately above and below the drift opened after drift excavation. Joint opening zone extends slightly outward from the drift walls after applying the thermal loads due to the effect of thermally induced expansion. Increased separation along those joints in the drift side-wall, as well as portions of the subhorizontal joints above and below the drift, is a result of drift heating. In all cases, closure along subvertical joints above and below the drift increases with heating. Figures 4-25 through 4-27 show the distribution of joint opening and closing zones immediately after drift excavation, 50 yr and 100 yr after waste emplacement, respectively for Case 12 (as identified in table 4-3). In these figures, red lines represent joints with zero normal stress and the thickness of green lines is proportional to the magnitude of joint closure. The figures show that thermal loading primarily causes joints in most areas around the drift to close, except in areas near drift side-walls where joints show the tendency of opening up. The thermally induced joint closure decreases near the drift wall as the waste decays with time after the preclosure period. This is reflected by the slight decrease in joint closure from 50 to 100 yr in most cases. However, the joint opening zone which occurs almost immediately after drift excavation would remain as it is so long as the drift exists. The maximum joint opening after 100 yr ranges from 0.02 cm (Case 8) to 1.4 cm (Case 26) for the high thermal loading (100 MTU/acre) cases and from 0.01 cm (Case 49) to 1.2 cm (Case 54) for the low thermal loading (20 MTU/acre) cases. The maximum joint opening after 50 yr ranges from 0.003 (Case 2) to 1.14 cm (Cases 25 and 30) for the high thermal loading cases and from 0.01 cm (Case 49) to 1.16 cm (Case 54) for the low thermal loading

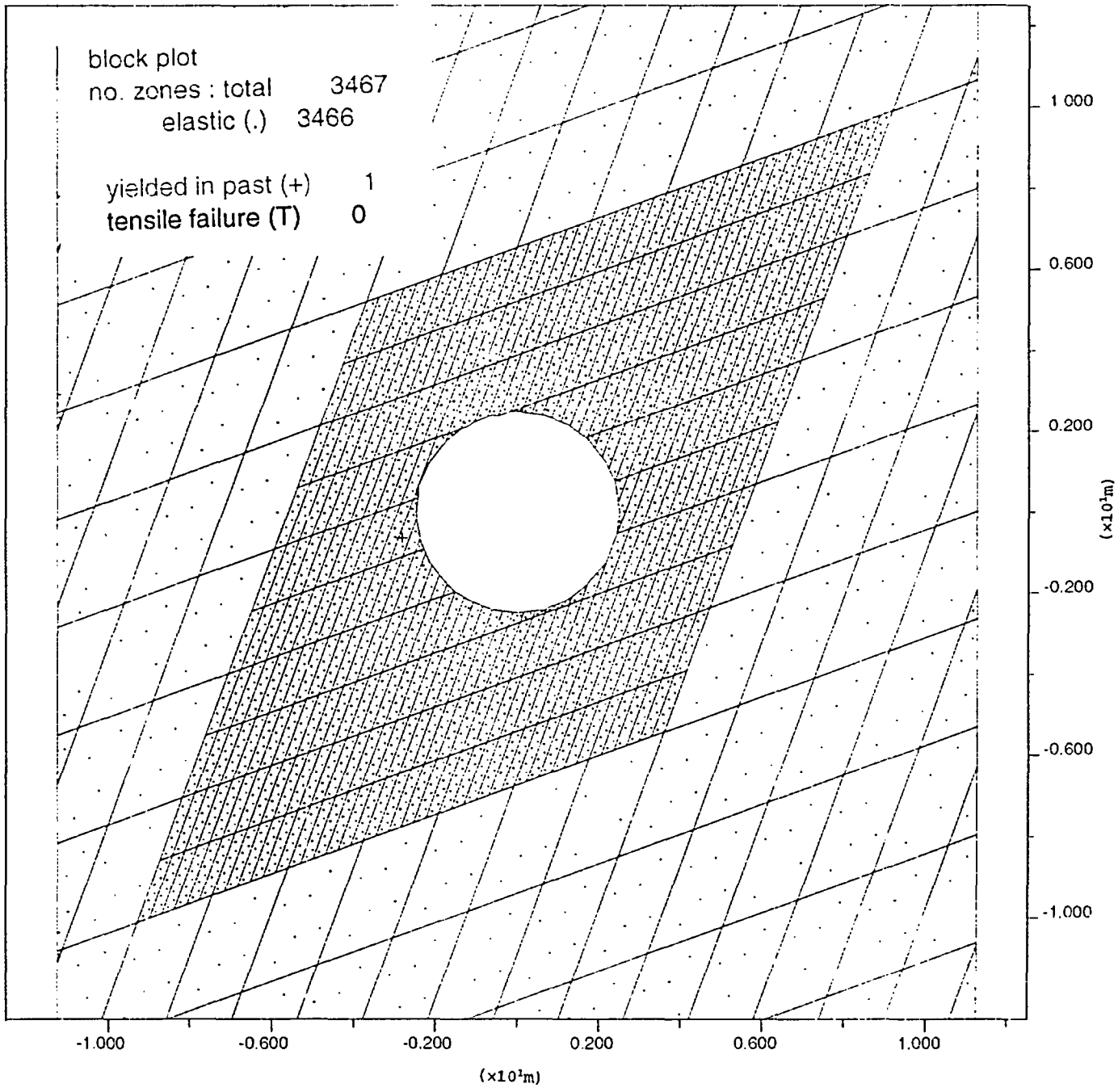

Figure 4-22. Failure distribution following drift excavation for Case 26

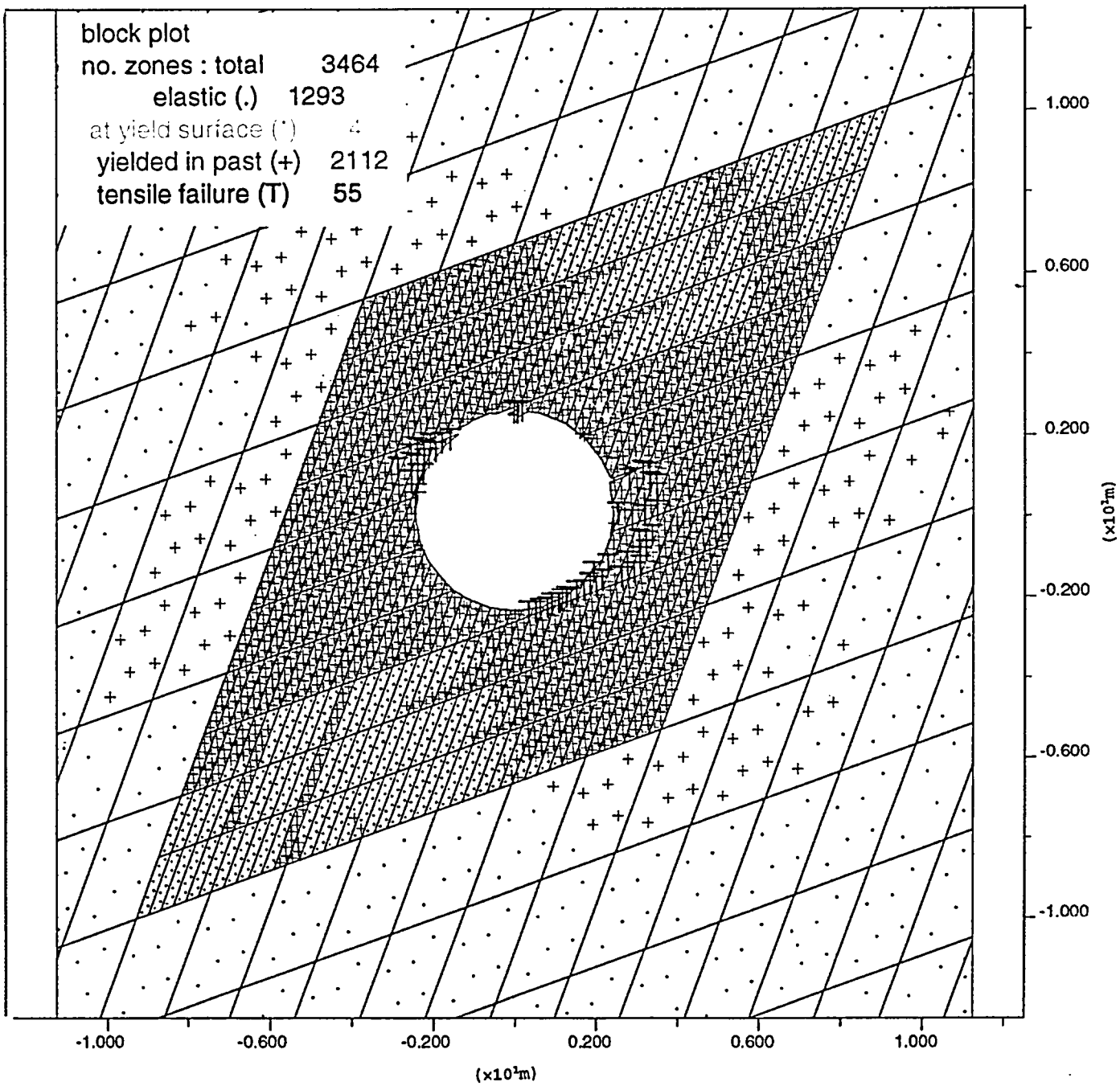

Figure 4-23. Failure distribution after 50 yr of heating for Case 26

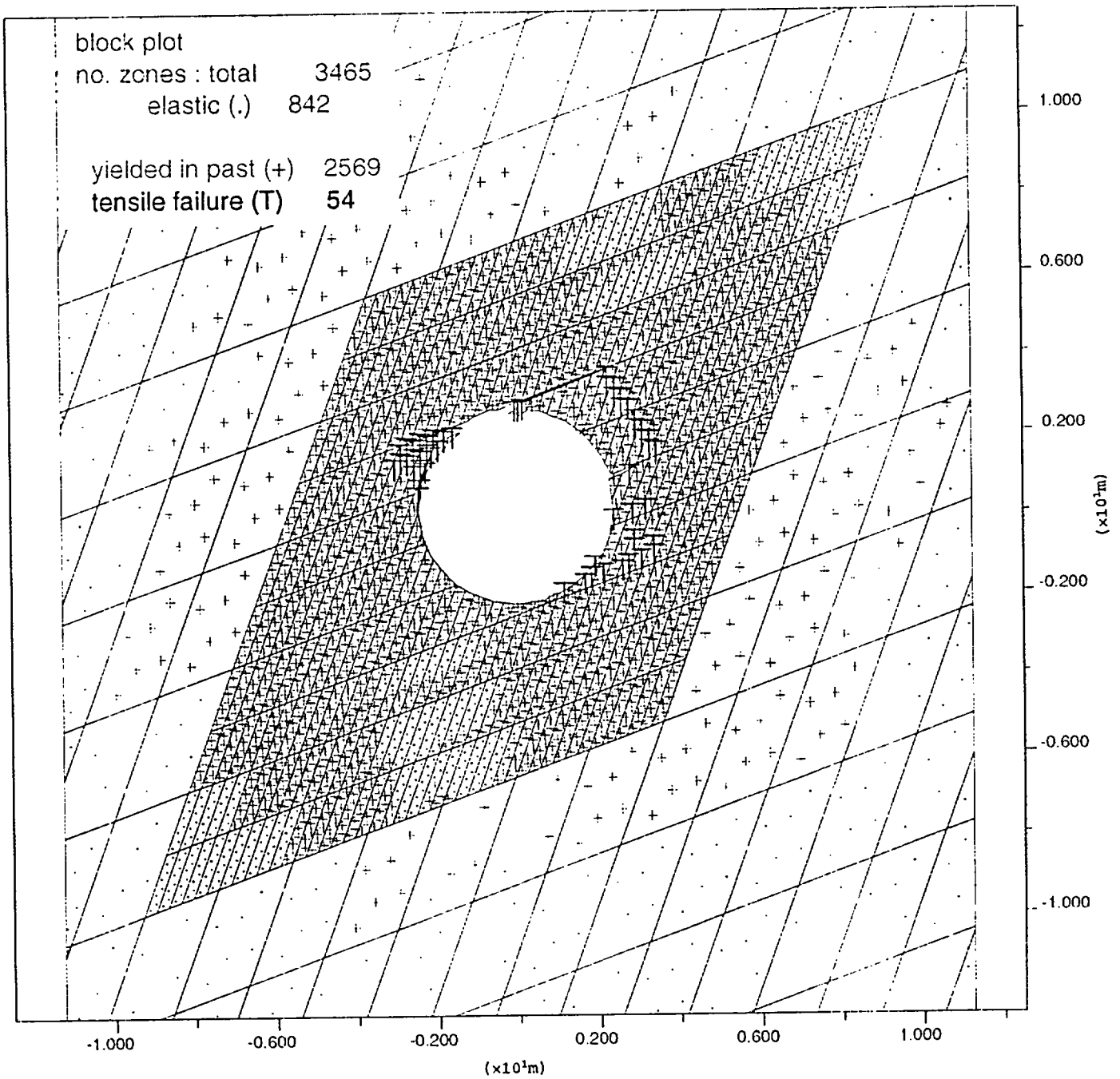

Figure 4-24. Failure distribution after 100 yr of heating for Case 26

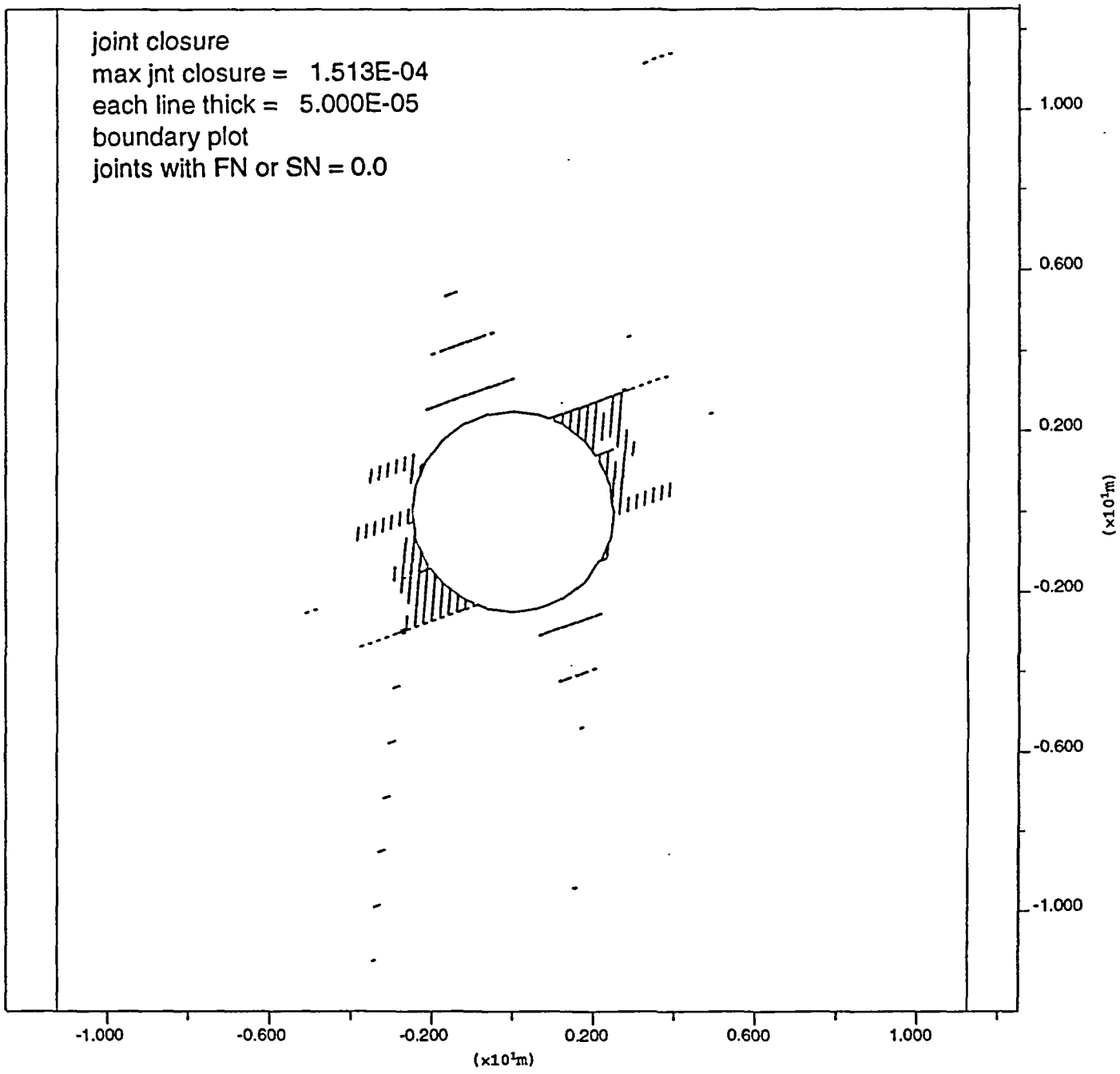

Figure 4-25. Distribution of joint opening and closure following drift excavation for Case 12. Red lines represent joints with zero normal stress. Thickness of green lines is proportional to magnitude of joint closure. Joint closure unit is meter.

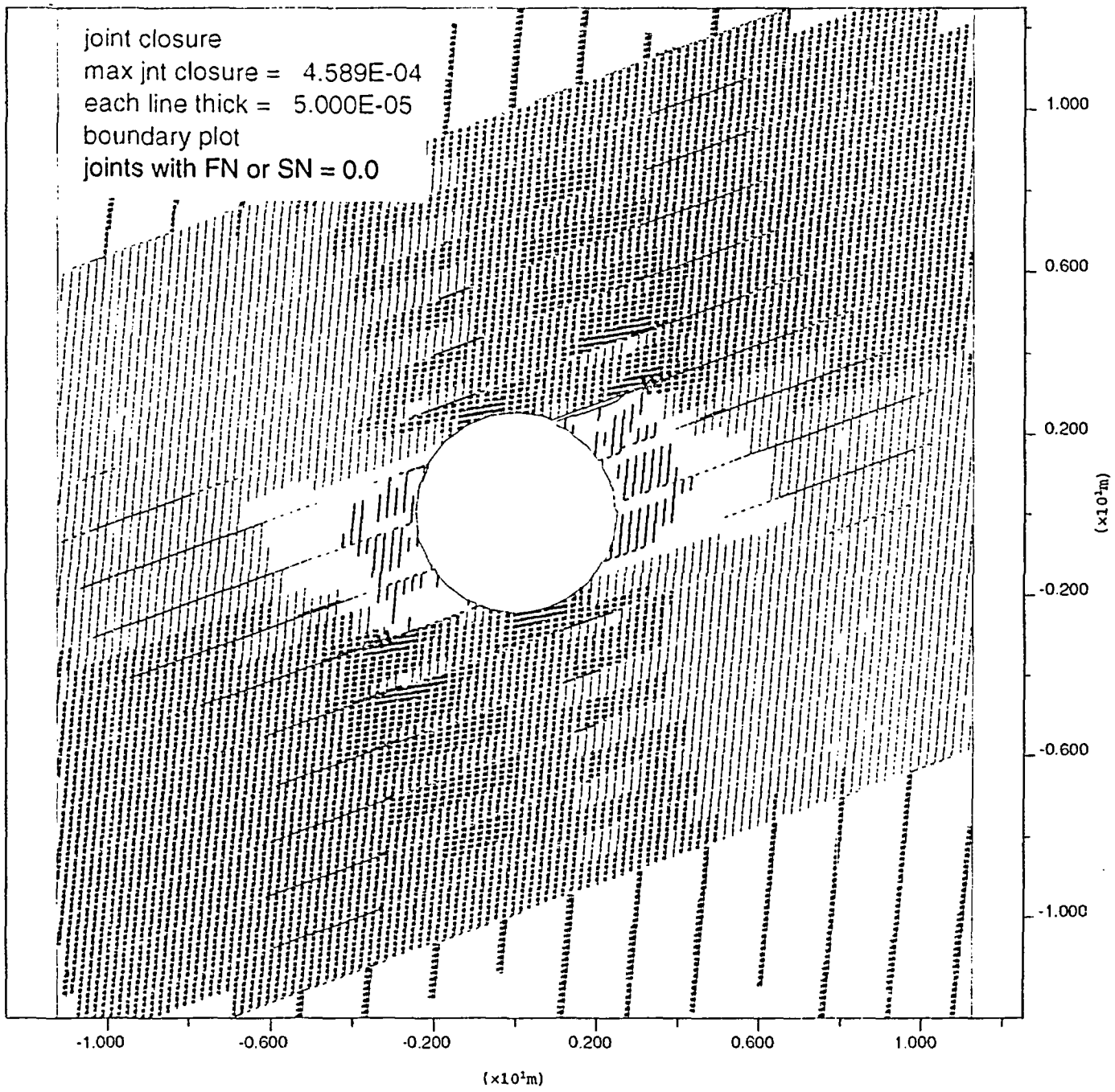

Figure 4-26. Distribution of joint opening and closure after 50 yr of heating for Case 12. Joint closure unit is meter.

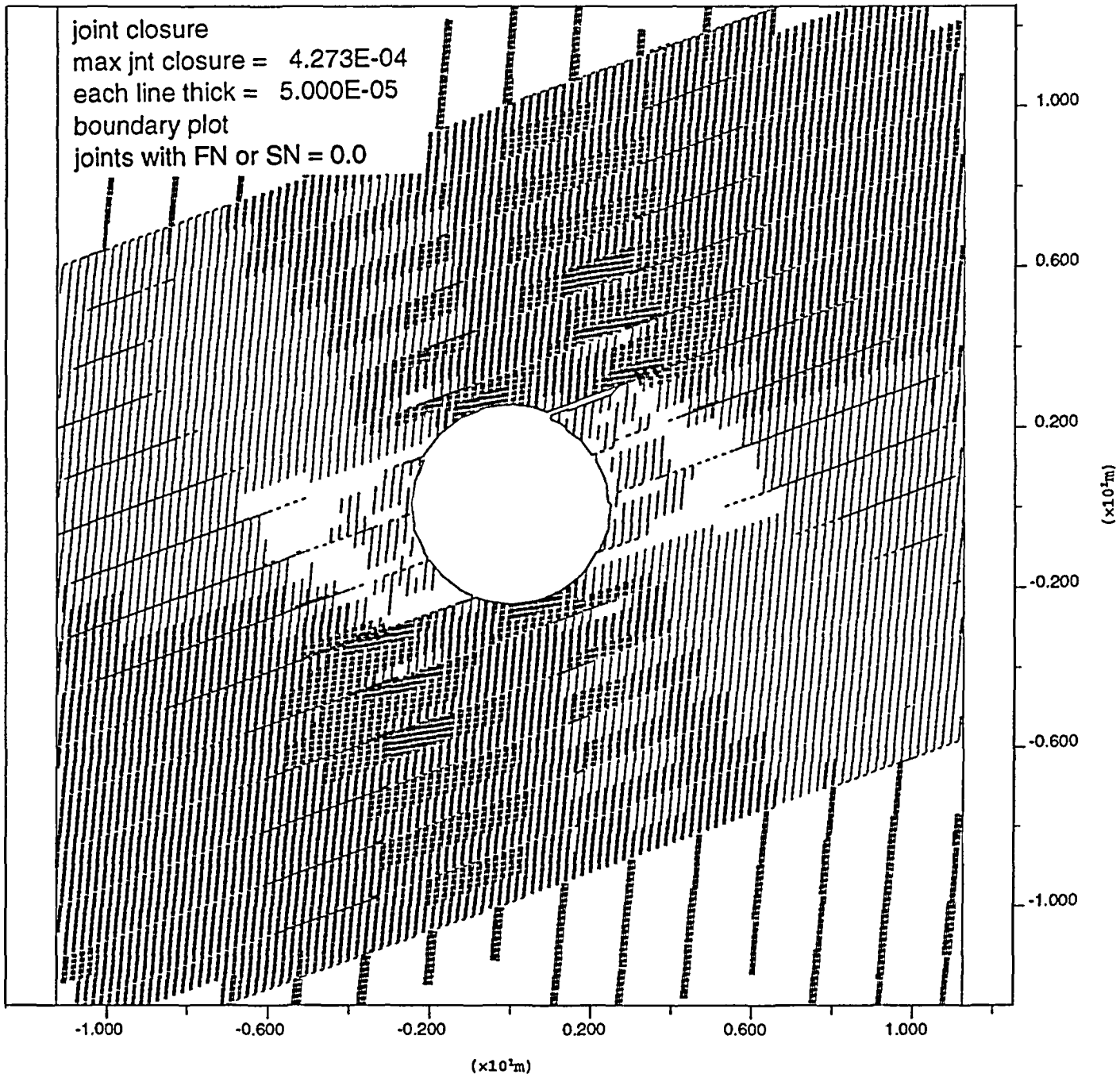

Figure 4-27. Distribution of joint opening and closure after 100 yr of heating for Case 12. Joint closure unit is meter.

cases. The maximum joint closure after 100 yr ranges from 0.0005 cm (Case 3) to 0.1 cm (Case 27), while the maximum joint closure after 50 yr ranges from 0.02 cm (Case 1) to 0.1 cm (Case 27) for the high thermal loading. The maximum joint closure after 100 yr ranges from 0.003 cm (Case 61) to 0.158 cm (Case 60), while the maximum joint closure after 50 yr ranges from 0.007 cm (Case 38) to 0.160 cm (Case 60) for the low thermal loading. Table 4-3 lists the maximum joint opening and closure for each of the factorial runs.

As a quantitative measure, table 4-4 presents the maximum depth of joint opening zone into the pillar from drift side wall. The maximum depth of joint opening zone ranges from 0.41 m (Case 8) to 3.81 m (Case 11) for high thermal loading cases and from zero (Case 45) to 3.33 m (Case 54) for low thermal loading cases. The similarity of the extent of joint opening zones in the high and low loading cases (table 4-3), as well as figures 4-1 through 4-3, show that while the thermal loading may affect the magnitude of joint separation, the size or zone of joint opening does not change significantly from mechanical excavation through a period of thermal loading of 100 yr for a particular case. While the extent of joint opening zone might be affected by joint mechanical properties, it does not appear to depend on the joint pattern. In fact, such a stress relaxation zone adjacent to the sidewalls of the opening is a commonly observed phenomenon in underground mining and rock engineering (Feder, 1978; Chen et al., 1993). Due to the limited extent of the stress relaxation zone (less than one diameter of the drift), its effect on groundwater inflow may be nominal. It should be noted that the increase in closure along subvertical joints above and below the drift with heating may have a greater impact on groundwater flow in the near field.

Table 4-4. Maximum depth of opening zone from drift wall after 100 yr

UDEC RUNS	Parameter Values	Depth (m)
Case1.dat	de	0.48
Case2.dat	abde	0.48
Case3.dat	acef	1.01
Case4.dat	bcef	1.25
Case5.dat	aegh	1.67
Case6.dat	beg	2.02
Case7.dat	cdefg	2.02
Case8.dat	abcdefg	0.41
Case9.dat	acdeh	0.95
Case10.dat	bcdeh	0.83
Case11.dat	efh	3.81
Case12.dat	abefh	1.67
Case13.dat	cegh	0.60
Case14.dat	abcegh	0.48

Table 4-4 Maximum depth of opening zone from drift wall after 100 yr (cont'd)

UDEC RUNS	Parameter Values	Depth (m)
Case15.dat	adefgh	1.43
Case16.dat	bdefgh	0.60
Case17.dat	ce	2.62
Case18.dat	abcei	2.26
Case19.dat	adefi	1.49
Case20.dat	bdefi	0.71
Case21.dat	acdegi	0.83
Case22.dat	bcdegi	1.47
Case23.dat	efgi	1.66
Case24.dat	abefgi	2.76
Case25.dat	aehi	2.28
Case26.dat	behi	3.17
Case27.dat	cdefhi	1.86
Case28.dat	abcdefhi	2.48
Case29.dat	deghi	1.72
Case30.dat	abdeghi	1.93
Case31.dat	acefghi	3.79
Case32.dat	bcefghi	2.28
Case33.dat	(1)	2.58
Case34.dat	ab	2.73
Case35.dat	acdf	1.04
Case36.dat	bcdf	0.77
Case37.dat	adgh	0.76
Case38.dat	bdg	0.91
Case39.dat	cfg	3.28
Case40.dat	abcfg	0.61
Case41.dat	ach	0.68

Table 4-4 Maximum depth of opening zone from drift wall after 100 yr (cont'd)

UDEC RUNS	Parameter Values	Depth (m)
Case42.dat	bch	4.03
Case43.dat	dfg	0.61
Case44.dat	abdfh	0.89
Case45.dat	cdgh	2.24
Case46.dat	abcdgh	0.44
Case47.dat	afgh	1.59
Case48.dat	bfgh	2.5
Case49.dat	cdi	0.60
Case50.dat	abcdi	0.30
Case51.dat	afi	1.74
Case52.dat	bfi	3.03
Case53.dat	acgi	0.52
Case54.dat	bcgi	3.33
Case55.dat	dfgi	0.47
Case56.dat	abdfgi	1.82
Case57.dat	adhi	1.21
Case58.dat	bdhi	1.74
Case59.dat	cfhi	0.45
Case60.dat	abcfhi	3.10
Case61.dat	ghi	3.11
Case62.dat	abghi	1.49
Case63.dat	acdfghi	0.61
Case64.dat	bcdfghi	1.51

4.3 SIGNIFICANCE OF MAIN PARAMETERS AND TWO-PARAMETER INTERACTIONS

In this study, attempts were made to identify several performance measures (responses) that can be used to assess the effects of the nine main parameters and their interactions on the performance of

underground excavations. The responses selected include maximum and minimum principal stresses around the excavation, maximum joint closure and opening (or separation), maximum joint shear displacement, roof-to-floor convergence, and area of yield zone around the excavation. Calculated values of these responses after 50 yr and 100 yr of heating are provided in table 4-3a and 4-3b, respectively.

In this study, the main parameters and two-parameter interactions are of interest. Higher-order interactions (three or more parameters interactions) are assumed to be negligible. Consequently, it is possible to pool the sum of squares of responses associated with these high-order interactions and use it as an alternate measure of error in the modeling results, allowing estimating or testing significance of the main and the two-parameter interaction effects. Since there are 64 nonreplicated UDEC runs in the analysis, there are 63 degrees of freedom. Also, there are 45 main and two-parameter interactions. This provides a total of 63 − 45 = 18 degrees of freedom for error estimation. An analysis of variance for each of the response types is performed. In the analysis, difference between variation of response of one parameter and the error term is evaluated to determine if this difference is significantly different from zero such that the null hypothesis should be rejected. A t-test was also performed to determine significant interacting between two parameters.

All the main parameters and the two-parameter interactions are tested for significance at the $\alpha=0.05$ level. A summarized result of the analysis of variance and t-tests are presented in the following sections and table 4-5. A detailed discussion is provided in appendix A. Note that no information regarding interaction effects is included in table 4-5.

4.3.1 Thermal Load

Thermal load appears to be an important parameter to all responses (performance measures) selected for assessment in this study. To reiterate, these responses include minimum principal stress, maximum principal stress, maximum joint shear displacement, maximum joint closure, maximum joint separation, roof-to-floor convergence, and extent of yield zone. Over the range of values investigated, no parameters were identified to have effect on minimum principal stress. Therefore, no further discussion related to this response is provided. An increase in thermal load tends to increase almost all responses. Increase in thermal load tends to reduce roof-to-floor convergence. There are some exceptions when the effect of thermal load may be negligible:

- when heating is under one of the following conditions: at large subvertical joint spacing, high intact rock cohesion, low intact rock Young's modulus, or low thermal expansion coefficient, a negligible effect on extent of yield zone for 50 and 100 yr of heating occurs.

- the effect of thermal load on extent of yield zone for 100 yr of heating will also be negligible for either large joint friction angle or high intact rock friction angle.

- a negligible effect on maximum joint separation for 50 yr of heating is produced when intact rock Young's modulus is small.

Table 4-5. General summary of factorial experiment

Parameter Increased	Performance Affected						
	Minimum Principal Stress	Maximum Principal Stress	Maximum Joint Shear Displacement	Maximum Joint Closure	Maximum Joint Separation	Maximum Roof-to-Floor Convergence	Extent of Yield Zone
Subvertical Joint Inclination	N	I	N (50 yr) I (100 yr)	N	D	D (50 yr) N (100 yr)	N
Subhorizontal Joint Inclination	N	N	N	N	I	N	N
Subvertical Joint Spacing	N	I	N (50 yr) D (100 yr)	N	N	N (50 yr) D (100 yr)	D
Joint Friction Angle	N	N	N	N	D	D	D
Thermal Load	N	I	I	I	I	D	I
Intact Rock Cohesion	N	N	N	N	N	N	N (50 yr) D (100 yr)
Intact Rock Friction Angle	N	N	N	N	N	N	D
Intact Rock Young's Modulus	N	I	N (50 yr) I (100 yr)	N (50 yr) I (100 yr)	I	D (50 yr) N (100 yr)	I
Thermal Expansion Coefficient	N	I	N	I	I	D (50 yr) N (100 yr)	I

Note: I = increase; D = decrease; N = no effect

4.3.2 Thermal Expansion Coefficient

High thermal expansion coefficient will cause high responses in maximum principal stress, maximum joint separation, maximum joint closure, and extent of yield zone for both 50 and 100 yr of heating. The exceptions where the effect of thermal expansion coefficient may be neglected include

- maximum joint closure for 100 yr of heating when thermal load is low.
- extent of yield zone for both 50 and 100 yr of heating at large joint friction angle, high intact rock friction angle, low thermal load, or low intact rock Young's modulus.

In general, thermal expansion coefficient does not have an effect on maximum joint shear displacement for either 50 or 100 yr of heating. A change in thermal expansion coefficient has an effect only when one of the following conditions is met:

- large subvertical joint spacing for both 50 and 100 yr of heating.
- high thermal load for 100 yr of heating.
- high intact rock friction angle for 100 yr of heating.

- small joint friction angle.

A high thermal expansion coefficient tends to reduce roof-to-floor convergence after 50 yr of heating. There is one exception where a change in thermal expansion coefficient does not have an effect when subhorizontal joint inclination is large. Most of the effect of thermal expansion coefficient on roof-to-floor convergence diminishes after 100 yr of heating. The effect remains to be significant after 100 yr of heating only when subhorizontal joint inclination is small.

4.3.3 Intact Rock Young's Modulus

The maximum principal stress, maximum joint separation , and extent of yield zone tends to be larger at high intact rock Young's modulus. The exceptions include

- no effect on maximum joint separation after 50 yr of heating when thermal load is low; no effect for 100 yr of heating when thermal load is low, subvertical joint spacing is large, or intact rock friction angle is large.

- no effect on extent of yield zone for both 50 and 100 yr of heating when joint or intact rock friction angle is large, thermal load is low, or thermal expansion coefficient is low.

- no effect on extent of yield zone after 100 yr of heating when subvertical joint spacing is large and intact rock cohesion is high.

Intact rock Young's modulus does not influence maximum joint shear displacement or maximum joint closure after 50 yr of heating. However, the effect does becomes significant after 100 yr of heating. Maximum joint shear displacement and maximum joint closure tends to be larger at a higher intact rock Young's modulus. There are exceptions:

- negligible effect on maximum joint shear displacement at small joint friction angle, low thermal load, or large intact rock friction angle.

- negligible effect on maximum joint closure when thermal load is low.

High intact rock Young's modulus will result in a small roof-to-floor convergence for 50 yr of heating. This effect diminishes after 100 yr of heating.

4.3.4 Subvertical Joint Inclination

Subvertical joint inclination over the range of values studied has no influence on either maximum joint closure or extent of yield zone. Large subvertical joint inclination tends to limit maximum joint separation and roof-to-floor convergence after 50 yr of heating. The effect is not important to roof-to-floor convergence when joint friction angle is large or thermal load is low. After 100 yr of heating, subvertical joint inclination remains important to maximum joint separation except when intact rock friction angle is small and the effect becomes insignificant for roof-to-floor convergence after 100 yr of heating. The only possible significant impact is when joint friction angle is small.

friction angle is small and the effect becomes insignificant for roof-to-floor convergence after 100 yr of heating. The only possible significant impact is when joint friction angle is small.

Subvertical joint inclination has a positive effect on maximum principal stress. The following are exceptions:

- no effect after 50 yr of heating when either subhorizontal joint inclination or thermal expansion coefficient is low.
- no effect after 100 yr of heating when joint friction angle is large.

Subvertical joint inclination is insignificant for maximum joint shear displacement after 50 yr of heating. However, it has a significant effect after 100 yr of heating except when subvertical joint spacing is large or thermal load is low; an increase in subvertical joint inclination tends to increase maximum joint shear displacement.

4.3.5 Subhorizontal Joint Inclination

In general, subhorizontal joint inclination does not play a significant role in controlling maximum principal stress, maximum joint shear displacement, maximum joint closure, roof-to-floor convergence, and extent of yield zone. There are, of course, some exceptions to this general rule as follows:

- significant negative effect on maximum principal stress when subvertical joint inclination is low and significant positive impact when subvertical joint inclination is large for 50 yr of heating. The terms positive and negative effects are used frequently in section 4.3. A positive effect means a higher or larger response resulting from a higher value of a parameter while a negative effect indicates that a decrease in the value of a parameter results in an increase in response.
- significant negative effect on maximum principal stress when thermal load is high for 100 yr of heating.
- significant positive effect on roof-to-floor convergence when thermal expansion coefficient is high for both 50 and 100 yr of heating.
- significant positive effect on extent of yield zone when subvertical joint inclination is small.

When subhorizontal joint inclination becomes large, maximum joint separation increases for both 50 and 100 yr of heating. For a case where subvertical joint spacing is small, the effect of subhorizontal joint inclination is negligible.

4.3.6 Subvertical Joint Spacing

A change in subvertical joint spacing provides no effect on either maximum joint closure or maximum joint separation. However, for a small subhorizontal joint inclination, high thermal load, or

high intact rock Young's modulus condition, subvertical joint spacing will have a negative effect on maximum joint separation after 100 yr of heating.

Variation of subvertical joint spacing does not seem to affect the maximum joint shear displacement or roof-to-floor convergence after 50 yr of heating. The only exception is when thermal expansion coefficient is low for maximum joint shear displacement and intact rock friction angle is low for roof-to-floor convergence. The effect of subvertical joint spacing becomes important as the excavation is heated for 100 yr. Large subvertical joint spacing tends to limit the amount of maximum joint shear displacement and roof-to-floor convergence. Subvertical joint spacing has no effect for a case where thermal load is high on maximum joint shear displacement.

Large subvertical joint spacing will increase the maximum principal stress while limit the extent of yield zone around an excavation for both 50 and 100 yr of heating. The exceptions include

- negligible effect on maximum principal stress when joint friction angle is small, intact rock Young's modulus is low, or intact rock friction angle is high for 50 yr of heating.
- negligible effect on maximum principal stress for 100 yr of heating when intact rock friction angle is large.
- negligible effect on extent of yield zone when thermal load is low for 50 and 100 yr of heating.
- negligible effect on extent of yield zone when joint friction angle is large, intact rock friction angle is large, or intact rock Young's modulus is low.

4.3.7 Joint Friction Angle

A change in joint friction angle does not impact maximum principal stress, maximum joint shear displacement, or maximum joint closure. It has a significant negative effect on maximum joint separation, roof-to-floor convergence, and extent of yield zone. Some exceptions are recognized:

- significant negative effect on maximum principal stress when subvertical joint inclination is large for 100 yr of heating.
- marginal negative effect on maximum joint shear displacement when intact rock Young's modulus is low or thermal expansion coefficient is high.
- insignificant effect on roof-to-floor convergence for a case where subvertical joint inclination is high for 100 yr of heating.
- no effect on extent of yield zone when intact rock friction angle is large, intact rock Young's modulus is low, or thermal expansion coefficient is low for both 50 and 100 yr of heating.
- no effect on extent of yield zone for cases where subvertical joint spacing is large, intact rock cohesion is high, or thermal load is low.

A change in intact rock cohesion does not appear to have an effect on any performance measures (responses) of interest other than it shows a significant negative impact on extent of yield zone after 100 yr of heating. Exceptions are

- significant negative effect on extent of yield zone after 50 yr of heating when thermal load is high.

- negligible effect on extent of yield zone for conditions where joint friction angle is large, intact rock friction angle is large, intact rock Young's modulus is low, or thermal load is low.

4.3.9 Intact Rock Friction Angle

Intact rock friction angle has shown significance only to extent of yield zone. When the intact rock friction angle becomes larger, the extent of yield zone tends to be smaller. A number of exceptions are

- intact rock friction angle has a positive effect on maximum principal stress when subvertical joint spacing is low for both 50 and 100 yr of heating.

- intact rock friction angle has a negative effect on maximum joint shear displacement after 100 yr of heating when either intact rock Young's modulus is high or thermal expansion coefficient is small.

- intact rock friction angle has a negative effect on maximum joint separation after 100 yr of heating for cases where subvertical joint inclination is large, intact rock Young's modulus is high, or joint friction angle is small.

- intact rock friction angle has a negative effect on roof-to-floor convergence after 50 yr of heating when vertical joint spacing is small.

- intact rock friction angle does not appear to have an effect on extent of yield zone when joint friction angle is large, intact rock Young's modulus is low, or thermal expansion coefficient is low for both 50 and 100 yr of heating.

- intact rock friction angle has no impact on extent of yield zone after 100 yr of heating for cases where subvertical joint spacing is large, intact rock cohesion is high, or thermal load is low.

5 CONCLUSIONS AND RECOMMENDATIONS

5.1 CONCLUSIONS

The TM parametric study of emplacement drifts without backfill, rock support, and seismic load for 100 yr of heating shows that thermal load is the most important parameter to affect most of the performance measures studied herein. The magnitude of maximum principal stress, maximum joint shear displacement, maximum joint closure, maximum joint separation, and extent of yield zone increases as thermal load increases from 20 MTU/acre to 100 MTU/acre. An increase in thermal load from 20 MTU/acre to 100 MTU/acre either reduces opening convergence or causes opening divergence. Increase in rock mass yield zone, rock joint shear displacement, and corresponding dilation will decrease the stability of the underground opening, increase fracture opening in some areas, but decrease fracture opening in other areas that could change groundwater flow and radionuclide transport pathways.

Magnitude of maximum principal stress, maximum joint separation, maximum joint closure, and extent of yield zone increases with the increase of coefficient of thermal expansion. Increase in the coefficient of thermal expansion reduces the short-term convergence of the opening, but the long-term opening convergence is not reduced by the increase of coefficient of thermal expansion. As in the case of thermal load, an increase in the coefficient of thermal expansion will increase both the instability of the underground opening and fracture dilation.

Increase in intact rock Young's modulus causes increases in maximum principal stress, maximum joint separation, and extent of yield zone. Like the coefficient of thermal expansion, increase in intact rock Young's modulus reduces the short-term convergence of the opening, but the long-term opening convergence is not reduced by increase of intact rock Young's modulus. Intact rock Young's modulus does not have an effect on either maximum joint shear displacement or maximum joint closure for 50 yr of heating, however, these quantities increase with increase of intact rock Young's modulus for 100 yr of heating. Intact rock Young's modulus affects both the stability of underground openings and fracture dilation.

The maximum principal stress increases with the increase of subvertical joint inclination when either subhorizontal joint inclination or the coefficient of thermal expansion is at its higher value. The effect of subvertical joint inclination on maximum joint separation and maximum joint shear displacement is more dominant after 100 yr of heating than after 50 yr. Increase in subhorizontal joint inclination increases maximum joint separation for both 50 and 100 yr of heating. The orientations of both vertical and horizontal joints influence the stability and fracture dilation behaviors of rock mass around the underground opening.

A change in subvertical joint spacing generally has no effect on either maximum joint closure or maximum joint separation. Variation of subvertical joint spacing does not affect maximum joint shear displacement or opening convergence after 50 yr of heating, however, the effect becomes important as the excavation is heated for 100 yr. Large subvertical joint spacing tends to limit the maximum joint shear displacement, opening convergence, and extent of yield zone around an excavation while it tends to increase the maximum principal stress for both 50 and 100 yr of heating. Both opening stability and fracture dilation are sensitive to change of subvertical joint spacing.

Joint friction angle has a significant effect on maximum joint separation, opening convergence, and extent of yield zone. Intact rock friction angle has a significant effect on only the extent of yield zone. When the intact rock friction angle becomes larger, the extent of yield zone tends to be smaller. Both joint friction angle and intact rock friction angle affect opening stability and fracture dilation.

Variation of intact rock cohesion does not appear to have an effect on any performance measures (responses) of interest other than having a significant negative effect on extent of yield zone after 100 yr of heating; that is, an increase in intact rock cohesion will reduce the extent of yield zone around an excavation.

In general, thermal loading causes ground heave which leads to upward movement of both the roof and floor. In some cases, floor upward movement is greater than roof upward movement, resulting in positive convergence. In other cases, floor upward movement is less than roof upward movement, resulting in negative convergence. Most of the low thermal loading cases have positive convergence. Negative convergence occurs in about one-half of the high thermal loading cases.

Shear displacement usually occurs along joints near the drift following drift excavation. Thermal load increases joint shear displacement, especially along the horizontal-subhorizontal joint set. Although in most cases the extensiveness and magnitude of joint shear displacement are rather limited, there are cases where thermally-enhanced joint shear displacement becomes so extensive that it could greatly increase shear-induced permeability and, therefore, increase the possibility of groundwater inflow into the drift.

Yielding occurs in some of the UDEC run cases, mostly by tensile failure. Although yielding zones are localized to the immediate areas around the drift, they extend to cover the entire pillar in the worst cases. Most studies show that yielding of intact rock causes rock to dilate which, in turn, could increase rock permeability. It is therefore important in the design of the emplacement drift to make sure the extent of yielding zone is limited to avoid direct connections between the drifts or with overlying strata which could facilitate groundwater inflow.

In most of the UDEC runs conducted in this study, subvertical joints near the side-walls of the drift as well as horizontal-subhorizontal joints in the immediate vicinity of the drift tend to open up due to stress relaxation. This joint opening phenomenon occurs immediately after drift excavation and the extent of this zone does not appear to increase significantly during the heating stage. Thermal loading increases the closure along subvertical joints above and below the drift except in zones where increased separation occurs. In general, the extent of these zones is less than one drift diameter. It is anticipated that the extent of joint opening zones will increase significantly when the drifts are subjected to repeated seismic loads.

Maximum compressive stress usually occurs in drift side-walls immediately after excavation. The maximum compressive principal stress increases and its location shifts to the immediate roof and floor areas after heating. Tensile stresses are predicted following drift excavation as well as after heating for most of the UDEC run cases. Heating appears to change the location of the maximum tensile stress from roof and floor areas following drift excavation to the side-walls of the drift. It is usually noticed that the circumferential stress increases in the roof with heating, while it decreases in the ribs of the drift due to thermal expansion.

5.2 RECOMMENDATIONS

The overall objective of the TM parametric study was to identify thermal and site specific natural phenomena and rock mechanical and thermal parameters that may significantly influence the pre- and postclosure performance of the proposed repository under heated and seismic conditions. The Phase I TM parametric study reported herein involved a parametric investigation of emplacement drifts without backfill, rock support, and seismic load for 100 yr of heating using the distinct element computer code UDEC. Based on the overall objective of the TM parametric study and results of Phase I TM parametric study, the following recommendations are made.

(i) The pre- and postclosure performance of the proposed repository under heated conditions is sensitive, in addition to thermal load, to the following rock mechanical and thermal parameters: thermal expansion coefficient, intact rock Young's modulus, subvertical joint inclination, subhorizontal joint inclination, subvertical joint spacing, joint friction angle, and intact rock friction angle. These parameters should be used for subsequent parametric studies, as applicable. Parametric study of selected cases should be conducted for more than 100 yr of heating to contribute toward addressing postclosure performance of the proposed repository under heated and seismic conditions.

(ii) Provide seismic analysis on 5 to 10 of the most sensitive runs of Phase I TM parametric study, including consideration of effect of repeated seismic loads. The dynamic ground motion at YM due to earthquakes and nearby underground nuclear weapons testing will take place in the environment of *in situ* stresses and thermal load for which Phase I TM parametric study was conducted. It is anticipated that the response of the jointed rock mass will increase significantly when subjected to dynamic ground motion, including repeated seismic loads (Kana et al., 1991 and 1995; Hsiung et al., 1992; Ghosh et al., 1996). Results of Phase I TM parametric study should be used to select 5 to 10 UDEC runs that will provide the most sensitive combination of parameters.

(iii) Conduct TM parametric study on backfilled drifts, including consideration of effect of repeated seismic loads. The stability of emplacement drifts, the thermal environment in the emplacement drifts and waste packages, and groundwater flow and radionuclide transport may be significantly affected by the absence or presence of backfill in the emplacement drifts. Emplacement drifts could be backfilled (TRW Environmental Safety Systems, Inc., 1994a) for four major reasons: (i) to prevent deleterious rock movement in the strata between the ground surface and repository horizon that may cause subsidence; (ii) to provide a predetermined environment around waste packages to enhance the long-term performance of the waste package exterior; (iii) to protect, or cushion, the waste package from damage caused by rock falling onto the waste package; and (iv) to retard transport of radionuclides to the accessible environment. A parametric study on backfilled drifts would contribute to addressing the first three topics.

(iv) Consider temperature- and time-dependent degradation of rock and joint properties for parametric studies. It is well recognized that rock mass deteriorates as temperature increases and/or time passes (Martin, 1972; Nimick and Connolly, 1991; Price et al., 1987; Carter, 1975 and 1976). Degraded rock and joint properties should be considered for parametric studies.

(v) Conduct TM parametric study for selected cases using an alternative model, such as ABAQUS, to enhance confidence in the numerical analysis results.

(vi) Conduct TM parametric study on rock-bolts, including consideration of effect of repeated seismic loads.

(vii) Provide abstracted input to the SEISMO (i.e., seismic effects) module (Freitas et al., 1994) in the Total Performance Assessment code (Sagar and Janetzke, 1993), and Engineered Barrier System Performance Assessment Code (Lichtner, 1994).

Details of the scope of the previously recommended studies will be developed to enable the NRC staff to address issues relevant to time-dependent TM coupled response of a jointed rock mass as identified in the Repository Design and TM Effects KTI Implementation Plan[1].

[1] Nuclear Regulatory Commission. 1996. NRC Key Technical Issue Implementation Plans for FY1996.

6 REFERENCES

Althaus, E.A., Friz-Topfer, C. Lempp, and O. Hatau. 1994. Effects of water on strength and failure mode of coarse-grained granites at 300 °C. *Rock Mechanics and Rock Engineering* 27: 21.

Barton, N., S. Bandis, and K. Bakhtar. 1985. Strength, deformation and conductivity coupling of rock joints. *International Journal Rock Mechanics Mining Science & Geomechanical Abstracts* 22: 121–140.

Bieniawski, Z.T. 1969. Behaviour of fractured rock under multiaxial compression. *Structure, Solid Mechanics and Engineering Design*. Vol. 1. M. Te'eni, ed. Toronto, Canada: Wiley Interscience: 589–598.

Board, M. 1989. *UDEC (Universal Distinct Element Code) Version ICG 1.5*. Volume 1–3. NUREG/CR-5429. Washington, DC: Nuclear Regulatory Commission.

Brechtel, C.E., and D.S. Kessler. 1995. *Geotechnical Characterization of the North Ramp of the Exploratory Studies Facility*. Volume I - Data Summary. SAND95-0488/1. Albuquerque, NM: Sandia National Laboratories.

Buscheck, T.A., and J.J. Nitao. 1993. The analysis of repository-heat-driven hydrothermal flow at Yucca Mountain. *Proceedings of the Fourth Annual International Conference on High-Level Radioactive Waste Management*. New York, NY: American Society of Civil Engineers.

Buscheck, T.A., and J.J. Nitao. 1994. The impact of buoyant, gas-phase flow and heterogeneity on thermo-hydrological behavior at Yucca Mountain. *Proceedings of the Fifth Annual International Conference on High-Level Radioactive Waste Management*. La Grange Park, IL: American Nuclear Society: 2,450–2,474.

Carter, N.L. 1975. High-temperature flow of rocks. *Reviews of Geophysics and Space Physics*. 14(3): 301–360.

Carter, N.L. 1976. Steady state flow of rocks. *Reviews of Geophysics and Space Physics*. 14(3): 344–349.

Chen, R., W.C. Brisbin, and B. Stimpson. 1993. Mining-induced deformation in potash yield pillars, Vanscoy, Saskatchewan. *Canada Geotechnical Journal* 30: 297–307.

Christianson, M. 1979. *TEMP3D: A Computer Program for Determining Temperatures Around Single or Arrays of Constant or Decaying Heat Sources, User's Guide and Manual*. Minneapolis, MN: University of Minnesota, Department of Civil & Mineral Engineering.

Christianson, M.C., and B. Brady. 1989. *Analysis of Alternative Waste Isolation Concepts*. NUREG/CR-5389. Washington, DC: Nuclear Regulatory Commission.

de Marsily, G. 1987. An overview of coupled processes with emphasis on geohydrology. *Coupled Processes Associated with Nuclear Waste Repositories*. C.F. Tsang, ed. San Diego, CA: Academic Press: 27–37.

Feder, G. 1978. Shear fracture of rock mass in vicinity of deep cavities-test results and analytical concepts (in German). *Rock Mechanics* 6: 71–102.

Freitas, C.J., R.B. Codell, and N.A. Eisenberg. 1994. *SEISMO Version 1.0-A Module for Simulation of Seismo—Mechanical Scenarios, Model Description, and User Guide*. CNWRA 94-008. San Antonio, TX: Center for Nuclear Waste Regulatory Analyses.

Ghosh, A., S.M. Hsiung, G.I. Ofoegbu, and A.H. Chowdhury. 1994. *Evaluation of Computer Codes for Compliance Determination Phase II*. CNWRA 94-001. San Antonio, TX: Center for Nuclear Waste Regulatory Analyses.

Ghosh, A., S.M. Hsiung, and A.H. Chowdhury. 1996. *Seismic Response of Rock Joints and Jointed Rock Mass*. NUREG/CR-6388. Washington, DC: Nuclear Regulatory Commission.

Hibbitt, Karlsson, and Sorensen, Inc. 1995. *ABAQUS Users' Manual, Version 5.5*. Pawtucket, RI: Hibbitt, Karlsson, and Sorensen, Inc.

Hill, D.P., et al. 1993. Seismicity remotely triggered by the magnitude 7.3 earthquake. *Science* 260: 1,617–1,623.

Hoek, E., and E.T. Brown. 1980. *Underground Excavation in Rock*. London, UK: The Institution of Mining and Metallurgy.

Hsiung, S.M., W. Blake, A.H. Chowdhury, and T.J. Williams. 1992. Effects of mining-induced seismic events on a deep underground mine. *PAGEOPH* 139(3/4): 741–762.

Itasca Consulting Group, Inc. 1993. *UDEC: Universal Distinct Element Code. Volume I: User's Manual*. Version 2.0. Minneapolis, MN: Itasca Consulting Group, Inc.

Jaeger, J.C., and N.G.W. Cook. 1979. *Fundamentals of Rock Mechanics*. 3rd Edition. London, UK: Chapman and Hall, Ltd.

Kana, D.D., B.H.G. Brady, B.W. Vanzant, and P.K. Nair. 1991. *Critical Assessment of Seismic and Geomechanics Literature Related to a High-Level Nuclear Waste Underground Repository*. NUREG/CR-5440. Washington, DC: Nuclear Regulatory Commission.

Kana, D.D., D.J. Fox, S.M. Hsiung, and A.H. Chowdhury. 1995. *An Experimental Model Study of Seismic Response of an Underground Opening in Jointed Rock*. CNWRA 95-012. San Antonio, TX: Center for Nuclear Waste Regulatory Analyses.

Kemeny, J., and N. Cook. 1990. Rock mechanics and crustal stress. *Demonstration of Risk-Based Approach to High-Level Waste Repository Evaluation*. R.K. McGuire, ed. EPRI NP-7057. Golden, CO: Risk Engineering Inc.: 5-1 to 5-20.

Klavetter, E.A., and R.R. Peters. 1986. *Estimation of Hydrologic Properties of an Unsaturated Fracture Rock Mass*. SAND84-2642. Albuquerque, NM: Sandia National Laboratories.

Lichtner, P.C. 1994. *Engineered Barrier System Performance Assessment Codes (EBSPAC) Progress Report October 1, 1993 through September 25, 1994*. CNWRA 94-026. San Antonio, TX: Center for Nuclear Waste Regulatory Analyses.

Lin, W., and W.D. Daily. 1989. Laboratory study of fracture healing in Topopah Spring tuff — implications for near field hydrology. *Nuclear Waste Isolation in Unsaturated Zone Focus '89 Proceedings*. La Grange Park, IL: American Nuclear Society: 443–449.

Manteufel, R.D., M.P. Ahola, D.R. Turner, and A.H. Chowdhury. 1993. *A Literature Review of Coupled Thermal-Hydrologic-Mechanical-Chemical Processes Pertinent to the Proposed High-Level Nuclear Waste Repository at Yucca Mountain*. NUREG/CR-6021. Washington, DC: Nuclear Regulatory Commission.

Martin III, R.J. 1972. Time-dependent crack growth in quartz and its application to the creep of rocks. *Journal of Geophysical Research* 77(8).

Mohanty, S., A.H. Chowdhury, S.M. Hsiung, and M.P. Ahola. 1994. *Single Fracture Flow Behavior of Apache Leap Tuff Under Normal and Shear Loads*. CNWRA 94-024. San Antonio, TX: Center for Nuclear Waste Regulatory Analyses.

Nataraja, M.S., and T.Brandshaug. 1992. *Staff Technical Position on Geologic Repository Operations Area Underground Facility Design — Thermal Loads*. NUREG-1466. Washington, DC: Nuclear Regulatory Commission.

Nimick, F.B., and J.R. Connolly. 1991. *Calculation of Heat Capacities for Tuffaceous Units from the Unsaturated Zone at Yucca Mountain, Nevada*. SAND 88-3050. Albuquerque, NM: Sandia National Laboratories.

Nuclear Regulatory Commission. 1996. *Disposal of High-Level Radioactive Wastes in Geologic Repositories*. Title 10, Energy, Part 60 (10 CFR Part 60). Washington, DC: U.S. Government Printing Office.

Ofoegbu, G.I., and J.H. Curran. 1992. Deformability of intact rock. *International Journal of Rock Mechanics and Mining Science & Geomechanics Abstract* 29(1): 35–48.

Ofoegbu, G.I., S.M. Hsiung, A.H. Chowdhury, and J. Philip. 1994. *Field Site Investigation: Effect of Mine Seismicity on Groundwater Hydrology*. NUREG/CR-6283. Washington, DC: Nuclear Regulatory Commission.

Price, R.H., J.R. Connolly, and K. Keil. 1987. *Petrologic and Mechanical Properties of Outcrop Samples of the Welded, Devitrified Topopah Spring Member of the Paintbrush Tuff*. SAND86-1131. Albuquerque, NM: Sandia National Laboratories.

Rojstaczer, S., and S. Wolf. 1992. Permeability changes associated with large earthquakes: An example from Loma Prieta, California. *Geology* 20: 211–214.

Sagar, B., R.W. Janetzke. 1993. *Total-System Performance Assessment (TPA) Computer Code: Description of Executive Module, Version 2.0, Iterative Performance Assessment, Phase 2.* CNWRA 93-017. San Antonio, TX: Center for Nuclear Waste Regulatory Analyses.

St. John, C.M. 1985. *Thermal Analysis of Spent Fuel Disposal in Vertical Boreholes in a Welded Tuff Repository.* SAND84-7207. Albuquerque, NM: Sandia National Laboratories.

TRW Environmental Safety Systems, Inc. 1994a. *Initial Summary Report for Repository/Waste Package Advanced Conceptual design.* Prepared for the U.S. Department of Energy. Document No. B00000000-01717-5705-00015, Volume I, Revision 00. Las Vegas, NV: TRW Environmental Safety Systems, Inc.

TRW Environmental Safety Systems, Inc. 1994b. FY93 *Thermal Loading Systems Study Final Report.* Volumes I & II, Revision 1. Las Vegas, NV: TRW Environmental Safety Systems, Inc.

TRW Environmental Safety Systems, Inc. 1995. *Thermomechanical Analyses.* Prepared for the U.S. Department of Energy. Document No. BC0000000-01717-5705-00013, Revision 00. Las Vegas, NV: TRW Environmental Safety Systems, Inc.

TRW Environmental Safety Systems, Inc. 1996. *Thermal Loading Study for FY1995.* Las Vegas, NV: TRW Environmental Safety Systems, Inc.

Tsang, C.F. 1987. Introduction to coupled processes. *Coupled Processes Associated with Nuclear Waste Repositories.* C.F. Tsang, ed. San Diego, CA: Academic Press: 1–6.

Tsang, C.F. 1991. Coupled hydromechanical-thermochemical process in rock fractures. *Reviews of Geophysics* 29(4): 537–551.

U.S. Department of Energy. 1987. Characteristics of Spent Fuel, High-Level Waste, and Other Radioactive Wastes Which May require Long-Term Isolation. DOE/RW-0184, Volume 2 of 6. Washington, DC: U.S. Department of Energy.

U.S. Department of Energy. 1988. *Site Characterization Plan: Yucca Mountain Site, Nevada Research and Development Area.* DOE/RW-0199. Washington, DC: U.S. Department of Energy.

U.S. Department of Energy. 1994. *Reference Information Base (RIB), Yucca Mountain Site Characterization Project.* Washington, DC: U.S. Department of Energy.

Walpole, R.E., and R.H. Myers. 1993. *Probability and Statistics for Engineers and Scientists.* 5th edition. New York, NY: Macmillan Publishing Company.

Wawersik, W.R., and C.A. Fairhurst. 1970. A study of brittle rock fracture in laboratory compression experiments. *International Journal of Rock Mechanics and Mining Science & Geomechanics Abstract* 7: 561–575.

Wawersik, W.R., and W.F. Brace. 1971. Post-failure behavior of a granite and diabase. *Rock Mechanics* 3: 61–85.

Wang, J.S.Y., D.C. Mangold, R.K. Spencer, and C.F. Tsang. 1983. *Thermal Impact of Waste Emplacement and Surface Cooling Associated with Geologic Disposal of Nuclear Waste.* NUREG/CR-2910. Washington, DC: Nuclear Regulatory Commission.

APPENDIX A

A.1 DESIGN OF 2^k FRACTIONAL FACTORIAL EXPERIMENTS

2^k factorial experimental design is a method that can be used to study the effect on a response of k parameters, each at two levels. Note that the response in the context of stability evaluation of an underground excavation could be the state of stresses, joint slip, extent of roof falls, etc. These two levels are often denoted as high and low for convenience. The complete factorial design requires that each level of every parameter occur with each level of every other factor, thus giving a total of 2^k treatment combinations (Walpole and Myers, 1993). The 2^k factorial design offers a distinct advantage in that any two treatment combinations are orthogonal and therefore the effect of each treatment combination can be assessed independently. As discussed in section 3.3, nine parameters were selected in the design.

To facilitate the design and discussion, each parameter was assigned an alphabet letter:

Parameter A = subvertical joint inclination (measured upward from horizontal axis)
B = subhorizontal joint inclination
C = subvertical joint spacing
D = joint friction angle
E = thermal load
F = intact rock cohesion
G = intact rock friction angle
H = intact rock Young's modulus
I = thermal expansion coefficient

Higher level values of the parameters (A, B, C,...) were denoted by letters a, b, c,... and lower level values by the notation (1) (Walpole and Myers, 1993). A treatment combination was expressed as a combination of letters and notations. Hence, a treatment combination in which all the parameters consisted of high level values was expressed as abcdefghi. In the presence of high level letters for some parameters, the low level symbols (1) were omitted for clarity. For example, the treatment combination abc indicates the values for parameters A, B, and C are at high level while the rest of the parameters have low level values.

As discussed in section 3.3, with nine parameters chosen for the study (k=9), a full 2^k factorial plan requires 512 UDEC runs. Since available resources and time did not support this level of effort, it was decided to carry out only 1/8 fraction of the 2^k factorial plan. The process for selecting appropriate UDEC runs was the same as that of allocating the 512 factorial UDEC runs into eight equal size blocks. To develop a 1/8 fraction of a 2^k factorial plan, three defining contrasts need to be chosen. Note that a contrast of a parameter or parameter interaction is the sum of differences of responses at low and high levels of the parameter or parameter interaction. These defining contrasts should be chosen in such a way that information regarding the treatment combinations of interest can be obtained for analysis. In this study, interest was placed on the potential effects of the nine parameters and their second-order interactions (two-parameter interactions). The higher-order interactions (three or more parameters

interactions) were assumed to be negligible. Given this objective, three defining contrasts were selected after some trial and error effort (Walpole and Myers, 1993). These three defining contrasts were

ABCDEF
ABCGI, and
CDEGH

Since each block has 2^3-1 = 7 degrees of freedom, there exist four additional effects confounded with the blocks. They can be determined as follows

$$(ABCDEF)(ABCGI) = A^2B^2C^2DEFGI = DEFGI$$
$$(ABCDEF)(CDEGH) = ABFGH$$
$$(ABCGI)(CDEGH) = ABDEHI$$
$$(ABCDEF)(ABCGI)(CDEGH) = CFHI$$

Note that the powers associated with each parameter were reduced to either zero or one using the approach of modulo 2 (i.e., to calculate the remainder of the powers when divided by two). Information regarding these seven contrasts was sacrificed in the analysis because these contrasts are not independent of the blocks. In other words, there is no way to assess the effects of these contrasts independent of the blocks. Since these seven contrasts are high order interactions, the sacrifice is acceptable. For a 1/8 fractional factorial design, there exist seven aliases for each treatment combination. The word alias is given to the effects of two treatment combinations that have the same contrast. Effect is defined as the difference between the mean response (contrast) at the low and high levels of a parameter (Walpole and Myers, 1993) and is equal to the contrast of the parameter divided by 2^{k-1}. In this study, k=9. For example, the alias structure for the effect of CF (interaction between subvertical joint spacing and intact rock cohesion) is written as

$$cf \equiv abde \equiv abfgi \equiv defgh \equiv cdegi \equiv abcdefhi \equiv hi \equiv abcgh$$

The symbol $\equiv$ implies aliased with. Without supplementary evidence, there is no way to determine which of the two aliased effects is actually providing the influence on the response. This is a notable disadvantage of fractional factorial experiments. However, its benefits seem to outweigh the disadvantages in the context of this study. Notice from the previous alias structure there is an aliasing between the two-parameter interactions CF and HI. In fact, with the three defining contrasts chosen, there exists three alias structures that are aliasing between two-parameter interactions,

$$CF \equiv HI$$
$$CH \equiv FI$$
$$CI \equiv FH$$

Some judgment needs to be applied to determine which of the two aliased effects are important.

The numerical modeling plan was constructed by evaluating the expressions

$$L_1 = \gamma_A + \gamma_B + \gamma_C + \gamma_D + \gamma_E + \gamma_F \qquad \text{(A-1)}$$

$$L_2 = \gamma_A + \gamma_B + \gamma_C + \gamma_G + \gamma_I \tag{A-2}$$

$$L_3 = \gamma_C + \gamma_D + \gamma_E + \gamma_G + \gamma_H \tag{A-3}$$

where γ is equal to one if its subscript is found in the treatment combination of interest—in other words, the corresponding parameter in the treatment combination to the subscript has a high level value. Otherwise, it is equal to zero. Note that the subscripts in the right hand side of Eqs. (A-1) to (A-3) are related to the three defining contrasts. The treatment combinations were assigned into corresponding blocks using the following scheme:

Block 1: $L_1 = 0, L_2 = 0, L_3 = 0$
Block 2: $L_1 = 0, L_2 = 0, L_3 = 1$
Block 3: $L_1 = 0, L_2 = 0, L_3 = 0$
Block 4: $L_1 = 0, L_2 = 1, L_3 = 1$
Block 5: $L_1 = 1, L_2 = 0, L_3 = 0$
Block 6: $L_1 = 1, L_2 = 0, L_3 = 1$
Block 7: $L_1 = 1, L_2 = 1, L_3 = 0$
Block 8: $L_1 = 1, L_2 = 1, L_3 = 1$

For example, for the treatment combination ab, γ_A and γ_B in Eqs. (A-1) to (A-3) are equal to one due to the presence of the high level values for these two parameters in the combination while the rest of the γ in the equations are zero due to the presence of the low level values. The related L_1, L_2, L_3 can be calculated as

$$\begin{aligned} L_1 &= 1 + 1 + 0 + 0 + 0 + 0 &&= 2 = 0 \text{ (modulo 2)} \\ L_2 &= 1 + 1 + 0 + 0 + 0 = 2 &&= 0 \text{ (modulo 2)} \\ L_3 &= 0 + 0 + 0 + 0 + 0 = 0 &&= 0 \text{ (modulo 2)} \end{aligned}$$

Consequently, this treatment combination should belong to Block 1.

Any of the blocks using this scheme is a suitable set for the experiment. In this study, the principal block was selected. The principal block is the block containing the treatment combination (1), in which all parameters are with low level values. The 64 treatment combinations contained in the principal block are listed in table A-1.

Table A-1. Treatment combinations selected for performing UDEC analysis

(1)	ach	cdi	adhi
ab	bch	abcdi	bdhi
de	acdeh	cei	aehi
abde	bcdeh	abcei	behi
acdf	dfh	afi	cfhi

Table A-1. Treatment combinations selected for performing UDEC analysis (cont'd)

bcdf	abdfh	bfi	abcfhi
acef	efh	adefi	cdefhi
bcef	abefh	bdefi	abcdefhi
adg	cdgh	acgi	ghi
bdg	abcdgh	bcgi	abghi
aeg	cegh	acdegi	deghi
beg	abcegh	bcdegi	abdeghi
cfg	afgh	dfgi	acdfghi
abcfg	bfgh	abdfgi	bcdfghi
cdefg	adefgh	efgi	acefghi
abcdefg	bdefgh	abefgi	bcefghi

A.2 SIGNIFICANCE OF MAIN PARAMETERS AND TWO-PARAMETER INTERACTIONS

The effects of the nine parameters and their two-parameter interactions on seven performance measures as discussed in section 4.3 using data listed in tables 4-3a and 4-3b were analyzed through analysis of variance and t-tests. The results are presented in the following sections.

A.2.1 Minimum Principal Stress

Analysis of variance for minimum principal stress around the excavation after 50 yr of heating is given in table A-2. The term "effects" used in table A-2 represents the difference of mean response of a particular parameter of interest (Walpole and Myers, 1993). The last column of table A-2 is the computed F-statistic and is the ratio of the mean square response of a parameter to that of the error term. This value is used to test the significance of that parameter by testing the null hypothesis between that parameter relative to the error term. In this study, the critical value for $F_{\alpha=0.05}(1,18)$ to reject the null hypothesis is equal to 4.41. The value 1 in the parentheses is the degree of freedom of each parameter and 18 is the degree of freedom of the error term. If the computed F exceeds the critical value [$F_{\alpha=0.05}(1,18) = 4.41$], it can be concluded that there is a significant amount of variation in the response due to the variation of a parameter. Consequently, the effect of that parameter is statistically significant or important.

As can be observed from table A-2, none of the main parameters (including thermal load which is represented by the capital letter E in table A-2) nor the two-parameter interactions are statistically significant since the corresponding F-ratios are substantially smaller than the critical value. Therefore, it can be concluded that they have no impact or effect on the minimum principal stress around the

excavation at 50 yr. It should be noted that whether or not a parameter is significant to or has an effect on a performance measure is assessed over the range of high and low values of that parameter. This notion is used throughout this report. It is possible to extrapolate the evaluation of significance or effect of a parameter from the range of the high and low values of the parameter through building a regression model.

Table A-2. Analysis of variance for the minimum principal stress after 50 yr of heating

Source of Variation	Effects	Sum of Squares	Degrees of Freedom	Mean Square	Computed F
A	0.89625	12.8522	1	12.8522	0.4975
B	1.52631	37.2741	1	37.2741	1.4429
C	1.18300	22.3918	1	22.3918	0.8668
D	-1.42150	32.3306	1	32.3306	1.2515
E	0.47044	3.5410	1	3.5410	0.1371
F	1.37950	30.4483	1	30.4483	1.1787
G	-1.20931	23.3990	1	23.3990	0.9058
H	1.91844	58.8865	1	58.8865	2.2795
I	1.90069	57.8018	1	57.8018	2.2375
AB	1.11425	19.8649	1	19.8649	0.7690
AC	1.11831	20.0100	1	20.0100	0.7746
AD	−1.31994	27.8758	1	27.8758	1.0791
AE	1.21000	23.4256	1	23.4256	0.9068
AF	1.58919	40.4083	1	40.4083	1.5642
AG	−1.54363	38.1245	1	38.1245	1.4758
AH	1.03363	17.0941	1	17.0941	0.6617
AI	1.20650	23.2903	1	23.2903	0.9016
BC	1.20162	23.1024	1	23.1024	0.8943
BD	−1.21613	23.6634	1	23.6634	0.9160
BE	−1.59756	40.8353	1	40.8353	1.5808
BF	1.24000	24.6016	1	24.6016	0.9523
BG	−1.18819	22.5886	1	22.5886	0.8744
BH	1.41606	32.0837	1	32.0837	1.2420
BI	1.23769	24.5099	1	24.5099	0.9488

Table A-2. Analysis of variance for the minimum principal stress after 50 yr of heating (cont'd)

Source of Variation	Effects	Sum of Squares	Degrees of Freedom	Mean Square	Computed F
CD	−1.20744	23.3265	1	23.3265	0.9030
CE	−1.15175	21.2244	1	21.2244	0.8216
CF	0.82631	10.9247	1	10.9247	0.4229
CG	−1.22875	24.1572	1	24.1572	0.9351
CH	1.34750	29.0521	1	29.0521	1.1246
CI	1.23000	24.2064	1	24.2064	0.9370
DE	1.31525	27.6781	1	27.6781	1.0714
DF	−1.27969	26.2016	1	26.2016	1.0143
DG	1.38500	30.6916	1	30.6916	1.1881
DH	−1.17875	22.2312	1	22.2312	0.8606
DI	−1.35050	29.1816	1	29.1816	1.1296
EF	−1.36700	29.8990	1	29.8990	1.1574
EG	1.54806	38.3440	1	38.3440	1.4843
EH	−1.13719	20.6911	1	20.6911	0.8010
EI	−1.10069	19.3842	1	19.3842	0.7504
FG	−1.36925	29.9975	1	29.9975	1.1612
FH	1.23000	24.2064	1	24.2064	0.9370
FI	1.34750	29.0521	1	29.0521	1.1246
GH	−1.33744	28.6198	1	28.6198	1.1079
GI	−1.14094	20.8278	1	20.8278	0.8063
HI	0.82631	10.9247	1	10.9247	0.4229
ERROR		464.9890	18	25.8327	
Total		1666.2150	63		

The analysis of variance for the minimum principal stress around the excavation after 100 yr of heating indicated a negative value of mean square for the error term which is not possible. This negative value may be related to level of precision used in the calculation since the error term involved could be small originally. Consequently, the significance of the main parameters and the two-parameter interaction cannot be assessed. No further attempt is made for significance assessment of main parameters on the minimum principal stress around the excavation.

A.2.2 Maximum Principal Stress

The analysis of variance for the maximum principal stress around the excavation after 50 yr of heating is given in table A-3. Notice that not all the main parameters and two-parameter interactions are listed in the table. Only those with the computed F-ratio greater than the critical value are listed. As can be observed from the table, the main parameters whose effects are considered significant to the variation of the maximum principal stress are subvertical joint inclination, subvertical joint spacing, thermal load, intact rock Young's modulus, and thermal expansion coefficient with the thermal load and the thermal expansion coefficient being dominant. All of these parameters have a positive effect on the maximum principal stress. The terms positive and negative effects are used frequently in this report. A positive effect means a higher or larger response resulting from a higher value of a parameter while a negative effect indicates that a decrease in the value of a parameter results in an increase in response. If there were no interaction effects, a general conclusion regarding the significance of the main parameter could be made directly from the variance analysis (Walpole and Myers, 1993). Otherwise, it is essential to understand the impact of the interactions so that the conditions that may be inconsistent with the general trend depicted by the marginal averages can be identified.

As can be seen in table A-3, there are statistically significant effects caused by interactions between

- subvertical joint inclination and horizontal joint inclination (AB)
- subvertical joint inclination and thermal expansion coefficient (AI)
- subvertical joint spacing and joint friction angle (CD)
- subvertical joint spacing and intact rock friction angle (CG)
- subvertical joint spacing and intact rock Young's modulus (CH)
- thermal load and intact rock Young's modulus (EH)
- thermal load and thermal expansion coefficient (EI)
- intact rock friction angle and intact rock Young's modulus (GH)
- intact rock Young's modulus and thermal expansion coefficient (HI)

Table A-3. Analysis of variance for the maximum principal stress after 50 yr of heating

Source of Variation	Effects	Sum of Squares	Degrees of Freedom	Mean Square	Computed F
A	7.40031	876.2341	1	876.2341	9.3739
C	6.87406	756.0436	1	756.0436	8.0881
E	34.08344	18586.8900	1	18586.8900	198.8424
H	16.56906	4392.5420	1	4392.5420	46.9914
I	25.42843	10345.6800	1	10345.6800	110.6781
AB	10.49031	1760.7470	1	1760.7470	18.8365
AI	5.39219	465.2109	1	465.2109	4.9768
CD	5.69781	519.4412	1	519.4412	5.5570

Table A-3. Analysis of variance for the maximum principal stress after 50 yr of heating (cont'd)

Source of Variation	Effects	Sum of Squares	Degrees of Freedom	Mean Square	Computed F
CG	−10.01469	1604.7030	1	1604.7030	17.1671
CH	6.42781	661.0684	1	661.0684	7.0721
EH	8.78469	1234.7320	1	1234.7320	13.2091
EI	15.93406	4062.3100	1	4062.3100	43.4586
GH	−5.53344	489.9033	1	489.9033	5.2410
HI	8.49844	1155.5750	1	1155.5750	12.3623
ERROR		1682.5590	18	93.4755	
Total		53301.4200		63	

A two-way table of means for testing the null hypothesis was constructed and the associated t-statistic determined for each of the two-parameter interactions listed previously to facilitate evaluation of their impacts. Table A-4 provides the two-way table of means of the nine statistically significant interactions. Note that t12, t34, t31, and t42 are t-statistics. The combination of the numbers denotes the comparison of the two response means. The number 1 indicates the response mean at the upper left corner (e.g., 36.64062 of the two-way table of means No. 1), 2 represents the response mean at upper right corner (e.g., 49.48875 of the two-way table of means No. 1), 3 represents the response mean at the lower left corner (e.g., 39.73062 of the two-way table of means No. 1), and 4 is the response mean at the lower right corner (e.g., 31.59812 of the two-way table of means No. 1). The t-statistic, t12, is calculated to test the difference between 36.64062 and 49.48875. The total degrees of freedom for each interaction listed in table A-4 are 30. The critical t-statistic for a two-tail test at an $\alpha = 0.05$ level is 2.042. A discussion regarding the interaction effects on the maximum principal stress after 50 yr of heating is provided in the following (notice that the discussion is structured in terms of main parameters).

- Subvertical joint inclination

  Although subvertical joint inclination is in general significant based on the variance analysis, it does not have an effect on the maximum principal stress and, therefore, is not significant when either the horizontal joint inclination or the thermal expansion coefficient has a low value (10° for the subhorizontal joint inclination and $6 \times 10^{-6}\ K^{-1}$ for the thermal expansion coefficient). Subvertical joint inclination has a significant positive effect on the maximum principal stress when either the subhorizontal joint inclination or the thermal expansion coefficient is at its high value, that is, the maximum principal stress increases with the subvertical joint inclination and the thermal expansion coefficient. The interaction impact is the largest when both parameters in each of the interactions are at their high values.

- Subhorizontal joint inclination

  As presented earlier, the subhorizontal joint inclination is not found to be significant to the maximum principal stress based on the analysis of variance. However, by examining the two-way table of means No. 1 in table A-4, it becomes clear why it is not important. The effect of the subhorizontal joint inclination changes from a significant negative effect for a subvertical joint inclination of 70° to what appears to be a significant positive effect for a subvertical joint inclination of 85°. The effect of subhorizontal joint inclination should not be ignored.

Table A-4. Two-way table of means for maximum principal stress after 50 yr of heating

Table A-4(a). Two-way table of means No.1

Parameters		B = 10°	B = 20°
A = 85°		36.64062	49.48875
A = 70°		39.73062	31.59812
t-statistic			
t12	t34	t31	t42
−3.7587	2.3791	0.9040	−5.2339

A = subvertical joint inclination
B = subhorizontal joint inclination

Table A-4(b). Two-way table of means No. 2

Parameters		I = 6	I = 12
A = 85°		27.65438	58.47500
A = 70°		25.64625	45.68251
t-statistic			
t12	t34	t31	t42
−9.0165	−5.8616	−0.5875	−3.7424

A = subvertical joint inclination
I = thermal expansion coefficient, $10^{-6}\ K^{-1}$

Table A-4. Two-way table of means for maximum principal stress after 50 yr of heating (cont'd)

Table A-4(c). Two-way table of means No. 3

Parameters		D = 28°	D = 38°
C = 0.5		39.71750	45.88563
C = 0.2		38.54125	33.31375
t-statistic			
t12	t34	t31	t42
−1.8045	1.5293	−0.3441	−3.6779

C = subvertical joint spacing, m
D = joint friction angle

Table A-4(d). Two-way table of means No. 4

Parameters		G = 20°	G = 50°
C = 0.5		46.11937	39.48375
C = 0.2		29.23063	42.62437
t-statistic			
t12	t34	t31	t42
1.9412	−3.9183	−4.9408	0.9188

C = subvertical joint spacing, m
G = intact rock friction angle

Table A-4(e). Two-way table of means No. 5

Parameters		H = 16	H = 32
C = 0.5		31.30312	54.30000
C = 0.2		30.85687	40.99812
t-statistic			
t12	t34	t31	t42
−6.7277	−2.9668	−0.1305	−3.8914

C = subvertical joint spacing, m
H = intact rock Young's modulus, GPa

Table A-4. Two-way table of means for maximum principal stress after 50 yr of heating (cont'd)

Table A-4(f). Two-way table of means No. 6

Parameters		H = 16	H = 32
E = 100		43.72938	69.08312
E = 20		18.43062	26.21500
t-statistic			
t12	t34	t31	t42
−7.4172	−2.2773	−7.4011	−12.5410

E = thermal load, MTU/acre
H = intact rock Young's modulus, GPa

Table A-4(g). Two-way table of means No. 7

Parameters		I = 6.0	I = 12.0
E = 100		35.72500	77.08749
E = 20		17.57562	27.07000
t-statistic			
t12	t34	t31	t42
−12.1005	−2.7776	−5.3096	−14.6325

E = thermal load, MTU/acre
I = thermal expansion coefficient, $10^{-6}\ K^{-1}$

Table A-4(h). Two-way table of means No. 8

Parameters		H = 16	H = 32
F = 43		35.53625	46.57188
F = 18		26.62375	48.72625
t-statistic			
t12	t34	t31	t42
−3.2284	−6.4660	−2.6073	0.6303

F = intact rock cohesion, MPa
H = intact rock Young's modulus, GPa

Table A-4. Two-way table of means for maximum principal stress after 50 yr of heating (cont'd)

Table A-4(i). Two-way table of means No. 9

Parameters		I = 6.0	I = 12.0
H = 32		30.68563	64.61250
H = 16		22.61500	39.54500
t-statistic			
t12	t34	t31	t42
−9.9252	−4.9528	−2.3610	−7.3334

H = intact rock Young's modulus, GPa
I = thermal expansion coefficient, 10^{-6} K^{-1}

- Subvertical joint spacing

  Variance analysis has shown the significance of subvertical joint spacing. A test on population means indicates that subvertical joint spacing has a positive effect for high joint friction angle and intact rock Young's modulus and low intact rock friction angle. However, it does not have a significant effect on the maximum principal stress when the joint friction angle and the intact rock Young's modulus are low and the intact rock friction angle is high.

- Joint friction angle

  The variance analysis indicates that joint friction angle does not have significant impact on the maximum principal stress. The interpretation of the interaction effect between the subvertical joint spacing and joint friction angle (two-way table of means No. 3) further confirms this observation.

- Thermal load

  The variance analysis of this parameter points out that the thermal load is one of the dominant factors affecting maximum principal stress around the excavation. This is further confirmed from the t-test results of its interaction with the intact rock Young's modulus and thermal expansion coefficient. Maximum principal stress increases as the thermal load increases at both low and high values of intact rock Young's modulus and thermal expansion coefficient. The interaction effects are not additive for high thermal load and high intact rock Young's modulus or high thermal expansion coefficient.

- Intact rock cohesion

  Intact rock cohesion is identified as not significant from the variance analysis and no other information is available to allow further evaluation of the effect of this main parameter. It

may, therefore, be concluded that the intact rock cohesion is not a controlling parameter responsible for the variation of the maximum principal stress.

- Intact rock friction angle

  Intact rock friction angle is not significant according to the variance analysis. This parameter has interactions with the subvertical joint spacing and intact rock Young's modulus. The t-test results indicate the intact rock friction angle has a significant positive effect; only when the subvertical joint spacing or the intact rock Young's modulus is at its low value. In other words, intact rock friction angle will contribute to the variation of the maximum principal stress only when the subvertical joint spacing becomes smaller. The effect of intact rock friction angle is not a concern when the intact rock Young's modulus is high.

- Intact rock Young's modulus

  Intact rock Young's modulus has been identified through variance analysis as important. It is also found to have a significant interaction with subvertical joint spacing, thermal load, intact rock friction angle, and thermal expansion coefficient. The positive effect of intact rock Young's modulus is significant at all values of subvertical joint spacing, thermal load, intact rock friction angle, and thermal expansion coefficient. Nonadditive interaction effects are observed for high intact rock Young's modulus and high subvertical joint spacing or high thermal load.

- Thermal expansion coefficient

  The variance analysis has indicated that the thermal expansion coefficient is a very important parameter that will affect the maximum principal stress. The t-test results have also shown that it has a significant positive interaction effect with subvertical joint inclination, thermal load, and intact rock Young's modulus irrespective of the values associated with these parameters.

After the emplacement drift has been heated for 100 yr, the controlling parameters identified through analysis of variance are the same as those at 50 yr. However, the number of interaction effects considered important has been reduced. Also, three interaction effects are identical to those for 50 yr. These effects are (i) subvertical joint spacing and intact rock friction angle, (ii) thermal load and thermal expansion coefficient, and (iii) intact rock Young's modulus and thermal expansion coefficient. The trend of the interaction effects is generally in line with that of 50 yr except the intact rock Young's modulus effect becomes insignificant when the thermal expansion coefficient is small. There are two new interactions identified as significant. The associated two-way table of means is provided in table A-5.

Table A-5. Two-way table of means of maximum principal stress under 100 yr of heating for subvertical joint inclination-joint friction angle and subhorizontal joint inclination-thermal load

Table A-5(a). Two-way table of means No. 1

Parameters		D = 28°	D = 38°
A = 85°		50.70563	37.64000
A = 70°		35.50063	37.14750
t-statistic			
t12	t34	t31	t42
2.9812	−0.3758	−3.4693	−.1124

A = subvertical joint inclination
D = joint friction angle

Table A-5(b). Two-way table of means No. 2

Parameters		E = 20	E = 100
B = 20°		25.05625	52.45125
B = 10°		20.05313	63.43313
t-statistic			
t12	t34	t31	t42
−6.2508	−9.8981	−1.1416	2.5058

B = subhorizontal joint inclination
E = thermal load, MTU/acre

The two-way table of means No. 1 shows that the joint friction angle is significant with a negative effect when subvertical joint inclination is large, while it has no effect when subvertical joint inclination is small. On the other hand, the subvertical joint inclination is significant and has a positive effect when the joint friction angle is small. The two-way table of means No. 1 indicates that subhorizontal joint inclination will play an important role to the variation of the maximum principal stress only when thermal load is high. Therefore, although the variance analysis indicated that subhorizontal joint inclination is not significant, its role at high thermal load should not be ignored. It should be noted that the effect of subhorizontal joint inclination for 100 yr is somewhat different from that for 50 yr.

A.2.3 Maximum Joint Shear Displacement

The analysis of variance for the maximum joint shear displacement around the excavation after 50 yr of heating is given in table A-6. The nine main parameters used in this study seem to have much less effect on maximum joint shear displacement compared to maximum principal stress. Only thermal load is considered important while thermal expansion coefficient is marginal since its F-ratio is smaller then the critical value of 4.41. Both parameters have a positive effect.

One interaction effect is identified to be significant—subvertical joint spacing and thermal expansion coefficient (CI). Its two-way table of means is given in table A-7. This two-way table clearly shows that the thermal expansion coefficient is significant only when the subvertical joint spacing is large. Maximum joint shear displacement increases as the thermal expansion coefficient increases. Consequently, the importance of the thermal expansion coefficient should not be ignored. Subvertical joint spacing appears to have a negative effect on the maximum joint shear displacement when the thermal expansion coefficient is small; the effect diminishes for high thermal expansion coefficient. It can be concluded that subvertical joint spacing is a conditionally important parameter that may effect maximum joint shear displacement around the excavation with 50 yr of heating.

As the emplacement drift is heated to 100 yr, the number of significant main parameters and two-parameter interactions increases substantially. Table A-8 lists these important effects. Table A-8 in general indicates that subvertical joint inclination, subvertical joint spacing, thermal load, and intact rock Young's modulus are important parameters that effect maximum joint shear displacement at the 100th yr of heating. Subvertical joint inclination and subvertical joint spacing have a negative effect, while the other two have a positive effect.

The significant interactions shown in table A-8 are

- subvertical joint inclination and subvertical joint spacing (AC)
- subvertical joint inclination and thermal load (AE)
- subvertical joint spacing and thermal expansion coefficient (CI)
- joint friction angle and intact rock Young's modulus (DH)
- joint friction angle and thermal expansion coefficient (DI)
- thermal load and intact rock Young's modulus (EH)
- thermal load and thermal expansion coefficient (EI)
- intact rock friction angle and intact rock Young's modulus (GH)
- intact rock friction angle and thermal expansion coefficient (GI)

A two-way table of means was constructed for these interactions as shown in table A-9. Discussion of the interaction effects on the maximum joint shear displacement after 100 yr of heating is provided below.

- Subvertical joint inclination

  The variance analysis has shown that subvertical joint inclination in general has a negative effect on maximum joint shear displacement. This trend seems to hold according to results from two-way tables of means Nos. 1 and 2. These two-way tables of means also reveal that subvertical joint inclination is not significant when the subvertical joint spacing is large or thermal load is low.

Table A-6. Analysis of variance for the maximum joint shear displacement after 50 yr of heating

Source of Variation	Effects	Sum of Squares	Degrees of Freedom	Mean Square	Computed F
E	0.58197	5.4189	1	5.4189	5.2849
I	0.51912	4.3118	1	4.3118	4.2051
CI	0.73115	8.5532	1	8.5532	8.3416
ERROR		18.4565	18	1.0254	
Total		97.8239	63		

Table A-7. Two-way table of means of maximum joint shear displacement after 50 yr of heating for subvertical joint spacing and thermal expansion coefficient

Parameters		I = 6	I = 12
C = 0.5		0.49545	1.74572
C = 0.2		1.38378	1.17175
t-statistic			
t12	t34	t31	t42
−3.4923	0.5922	2.4813	−1.6032

C = subvertical joint spacing, m
I = thermal expansion coefficient, 10^{-6} K^{-1}

Table A-8. Analysis of variance for the maximum joint shear displacement after 100 yr of heating

Source of Variation	Effects	Sum of Squares	Degrees of Freedom	Mean Square	Computed F
A	−0.81631	10.6618	1	10.6618	20.4029
C	−0.62883	6.3268	1	6.3268	12.1072
E	1.09474	19.1753	1	19.1753	36.6948
H	0.39786	2.5327	1	2.5327	4.8466
AC	0.38633	2.3880	1	2.3880	4.5698
AE	−0.43188	2.9843	1	2.9843	5.7109
CI	0.57000	5.1985	1	5.1985	9.9480
DH	0.38330	2.3507	1	2.3507	4.4985

Table A-8. Analysis of variance for the maximum joint shear displacement after 100 yr of heating (cont'd)

Source of Variation	Effects	Sum of Squares	Degrees of Freedom	Mean Square	Computed F
DI	−0.39323	2.4741	1	2.4741	4.7345
EH	0.45008	3.2411	1	3.2411	6.2024
EI	0.48841	3.8167	1	3.8167	7.3038
GH	−0.42423	2.8796	1	2.8796	5.5105
GI	0.54997	4.8395	1	4.8395	9.2611
ERROR		9.4061	18	0.5226	
Total		97.7979	63		

Table A-9. Two-way table of means of maximum joint shear displacement under 100 yr of heating

Table A-9(a). Two-way table of means No. 1

Parameters		C = 0.2	C = 0.5
A = 85°		0.99294	0.75044
A = 70°		2.19558	1.18042
t-statistic			
t12	t34	t31	t42
0.9488	3.9720	4.7056	1.6824

A = subvertical joint inclination
C = subvertical joint spacing, m

Table A-9(b). Two-way table of means No. 2

Parameters		E = 20	E = 100
A = 85°		0.54026	1.20313
A = 70°		0.92469	2.45131
t-statistic			
t12	t34	t31	t42
−2.5936	−5.9732	1.5042	4.8838

A = subvertical joint inclination
E = thermal load, MTU/acre

Table A-9. Two-way tables of means of maximum joint shear displacement under 100 yr of heating (cont'd)

Table A-9(c). Two-way table of means No. 3

Parameters		I = 6	I = 12
C = 0.5		0.58179	1.34908
C = 0.2		1.78063	1.40790
t-statistic			
t12	t34	t31	t42
−3.0021	1.4584	4.6907	0.2302

C = subvertical joint spacing, m
I = thermal expansion coefficient, 10^{-6} K^{-1}

Table A-9(d). Two-way table of means No. 4

Parameters		H = 16	H = 32
D = 38°		0.83001	1.61118
D = 28°		1.33182	1.34638
t-statistic			
t12	t34	t31	t42
−3.0564	−0.0570	1.9634	−1.0361

D = joint friction angle
H = intact rock Young's modulus, GPa

Table A-9(e). Two-way table of means No. 5

Parameters		I = 6	I = 12
D = 38°		1.31857	1.12262
D = 28°		1.04385	1.63436
t-statistic			
t12	t34	t31	t42
0.7667	−2.3105	−1.0749	2.0023

D = joint friction angle
I = thermal expansion coefficient, 10^{-6} K^{-1}

Table A-9. Two-way tables of means of maximum joint shear displacement under 100 yr of heating (cont'd)

Table A-9(f). Two-way table of means No. 6

Parameters		H = 16	H = 32
E = 100		1.40325	2.25119
E = 20		0.75859	0.70637
t-statistic			
t12	t34	t31	t42
−3.3177	0.2043	−2.5224	−6.0444

E = thermal load, MTU/acre
H = intact rock Young's modulus, GPa

Table A-9(g). Two-way table of means No. 7

Parameters		I = 6	I = 12
E = 100		1.48438	2.17006
E = 20		0.87804	0.58691
t-statistic			
t12	t34	t31	t42
−2.6829	1.1391	−2.3724	−6.1944

E = thermal load, MTU/acre
I = thermal expansion coefficient, $10^{-6}\ K^{-1}$

Table A-9(h). Two-way table of means No. 8

Parameters		H=16	H=32
G = 50°		1.23965	1.21327
G = 20°		0.92219	1.74428
t-statistic			
t12	t34	t31	t42
0.1032	−3.2166	−1.2421	2.0777

G = intact rock friction angle
H = intact rock Young's modulus, GPa

Table A-9. Two-way tables of means of maximum joint shear displacement under 100 yr of heating (cont'd)

Table A-9(i). Two-way table of means No. 9

Parameters		I = 6	I = 12
G = 50°		0.85284	1.60009
G = 20°		1.50958	1.15689
t-statistic			
t12	t34	t31	t42
−2.9238	1.3800	2.5696	−1.7341

G = intact rock friction angle
I = thermal expansion coefficient, 10^{-6} K^{-1}

- Subhorizontal joint inclination

  According to the variance analysis, subhorizontal joint inclination is not important to the maximum joint shear displacement; nor does it have any significant interaction with any other parameters of interest. It is therefore reasonable to conclude that subhorizontal joint inclination is not a controlling factor for variation of maximum joint shear displacement.

- Subvertical joint spacing

  Subvertical joint spacing is an important parameter that affects the variation of maximum joint shear displacement. Its interaction with the thermal expansion coefficient takes place only at low thermal expansion coefficient. When the thermal expansion coefficient is high, subvertical joint spacing does not seem to have any effect on the maximum joint shear displacement. The interaction of subvertical joint spacing with subvertical joint inclination takes place at small subvertical joint inclination and the effect is negative.

- Joint friction angle

  The variance analysis indicates that joint friction angle does not have any significant impact on the maximum joint shear displacement. The interaction effect as shown in the two-way table of means Nos. 4 and 5 is only marginal. The joint friction angle is not significant under high intact rock Young's modulus or low thermal expansion coefficient, while it has a negative effect at low intact rock Young's modulus or high thermal expansion coefficient. The calculated t-statistics for both cases are slightly smaller than the critical value of 2.042.

- Thermal load

  The interpretation of the result of the two-way table of means confirms the assertion from the variance analysis that thermal load is the dominant factor on the maximum joint shear displacement around the emplacement drifts. Thermal load has a significant positive effect

irrespective of the values associated with subvertical joint inclination, intact rock Young's modulus, and thermal expansion coefficient.

- Intact rock cohesion

  Intact rock cohesion is not a significant parameter according to the result of the variance analysis and no other information is available to allow further evaluation. It may be concluded that the intact rock cohesion is not a controlling parameter responsible for the variation of the maximum joint shear displacement.

- Intact rock friction angle

  According to the variance analysis intact rock friction angle is not significant. This parameter has important interactions with intact rock Young's modulus and thermal expansion coefficient. An increase in intact rock friction angle will result in a decrease in the maximum joint shear displacement when the intact rock Young's modulus is high or the thermal expansion coefficient is small. For a low intact rock Young's modulus or high thermal expansion coefficient, the effect of intact rock friction angle is not significant.

- Intact rock Young's modulus

  Intact rock Young's modulus is identified through variance analysis as important. It is also found to have an interaction with joint friction angle, thermal load, and intact rock friction angle. A significant positive effect of this parameter is observed at large joint friction angle, high thermal load, or small intact rock friction angle.

- Thermal expansion coefficient

  Although thermal expansion coefficient has not been found to be important through the variance analysis, it has interactions with subvertical joint spacing, joint friction angle, thermal load, and intact rock friction angle. Results of the related two-way table of means indicate that thermal expansion coefficient has a significant positive effect on the maximum joint shear displacement at large subvertical joint spacing, high thermal load, high intact rock friction angle, or small joint friction angle. Consequently, the potential effect of thermal expansion coefficient should not be ignored.

A.2.4 Maximum Joint Closure

The analysis of variance for the maximum joint closure around the excavation after 50 yr of heating is given in table A-10. The only main parameters identified to have a significant impact on the maximum joint closure are thermal load and thermal expansion coefficient. Both have a positive effect. No interaction effect is determined to be significant.

As the emplacement drift is heated to 100 yr, besides the thermal load and thermal expansion coefficient, intact rock Young's modulus becomes important and has a positive effect. Two interaction effects are also identified as significant. These include interaction between thermal load and intact rock Young's modulus, and thermal load and thermal expansion coefficient. The thermal load appears to have

a positive effect irrespective of the value of intact rock Young's modulus or thermal expansion coefficient. Intact rock Young's modulus and thermal expansion coefficient are not significant when the thermal load is low. Table A-11 lists the results of variance analysis and table A-12 provides the two-way table of means for the two interaction effects listed in table A-11.

A.2.5 Maximum Joint Separation

The analysis of variance for the maximum joint separation around the excavation after 50 yr of heating is given in table A-13 and the two-way table of means is provided in table A-14. Table A-13 shows that six of the nine main parameters are important to maximum joint separation. Maximum joint separation tends to decrease as subvertical joint inclination or joint friction angle increase, but it becomes larger when subhorizontal joint inclination, thermal load, intact rock Young's modulus, or thermal expansion coefficient increases. Thermal load is the dominant factor. There is only one interaction effect—between thermal load and intact rock Young's modulus—that is significant in affecting the variation of maximum joint separation. This interaction suggests that thermal load may not be significant for low intact rock Young's modulus and intact rock Young's modulus is not important when thermal load is low.

Table A-10. Analysis of variance for the maximum joint closure after 50 yr of heating

Source of Variation	Effects	Sum of Squares	Degrees of Freedom	Mean Square	Computed F
E	0.04971	0.0395	1	0.0395	6.5152
I	0.04328	0.0300	1	0.0300	4.9388
ERROR		0.1092	18	0.0061	
Total		0.4120	63		

Table A-11. Analysis of variance for the maximum joint closure after 100 yr of heating

Source of Variation	Effects	Sum of Squares	Degrees of Freedom	Mean Square	Computed F
E	3.33549	178.0079	1	178.0079	49.9833
H	1.40507	31.5876	1	31.5876	8.8696
I	1.73046	47.9118	1	47.9118	13.4533
EH	1.16479	21.7078	1	21.7078	6.0954
EI	1.15480	21.3371	1	21.3371	5.9913
ERROR		64.1042	18	3.5613	
Total		443.5074	63		

Table A-12. Two-way table of means of maximum joint closure after 100 yr of heating for thermal load—intact rock Young's modulus and thermal load-thermal expansion coefficient interactions

Table A-12(a). Two-way table of means No. 1

Parameters		H = 16	H = 32
E = 100		3.75457	6.32444
E = 20		1.58388	1.82416
t-statistic			
t12	t34	t31	t42
−3.8517	−0.3601	−3.2534	−6.7449

E = thermal load, MTU/acre
H = intact rock Young's modulus, GPa

Table A-12(b). Two-way table of means No. 2

Parameters		I = 6	I = 12
E = 100		3.59687	6.48214
E = 20		1.41619	1.99184
t-statistic			
t12	t34	t31	t42
−4.3244	−0.8628	−3.2684	−6.7300

E = thermal load, MTU/acre
I = thermal expansion coefficient, $10^{-6}\ K^{-1}$

Table A-13. Analysis of variance for the maximum joint separation after 50 yr of heating

Source of Variation	Effects	Sum of Squares	Degrees of Freedom	Mean Square	Computed F
A	−0.18245	0.5326	1	0.5326	7.6912
B	0.19441	0.6047	1	0.6047	8.7329
D	−0.17114	0.4686	1	0.4686	6.7673
E	0.35544	2.0214	1	2.0214	29.1906
H	0.16810	0.4521	1	0.4521	6.5287
I	0.17923	0.5139	1	0.5139	7.4219

Table A-13. Analysis of variance for the maximum joint separation after 50 yr of heating (cont'd)

Source of Variation	Effects	Sum of Squares	Degrees of Freedom	Mean Square	Computed F
EH	0.19247	0.5927	1	0.5927	8.5591
ERROR		1.2465	18	0.0692	
Total		9.8043	63		

Table A-14. Two-way table of means of maximum joint separation under 50 yr of heating for thermal load—intact rock Young's modulus interaction

Parameters		H = 16	H = 32
E = 100		0.33187	0.69244
E = 20		0.16890	0.14453
t-statistic			
t12	t34	t31	t42
−3.8755	.2619	−1.7517	−5.8891

E = thermal load, MTU/acre
H = intact rock Young's modulus, GPa

The analysis of variance for the maximum joint separation around the excavation after 100 yr of heating is given in table A-15 and the two-way table of means for significant interactions is provided in table A-16. The important parameters that have an effect on the maximum joint separation for an emplacement drift at 50 yr of heating remain significant after 100 yr of heating. Furthermore, the trends of the effects are also the same. More interaction effects become important after a longer period of heating. These interactions include

- subvertical joint inclination and intact rock friction angle (AG)
- subhorizontal joint inclination and subvertical joint spacing (BC)
- subvertical joint spacing and thermal load (CE)
- subvertical joint spacing and intact rock Young's modulus (CH)
- joint friction angle and intact rock friction angle (DG)
- joint friction angle and thermal expansion coefficient (DI)
- thermal load and intact rock Young's modulus (EH)
- thermal load and thermal expansion coefficient (EI)
- intact rock friction angle and intact rock Young's modulus (GH)

Table A-15. Analysis of variance for the maximum joint separation after 100 yr of heating

Source of Variation	Effects	Sum of Squares	Degrees of Freedom	Mean Square	Computed F
A	−0.13076	0.2736	1	0.2736	7.0685
B	0.16422	0.4315	1	0.4315	11.1488
D	−0.25660	1.0535	1	1.0535	27.2193
E	0.35751	2.0450	1	12.0450	52.8353
H	0.13499	0.2916	1	0.2916	7.5329
I	0.32451	1.6849	1	1.6849	43.5309
AG	−0.17438	0.4865	1	0.4865	12.5702
BC	0.18233	0.5319	1	0.5319	13.7421
CE	−0.12039	0.2319	1	0.2319	5.9919
CH	−0.12368	0.2448	1	0.2448	6.3239
DG	0.11763	0.2214	1	0.2214	5.7197
DI	−0.11256	0.2027	1	0.2027	5.2370
EH	0.14720	0.3467	1	0.3467	8.9568
EI	0.14343	0.3292	1	0.3292	8.5045
GH	−0.13419	0.2881	1	0.2881	7.4440
ERROR		0.6967	18	0.0387	
Total		10.7461	63		

Table A-16. Two-way table of means of maximum joint separation under 100 yr of heating

Table A-16(a). Two-way table of means No. 1

Parameters		G = 20°	G = 50°
A = 85°		0.39564	0.18027
A = 70°		0.35203	0.48542
t-statistic			
t12	t34	t31	t42
3.0963	−1.9177	−0.6271	4.3870

A = subvertical joint inclination
G = intact rock friction angle

Table A-16. Two-way table of means of maximum joint separation under 100 yr of heating (cont'd)

Table A-16(b). Two-way table of means No. 2

Parameters		C = 0.2	C = 0.5
B = 20°		0.38637	0.48453
B = 10°		0.40448	0.13798
t-statistic			
t12	t34	t31	t42
−1.4112	3.8313	0.2603	−4.9823

B = subhorizontal joint inclination
C = subvertical joint spacing, m

Table A-16(c). Two-way table of means No. 3

Parameters		E = 20	E = 100
C = 0.5		0.19270	0.42981
C = 0.2		0.15647	0.63438
t-statistic			
t12	t34	t31	t42
−3.4089	−6.8707	−0.5208	2.9410

C = subvertical joint spacing, m
E = thermal load, MTU/acre

Table A-16(d). Two-way table of means No. 4

Parameters		H = 16	H = 32
C = 0.5		0.30560	0.31691
C = 0.2		0.26609	0.52476
t-statistic			
t12	t34	t31	t42
−0.1625	−3.7189	−0.5681	2.9883

C = subvertical joint spacing, m
H = intact rock Young's modulus, GPa

Table A-16. Two-way table of means of maximum joint separation under 100 yr of heating (cont'd)

Table A-16(e). Two-way table of means No. 5

Parameters		G = 20°	G = 50°
D = 38°		0.18672	0.26336
D = 28°		0.56095	0.40233
t-statistic			
t12	t34	t31	t42
−1.1018	2.2804	5.3802	1.9980

D = joint friction angle
G = intact rock friction angle

Table A-16(f). Two-way table of means No. 6

Parameters		I = 6	I = 12
D = 38°		0.11906	0.33101
D = 28°		0.26311	0.70017
t-statistic			
t12	t34	t31	t42
−3.0472	−6.2835	2.0709	5.3073

D = joint friction angle
I = thermal expansion coefficient, $10^{-6}\ K^{-1}$

Table A-16(g). Two-way table of means No. 7

Parameters		H = 16	H = 32
E = 0.5		0.39100	0.67319
E = 0.2		0.18069	0.16848
t-statistic			
t12	t34	t31	t42
−4.0570	0.1755	−3.0236	−7.2560

E = thermal load, MTU/acre
H = intact rock Young's modulus, GPa

Table A-16. Two-way table of means of maximum joint separation under 100 yr of heating (cont'd)

Table A-16(h). Two-way table of means No. 8

Parameters		I = 6	I = 12
E = 100		0.29813	0.76606
E = 20		0.08405	0.26512
t-statistic			
t12	t34	t31	t42
−6.7274	−2.6033	−3.0777	−7.2019

E = thermal load, MTU/acre
I = thermal expansion coefficient, 10^{-6} K^{-1}

Table A-16(i). Two-way table of means No. 9

Parameters		H = 16	H = 32
G = 50°		0.33245	0.33325
G = 20°		0.23924	0.50843
t-statistic			
t12	t34	t31	t42
−0.0115	−3.8700	−1.3400	2.5185

G = intact rock friction angle
H = intact rock Young's modulus, GPa

Discussion of the interaction effects is provided in the following paragraphs.

- Subvertical joint inclination and subhorizontal joint inclination

  Vertical and subhorizontal joint inclinations are two of the important parameters that affect maximum joint separation. Interaction between subvertical joint inclination and intact rock friction angle suggests that subvertical joint inclination is significant at high intact rock friction angle. However, it has no effect when the intact rock friction angle is small. The effect of the subhorizontal joint inclination is significant with a positive influence when subvertical joint spacing is large. The effect does not exist at small subvertical joint spacing.

- Subvertical joint spacing

  Although the variance analysis result suggests that subvertical joint spacing may not be an important parameter regarding maximum joint separation, its interactions with subhorizontal

joint inclination, thermal load, and intact rock Young's modulus indicate that its effect is significant and should not be ignored. This parameter in general has a negative impact on maximum joint separation whereas the effect becomes significant at small subhorizontal joint inclination, high thermal load, or high intact rock Young's modulus.

- Joint friction angle

  Joint friction angle has been identified from table A-15 to be important and its general trend is to have a negative effect on maximum joint separation. The two-way table of means Nos. 5 and 6 confirm this trend. Maximum joint separation tends to decrease with an increase in joint friction angle irrespective of the values associated with the intact rock friction angle or thermal expansion coefficient.

- Thermal load

  Thermal load is the predominant parameter affecting maximum joint separation. Its interactions with subvertical joint spacing, intact rock Young's modulus, and thermal expansion coefficient indicate that thermal load has a positive effect at all values of subvertical joint spacing, intact rock Young's modulus, or thermal expansion coefficient.

- Intact rock cohesion

  According to the result of variance analysis, intact rock cohesion does not seem to affect the maximum joint separation and no interactions of any significance related to this parameter have been found.

- Intact rock friction angle

  Variance analysis indicated that intact rock friction angle is not significant. However, analysis of the associated two-way table of means of its interaction with subvertical joint inclination, joint friction angle, and intact rock Young's modulus suggests this parameter should not be ignored. Maximum joint separation decreases with an increase in intact rock friction angle at large subvertical joint inclination, high intact rock Young's modulus, or small joint friction angle.

- Intact rock Young's modulus

  Variance analysis shows that intact rock Young's modulus is significant and has a positive effect. Its related interaction effects further suggest that the intact rock Young's modulus is important to maximum joint separation at small subvertical joint spacing, small intact rock friction angle, or high thermal load.

- Thermal expansion coefficient

  Thermal expansion coefficient is the most important parameter besides thermal load that will have a significant impact to maximum joint separation. The effect is positive. Its interactions with joint friction angle and thermal load suggest further that the effect of the thermal expansion coefficient is significant at all values of joint friction angle and thermal load.

A.2.6 Roof-to-Floor Convergence

The analysis of variance for the roof-to-floor convergence of the emplacement drift after 50 yr of heating is given in table A-17 and the two-way table of means for significant interaction effects are provided in table A-18. Five main parameters are identified to be significant to roof-to-floor convergence of emplacement drift; all of which tend to reduce the roof-to-floor convergence as these parameters increase their values. Joint friction angle and thermal load seem to be the most dominant parameters. The significant interaction effects identified from table A-17 include

- subvertical joint inclination and joint friction angle (AD)
- subvertical joint inclination and thermal load (AE)
- subhorizontal joint inclination and thermal expansion coefficient (BI)
- subvertical joint spacing and intact rock friction angle (CG)
- joint friction angle and thermal load (DE)
- thermal load and thermal expansion coefficient (EI)

Discussion of the interaction effects is provided in the following paragraphs.

- Subvertical joint inclination

  Subvertical joint inclination has no significant effect on the roof-to-floor convergence when joint friction angle is large or thermal load is low. Otherwise, its effect is significant with a negative impact.

- Subhorizontal joint inclination

  Subhorizontal joint inclination is not found to be significant from the variance analysis. However, its interaction with the thermal expansion coefficient seems to suggest that its effect should not be ignored. The effect of subhorizontal joint inclination is not obvious when the thermal expansion coefficient is small. But, it becomes significant at large thermal expansion coefficient. The effect of subhorizontal joint inclination is positive.

- Subvertical joint spacing

  The variance analysis result suggests that subvertical joint spacing may not be an important parameter as far as roof-to-floor convergence is concerned. However, its computed F-ratio is very close to the critical value. Therefore, further investigation seems warranted. Its interaction with intact rock friction angle suggests the effect of vertical joint friction angle may become significant with a negative impact at low intact rock friction angle.

Table A-17. Analysis of variance for the roof-to-floor convergence after 50 yr of heating

Source of Variation	Effects	Sum of Squares	Degrees of Freedom	Mean Square	Computed F
A	−0.21887	0.7665	1	0.7665	6.8353
C	−0.17187	0.4727	1	0.4727	4.2149
D	−0.56487	5.1053	1	5.1053	45.5272
E	−0.59750	5.7121	1	5.7121	50.9381
H	−0.40544	2.6301	1	2.6301	23.4539
I	−0.23513	0.8845	1	0.8845	7.8880
AD	0.22856	0.8359	1	0.8359	7.4538
AE	−0.17919	0.5137	1	0.5137	4.5812
BI	0.17725	0.5027	1	0.5027	4.4827
CG	0.18069	0.5224	1	0.5224	4.6583
DE	−0.17969	0.5166	1	0.5166	4.6068
EI	−0.24531	0.9629	1	0.9629	8.5863
ERROR		2.0185	18	0.1121	
Total		25.4237	63		

Table A-18. Two-way table of means for roof-to-floor convergence after 50 yr of heating

Table A-18(a). Two-way table of means No. 1

Parameters		D = 28°	D = 38°
A = 85°		0.22438	−0.11194
A = 70°		0.67181	−0.12163
t-statistic			
t12	t34	t31	t42
2.8406	6.7016	3.7792	−0.0818

A = subvertical joint inclination
D = joint friction angle

Table A-18. Two-way table of means for roof-to-floor convergence after 50 yr of heating (cont'd)

Table A-18(b). Two-way table of means No. 2

Parameters		E = 20	E = 100
A = 85°		0.44456	−0.33213
A = 70°		0.48425	0.06594
t-statistic			
t12	t34	t31	t42
6.5602	3.5332	0.3352	3.3622

A = subvertical joint inclination
E = thermal load, MTU/acre

Table A-18(c). Two-way table of means No. 3

Parameters		I = 6	I = 12
B = 20°		0.25513	0.19725
B = 10°		0.31131	−0.10106
t-statistic			
t12	t34	t31	t42
.4888	3.4831	0.4746	−2.5196

B = subhorizontal joint inclination
I = thermal expansion coefficient, $10^{-6}\ K^{-1}$

Table A-18(d). Two-way table of means No. 4

Parameters		G = 20°	G = 50°
C = 0.5		0.03956	0.11988
C = 0.2		0.39213	0.11106
t-statistic			
t12	t34	t31	t42
−.6783	2.3739	2.9779	−0.0744

C = subvertical joint spacing, m
G = intact rock friction angle

Table A-18. Two-way table of means for roof-to-floor convergence after 50 yr of heating (cont'd)

Table A-18(e). Two-way table of means No. 5

Parameters		E = 20	E = 100
D = 38°		0.27181	−0.50538
D = 28°		0.65700	0.23919
t-statistic			
t12	t34	t31	t42
6.5644	3.5290	3.2534	6.2888

D = joint friction angle
E = thermal load, MTU/acre

Table A-18(f). Two-way table of means No. 6

Parameters		I = 6	I = 12
E = 100		0.10712	−0.37331
E = 20		0.45931	0.46950
t-statistic			
t12	t34	t31	t42
4.0579	−0.0860	2.9747	7.1187

E = thermal load, MTU/acre
= thermal expansion coefficient, $10^{-6}\ K^{-1}$

- Joint friction angle

  Joint friction angle is one of the most important parameters having an impact on roof-to-floor convergence. High joint friction angle results in small roof-to-floor convergence. Its interactions with subvertical joint inclination and thermal load suggest the effect of joint friction angle is significant at all values of subvertical joint inclination or thermal load.

- Thermal load

  Thermal load is the other dominant parameter besides joint friction angle affecting roof-to-floor convergence. Its interactions with subvertical joint inclination, joint friction angle, and thermal expansion coefficient indicate that the effect of thermal load is significant at all values of subvertical joint inclination, joint friction angle, and thermal expansion coefficient.

- Intact rock cohesion and intact rock friction angle

  Intact rock cohesion and intact rock friction angle are not significant parameters according to the variance analysis. Intact rock cohesion is also not found to interact with other parameters. Therefore, it is reasonable to conclude that intact rock cohesion will not impact roof-to-floor convergence. On the other hand, the intact rock friction angle interacts with subvertical joint spacing and has a significant negative effect when subvertical joint spacing is small. Consequently, when subvertical joint spacing is small, the impact of intact rock friction angle should not be ignored.

- Intact rock Young's modulus

  No interaction of intact rock Young's modulus with other main parameters is identified as significant. Consequently, intact rock Young's modulus can be categorically concluded to be significant based on results of variance analysis shown in table 4-17.

- Thermal expansion coefficient

  Roof-to-floor convergence increases as thermal expansion coefficient decreases at low subhorizontal joint inclination and high thermal load.

The analysis of variance for the roof-to-floor convergence of the emplacement drift after 100 yr of heating and the two-way table of means for the interaction effects are given in tables A-19 and A-20, respectively. Only two of the five main parameters identified to be significant for 50 yr of heating remain significant at 100 yr. These two parameters are joint friction angle and thermal load. They tend to reduce the roof-to-floor convergence as their values increase. The number of significant interaction effects has also been reduced considerably. The remaining ones are (i) subvertical joint inclination and joint friction angle and (ii) subhorizontal joint inclination and thermal expansion coefficient. The two-way tables of means given in table A-20 indicate that vertical and subhorizontal joint inclinations, and the thermal expansion coefficient may become significant. Subvertical joint inclination should have important negative effect if joint friction angle is small. Subhorizontal joint inclination will have a positive impact if the thermal expansion coefficient is large. The effect of the thermal expansion coefficient will only take place when subhorizontal joint inclination is small. Also, joint friction angle is not going to have much effect if subvertical joint inclination is high.

Table A-19. Analysis of variance for the roof-to-floor convergence after 100 yr of heating

Source of Variation	Effects	Sum of Squares	Degrees of Freedom	Mean Square	Computed F
C	−0.30319	1.4708	1	1.4708	4.2285
D	−0.51131	4.1830	1	4.1830	12.0265
E	−0.50544	4.0875	1	4.0875	11.7517
AD	0.38825	2.4118	1	2.4118	6.9341

Table A-19. Analysis of variance for the roof-to-floor convergence after 100 yr of heating (cont'd)

Source of Variation	Effects	Sum of Squares	Degrees of Freedom	Mean Square	Computed F
BI	0.33469	1.7923	1	1.7923	5.1528
ERROR		6.2607	18	0.3478	
Total		30.3502	63		

Table A-20. Two-way table of means for roof-to-floor convergence after 100 yr of heating

Table A-20(a). Two-way table of means No. 1

Parameters		D = 28°	D = 38°
A = 85°		0.16756	0.04450
A = 70°		0.70550	−0.19406
t-statistic			
t12	t34	t31	t42
0.5902	4.3142	2.5799	−1.1441

A = subvertical joint inclination
D = joint friction angle

Table A-20(b). Two-way table of means No. 2

Parameters		I = 6	I = 12
B = 20°		0.22631	0.41512
B = 10°		0.28131	−0.19925
t-statistic			
t12	t34	t31	t42
−0.9055	2.3047	0.2638	−2.9465

B = subhorizontal joint inclination
I = thermal expansion coefficient, $10^{-6}\ K^{-1}$

A.2.7 Extent of Yield Zone Around Emplacement Drift

The analysis of variance for the extent of the yield zone around the emplacement drift after 50 yr of heating is given in table A-21 and the two-way table of means for the interaction effects is provided in table A-22. Five main parameters are identified to be significant to the extent of yield zone around the emplacement drift. Among them, joint friction angle and intact rock friction angle have a negative impact, while thermal load, intact rock Young's modulus, and thermal expansion coefficient have positive impacts. The effect of subvertical joint spacing is marginal as its F-ratio is somewhat smaller than the critical value. The significant interaction effects identified from table A-21 include

- subvertical joint spacing and thermal load (CE)
- joint friction angle and intact friction angle (DG)
- joint friction angle and intact rock Young's modulus (DH)
- joint friction angle and thermal expansion coefficient (CI)
- thermal load and intact rock cohesion (EF)
- thermal load and intact rock Young's modulus (EH)
- thermal load and thermal expansion coefficient (EI)
- intact rock friction angle and intact rock Young's modulus (GH)
- intact rock friction angle and thermal expansion coefficient (GI)
- intact rock Young's modulus and thermal expansion coefficient (HI)

Table A-21. Analysis of variance for the extent of yield zone around emplacement drift after 50 yr of heating

Source of Variation	Effects	Sum of Squares	Degrees of Freedom	Mean Square	Computed F
C	−8.71338	1214.7690	1	1214.7690	4.2818
D	−10.44024	1743.9770	1	1743.9770	6.1472
E	10.08567	1627.5310	1	1627.5310	5.7367
G	−10.16888	1654.4980	1	1654.4980	5.8318
H	11.40590	2081.5120	1	2081.5120	7.3369
I	11.57554	2143.8890	1	2143.8890	7.5568
CE	−10.14821	1647.7800	1	1647.7800	5.8081
DG	10.19279	1662.2870	1	1662.2870	5.8592
DH	−10.10348	1633.2840	1	1633.2840	5.7570
DI	−10.34895	1713.6130	1	1713.6130	6.0402
EF	−10.08665	1627.8490	1	1627.8490	5.7379
EH	9.95839	1586.7140	1	1586.7140	5.5929
EI	9.87317	1559.6710	1	1559.6710	5.4975

Table 4-21. Analysis of variance for the extent of yield zone around emplacement drift after 50 yr of heating (cont'd)

Source of Variation	Effects	Sum of Squares	Degrees of Freedom	Mean Square	Computed F
GH	−10.16124	1652.0140	1	1652.0140	5.8230
GI	−10.04262	1613.6680	1	613.6680	5.6879
HI	11.18047	2000.0480	1	2000.0480	7.0498
ERROR		5106.6640	18	283.7035	
Total		50403.9000	63		

Table A-22. Two-way table of means for extent of yield zone around emplacement drift after 50 yr of heating

Table A-22(a). Two-way table of means No. 1

Parameters		E = 20	E = 100
C = 0.5		1.57607	1.51352
C = 0.2		0.14124	20.37512
t-statistic			
t12	t34	t31	t42
.0105	−3.3978	−0.2409	3.1673

C = subvertical joint spacing, m
E = thermal load, MTU/acre

Table A-22(b). Two-way table of means No. 2

Parameters		F = 18	F = 43
C = 0.5		0.15311	2.93647
C = 0.2		20.04697	0.46939
t-statistic			
t12	t34	t31	t42
−0.4674	3.2875	3.3407	−0.4143

C = subvertical joint spacing, m
F = intact rock cohesion, MPa

Table A-22. Two-way table of means for extent of yield zone around emplacement drift after 50 yr of heating (cont'd)

Table A-22(c). Two-way table of means No. 3

Parameters		G = 20°	G = 50°
D = 38°		0.66941	0.69332
D = 28°		21.30244	0.94077
t-statistic			
t12	t34	t31	t42
−0.0040	3.4192	3.4648	0.0416

D = joint friction angle
G = intact rock friction angle

Table A-22(d). Two-way table of means No. 4

Parameters		H = 16	H = 32
D = 38°		0.03016	1.33257
D = 28°		0.36692	21.87629
t-statistic			
t12	t34	t31	t42
−0.2187	−3.6119	0.0566	3.4498

D = joint friction angle
H = intact rock Young's modulus, GPa

Table A-22(e). Two-way table of means No. 5

Parameters		I = 6.0	I = 12.0
D = 38°		0.06807	1.29466
D = 28°		0.15936	22.08385
t-statistic			
t12	t34	t31	t42
−0.2060	−3.6816	0.0153	3.4910

D = joint friction angle
I = thermal expansion coefficient, $10^{-6}\ K^{-1}$

Table A-22. Two-way table of means for extent of yield zone around emplacement drift after 50 yr of heating (cont'd)

Table A-22(f). Two-way table of means No. 6

Parameters		E = 18	F = 43
E = 100		20.18620	1.70244
F = 20		0.01388	1.70342
t-statistic			
t12	t34	t31	t42
3.1039	−.2837	−3.3874	0.0002

E = thermal load, MTU/acre
F = intact rock cohesion, MPa

Table A-22(g). Two-way table of means No. 7

Parameters		H = 16	H = 32
E = 100		0.26217	21.62647
E = 20		0.13490	1.58240
t-statistic			
t12	t34	t31	t42
−3.5876	−0.2431	−0.0214	−3.3659

E = thermal load, MTU/acre
H = intact rock Young's modulus, GPa

Table A-22(h). Two-way table of means No. 8

Parameters		I = 6.0	I = 12.0
E = 100		0.21997	21.66867
E = 20		0.00747	1.70984
t-statistic			
t12	t34	t31	t42
−3.6018	−0.2859	−0.0357	−3.3516

E = thermal load, MTU/acre
I = thermal expansion coefficient, $10^{-6}\ K^{-1}$

Table A-22. Two-way table of means for extent of yield zone around emplacement drift after 50 yr of heating (cont'd)

Table A-22(i). Two-way table of means No. 9

Parameters		H = 16	H = 32
G = 50°		0.19472	1.43937
G = 20°		0.20236	21.76950
t-statistic			
t12	t34	t31	t42
−0.2090	−3.6216	0.0013	3.4139

G = intact rock friction angle
H = intact rock Young's modulus, GPa

Table A-22(j). Two-way table of means No. 10

Parameters		I = 6.0	I = 12.0
G = 50°		0.05059	1.58350
G = 20°		0.17685	21.79501
t-statistic			
t12	t34	t31	t42
−0.2574	−3.6302	0.0212	3.3940

G = intact rock friction angle
I = thermal expansion coefficient, 10^{-6} K^{-1}

Table A-22(k). Two-way table of means No. 11

Parameters		I = 6.0	I = 12.0
H = 32		0.22643	22.98244
H = 16		0.00101	0.39607
t-statistic			
t12	t34	t31	t42
−3.8213	−0.0663	−0.0379	−3.7928

H = intact rock Young's modulus, GPa
I = thermal expansion coefficient, 10^{-6} K^{-1}

Discussion regarding the interaction effects is provided in the following paragraphs.

- Subvertical joint inclination and subhorizontal joint inclination

  The variance analysis indicates that subvertical joint inclination and subhorizontal joint inclination are not important parameters that will affect the extent of the yield zone, nor do they have any interaction with other main parameters.

- Subvertical joint spacing

  The variance analysis result suggests that effect of subvertical joint spacing may be marginal since its F-ratio is slightly smaller than the critical value. The analysis of the interaction effect of this parameter with thermal load indicates that subvertical joint spacing will have a negative effect on the extent of yield zone when the thermal load is high. However, the effect of subvertical joint spacing is negligible at low thermal load.

- Joint friction angle

  Joint friction angle has significant interactions with intact rock friction angle, intact rock Young's modulus, and thermal expansion coefficient. In general, the effect of joint friction angle is significant at small intact rock friction angle, high intact rock Young's modulus, or high thermal expansion coefficient. Its effect is not significant at large intact rock friction angle, low intact rock Young's modulus, or low thermal expansion coefficient.

- Thermal load

  Generally, thermal load has a positive effect on the extent of yield zone. It has significant interactions with subvertical joint spacing, intact rock cohesion, intact rock Young's modulus, and thermal expansion coefficient. The effect of changing thermal load becomes less important when subvertical joint spacing is large, intact rock cohesion is high, intact rock Young's modulus is low, or thermal expansion coefficient is low.

- Intact rock cohesion

  Intact rock cohesion does not appear to be important to the extent of yielding according to the corresponding variance analysis. However, an analysis of its interaction with thermal load suggests its effect may be significant at a high thermal load condition.

- Intact rock friction angle

  Intact rock friction angle is an important parameter that controls extent of yielding around an emplacement drift. Analysis of its interactions with joint friction angle, intact rock Young's modulus, and thermal expansion coefficient using the two-way table of means suggests intact rock friction angle may not contribute to the extent of yield zone if joint friction angle is large, intact rock Young's modulus is low, or thermal expansion coefficient is low.

- Intact rock Young's modulus

  As discussed earlier, an increase in intact rock Young's modulus tends to increase the extent of yielding. Further study from the results of the two-way table of means of its interaction with other parameters indicates that the effect of intact rock Young's modulus may not be significant if joint friction angle is at its high value, intact rock friction angle is large, thermal load is low, or thermal expansion coefficient is low.

- Thermal expansion coefficient

  Thermal expansion coefficient has a positive effect on the extent of yielding. Results of the two-way table of means indicates that the effect of thermal expansion coefficient may not be significant if joint friction angle is high, intact rock friction angle is large, thermal load is low, or intact rock Young's modulus is low. Note the similarity of the effects between this parameter and intact rock Young's modulus.

When the heating reaches 100 yr, two additional main parameters become significant in affecting the extent of yielding based on the results of corresponding variance analysis. These two parameters are subvertical joint spacing and intact rock cohesion. While subvertical joint spacing has a positive effect, the effect of intact rock cohesion is a negative one. Analysis of variance for the extent of the yield zone around the emplacement drift after 100 yr of heating is given in table A-23 and the two-way table of means for interaction effects is provided in table A-24. As can be observed, considerably more interaction effects become significant. Consequently, the effects become more complicated. Observations made for the significant interaction effects for 50 yr of heating are equally applicable to the conditions for 100 yr of heating. Other significant interaction effects added besides those for 50 yr of heating are

- subvertical and subhorizontal joint inclination (AB)
- subvertical joint spacing and joint friction angle (CD)
- subvertical joint spacing and intact rock friction angle (CG)
- subvertical joint spacing and intact rock Young's modulus (CH)
- joint friction angle and thermal load (DE)
- joint friction angle and intact rock cohesion (DF)
- thermal load and intact rock friction angle (EG)
- intact rock cohesion and intact rock friction angle (FG)
- intact rock cohesion and intact rock Young's modulus (FH)

Table A-23. Analysis of variance for the extent of yield zone around emplacement drift after 100 yr of heating

Source of Variation	Effects	Sum of Squares	Degrees of Freedom	Mean Square	Computed F
C	−12.65815	2563.6620	1	2563.6620	6.5451
D	−13.77865	3037.6210	1	3037.6210	7.7551
E	14.63804	3428.3560	1	3428.3560	8.7527

Table A-23. Analysis of variance for the extent of yield zone around emplacement drift after 100 yr of heating (cont'd)

Source of Variation	Effects	Sum of Squares	Degrees of Freedom	Mean Square	Computed F
F	−12.51385	2505.5420	1	2505.5420	6.3967
G	−13.77740	3037.0690	1	3037.0690	7.7537
H	15.93083	4060.6610	1	4060.6610	10.3670
I	16.17330	4185.2080	1	4185.2080	10.6850
AB	−11.79611	2226.3710	1	2226.3710	5.6840
CD	12.14427	2359.7310	1	2359.7310	6.0245
CE	−14.18606	3219.9110	1	3219.9110	8.2205
CG	11.84199	2243.7230	1	2243.7230	5.7283
CH	−12.56280	2525.1850	1	2525.1850	6.4469
DE	−11.97927	2296.0450	1	2296.0450	5.8619
DF	11.90099	2266.1350	1	2266.1350	5.7855
DG	14.35589	3297.4650	1	3297.4650	8.4185
DH	−13.36345	2857.3100	1	2857.3100	7.2948
DI	−13.62367	2969.6700	1	2969.6700	7.5817
EF	−14.22693	3238.4900	1	3238.4900	8.2680
EG	−11.97007	2292.5200	1	2292.5200	5.8529
EH	14.38236	3309.6390	1	3309.6390	8.4496
EI	14.43951	3335.9910	1	3335.9910	8.5169
FG	11.91688	2272.1940	1	2272.1940	5.8010
FH	−12.60920	2543.8690	1	2543.8690	6.4946
GH	−13.68643	2997.0930	1	2997.0930	7.6517
GI	−13.62832	2971.6980	1	2971.6980	7.5868
HI	15.65620	3921.8640	1	3921.8640	10.0126
ERROR		7050.4530	18	391.6918	
Total		93808.7800	63		

Table A-24. Two-way table of means for extent of yield zone around emplacement drift after 100 yr of heating

Table A-24(a). Two-way table of means No. 1

Parameters		B = 10°	B = 20°
A = 85°		11.56708	3.28212
A = 70°		1.38620	16.69345
t-statistic			
t12	t34	t31	t42
1.1840	−2.1876	−1.4550	1.9167

A = subvertical joint inclination
B = subhorizontal joint inclination

Table A-24(b). Two-way table of means No. 2

Parameters		D = 28°	D = 38°
C = 0.5		2.72033	1.08594
C = 0.2		27.52275	1.59983
t-statistic			
t12	t34	t31	t42
0.2336	3.7047	3.5446	0.0734

C = subvertical joint spacing, m
D = joint friction angle

Table A-24(c). Two-way table of means No. 3

Parameters		E = 20	E = 100
C = 0.5		1.67715	2.12913
C = 0.2		0.14924	28.97334
t-statistic			
t12	t34	t31	t42
−0.0646	−4.1193	−0.2184	3.8364

C = subvertical joint spacing, m
E = thermal load, MTU/acre

Table A-24. Two-way table of means for extent of yield zone around emplacement drift after 100 yr of heating (cont'd)

Table A-24(d). Two-way table of means No. 4

Parameters		G = 20°	G = 50°
C = 0.5		2.87084	0.93543
C = 0.2		27.37099	1.75159
t-statistic			
t12	t34	t31	t42
0.2766	3.6614	3.5014	0.1166

C = subvertical joint spacing, m
G = intact rock friction angle

Table A-24(e). Two-way table of means No. 5

Parameters		H = 16	H = 32
C = 0.5		0.21913	3.58715
C = 0.2		0.31447	28.80810
t-statistic			
t12	t34	t31	t42
−0.4813	−4.0721	0.0136	3.6044

C = subvertical joint spacing, m
H = intact rock Young's modulus, GPa

Table A-24(f). Two-way table of means No. 6

Parameters		E = 20	E = 100
D = 38°		0.01350	2.67228
D = 28°		1.81289	28.43019
t-statistic			
t12	t34	t31	t42
−0.3800	−3.8040	0.2572	3.6811

D = joint friction angle
E = thermal load, MTU/acre

Table A-24. Two-way table of means for extent of yield zone around emplacement drift after 100 yr of heating (cont'd)

Table A-24(g). Two-way table of means No. 7

Parameters		F = 18	F = 43
D = 38°		1.64932	1.03646
D = 28°		27.32896	2.91412
t-statistic			
t12	t34	t31	t42
0.0876	3.4892	3.6700	0.2683

D = joint friction angle
F = intact rock cohesion, MPa

Table A-24(h). Two-way table of means No. 8

Parameters		G = 20°	G = 50°
D = 38°		1.05364	1.63213
D = 28°		29.18819	1.05489
t-statistic			
t12	t34	t31	t42
−0.0827	4.0206	4.0208	−0.0825

D = joint friction angle
G = intact rock friction angle

Table A-24(i). Two-way table of means No. 9

Parameters		H = 16	H = 32
D = 38°		0.05920	2.62657
D = 28°		0.47440	29.76868
t-statistic			
t12	t34	t31	t42
−0.3669	−4.1865	0.0593	3.8790

D = joint friction angle
H = intact rock Young's modulus, GPa

Table A-24. Two-way table of means for extent of yield zone around emplacement drift after 100 yr of heating (cont'd)

Table A-24(j). Two-way table of means No. 10

Parameters		I = 6	I = 12
D = 38°		0.06807	2.61770
D = 28°		0.22306	30.02002
t-statistic			
t12	t34	t31	t42
−0.3644	−4.2584	0.0221	3.9162

D = joint friction angle
I = thermal expansion coefficient, 10^{-6} K^{-1}

Table A-24(k). Two-way table of means No. 11

Parameters		F = 18	F = 43
E = 100		28.92163	2.18084
E = 20		0.05665	1.76974
t-statistic			
t12	t34	t31	t42
3.8216	−0.2448	−4.1252	−0.0588

E = thermal load, MTU/acre
F = intact rock cohesion, MPa

Table A-24(l). Two-way table of means No. 12

Parameters		G = 20°	G = 50°
E = 100		28.42497	2.67750
E = 20		1.81686	0.00953
t-statistic			
t12	t34	t31	t42
3.6797	0.2583	−3.8027	−0.3813

E = thermal load, MTU/acre
G = intact rock friction angle

Table A-24. Two-way table of means for extent of yield zone around emplacement drift after 100 yr of heating (cont'd)

Table A-24(m). Two-way table of means No. 13

Parameters		H = 16	H = 32
E = 100		0.39464	30.70783
E = 20		0.13896	1.68743
t-statistic			
t12	t34	t31	t42
−4.3322	−0.2213	−0.0365	−4.1474

E = thermal load, MTU/acre
H = intact rock Young's modulus, GPa

Table A-24(n). Two-way table of means No. 14

Parameters		I = 6	I = 12
E = 100		0.24483	30.85764
E = 20		0.04630	1.78009
t-statistic			
t12	t34	t31	t42
−4.3750	−0.2478	−0.0284	−4.1556

E = thermal load, MTU/acre
I = thermal expansion coefficient, $10^{-6}\ K^{-1}$

Table A-24(o). Two-way table of means No. 15

Parameters		G = 20°	G = 50°
F = 43		2.90555	1.04503
F = 18		27.33628	1.64199
t-statistic			
t12	t34	t31	t42
0.2659	3.6721	3.4915	0.0853

F = intact rock cohesion, MPa
G = intact rock friction angle

Table A-24. Two-way table of means for extent of yield zone around emplacement drift after 100 yr of heating (cont'd)

Table A-24(p). Two-way table of means No. 16

Parameters		H = 16	H = 32
F = 43		0.31447	3.63611
F = 18		0.21913	28.75915
t-statistic			
t12	t34	t31	t42
−0.4747	−4.0788	−0.0136	3.5904

F = intact rock cohesion, MPa
H = intact rock Young's modulus, GPa

Table A-24(q). Two-way table of means No. 17

Parameters		H = 16	H = 32
G = 50°		0.22131	2.46571
G = 20°		0.31229	29.92955
t-statistic			
t12	t34	t31	t42
−0.3208	−4.2327	0.0130	3.9249

G = intact rock friction angle
H = intact rock Young's modulus, GPa

Table A-24(r). Two-way table of means No. 18

Parameters		I = 6	I = 12
G = 50°		0.07103	2.61600
G = 20°		0.22011	30.02172
t-statistic			
t12	t34	t31	t42
−0.3637	−4.2590	0.0213	3.9166

G = intact rock friction angle
I = thermal expansion coefficient, $10^{-6}\ K^{-1}$

Table A-24. Two-way table of means for extent of yield zone around emplacement drift after 100 yr of heating (cont'd)

Table A-24(s). Two-way table of means No. 19

Parameters		I = 6	I = 12
H = 32		0.28288	32.11237
H = 16		0.00825	0.52535
t-statistic			
t12	t34	t31	t42
−4.5489	−0.0739	−0.0392	−4.5142

H = intact rock Young's modulus, GPa
I = thermal expansion coefficient, 10^{-6} K^{-1}

A brief discussion regarding additional interaction effects is provided below.

- Subvertical joint inclination and subhorizontal joint inclination

  The variance analysis indicates that subvertical joint inclination and subhorizontal joint inclination are not important parameters over the range of values investigated that will affect the extent of the yield zone. However, the interaction between these two parameters seems to indicate that subhorizontal joint inclination will be significant if subvertical joint inclination is small, and the effect of subhorizontal joint inclination on extent of yield zone is positive. The significance for the negative effect of subvertical joint inclination at high subhorizontal joint inclination is marginal since the associated t-statistic (1.9167) is somewhat smaller than the critical value of 2.042.

- Subvertical joint spacing

  The variance analysis result suggests that effect of subvertical joint spacing is significant and negative. The analysis of the two-way table of means shows that subvertical joint spacing does not appear to have much effect on the extent of yield zone when joint friction angle is large, intact rock friction angle is large, or intact rock Young's modulus is low.

- Joint friction angle

  Besides interacting with intact rock friction angle, intact rock Young's modulus, and thermal expansion coefficient as is the case for 50 yr of heating, joint friction angle also has significant interactions with subvertical joint spacing, thermal load, and intact rock cohesion. The effect of joint friction angle may not be important if subvertical joint spacing is large, intact rock cohesion is high, or thermal load is low.

- Thermal load

  Two additional significant interaction effects are identified for thermal load after 100 yr of heating. Thermal load has a positive effect when either joint or intact rock friction angle is small.

- Intact rock cohesion

  Intact rock cohesion becomes an important parameter to the extent of yielding around an emplacement drift after 100 yr of heating. Also, intact rock cohesion is found to have a significant negative effect when joint friction angle is small, intact rock friction angle is small, or intact rock Young's modulus is high.

- Intact rock friction angle

  Three more parameters are found to have significant negative interaction with intact rock friction angle. The significant effect become obvious when subvertical joint spacing is small, intact rock cohesion is low, or thermal load is high.

- Intact rock Young's modulus

  Two additional parameters have significant positive interaction with intact rock Young's modulus. The effect of intact rock Young's modulus becomes important when either subvertical joint spacing or intact rock cohesion is low.

- Thermal expansion coefficient

  No additional interaction effects with thermal expansion coefficient have been added due to the additional 50 yr of heating.